

FINAL REPORT – PHASE III

Measurement and Modeling of Ecosystem Risk and Recovery for In Situ Treatment of Contaminated Sediments

SERDP Project ER-1552

AUGUST 2015

Richard Luthy
Yeo-Myoung Cho
Stanford University

Yongju Choi
Seoul National University

Yanwen Wu
Formerly Stanford University

David Werner
Newcastle University

Distribution Statement A
This document has been cleared for public release



This report was prepared under contract to the Department of Defense Strategic Environmental Research and Development Program (SERDP). The publication of this report does not indicate endorsement by the Department of Defense, nor should the contents be construed as reflecting the official policy or position of the Department of Defense. Reference herein to any specific commercial product, process, or service by trade name, trademark, manufacturer, or otherwise, does not necessarily constitute or imply its endorsement, recommendation, or favoring by the Department of Defense.

REPORT DOCUMENTATION PAGE				Form Approved OMB No. 0704-0188	
Public reporting burden for this collection of information is estimated to average 1 hour per response, including the time for reviewing instructions, searching existing data sources, gathering and maintaining the data needed, and completing and reviewing this collection of information. Send comments regarding this burden estimate or any other aspect of this collection of information, including suggestions for reducing this burden to Department of Defense, Washington Headquarters Services, Directorate for Information Operations and Reports (0704-0188), 1215 Jefferson Davis Highway, Suite 1204, Arlington, VA 22202-4302. Respondents should be aware that notwithstanding any other provision of law, no person shall be subject to any penalty for failing to comply with a collection of information if it does not display a currently valid OMB control number. PLEASE DO NOT RETURN YOUR FORM TO THE ABOVE ADDRESS.					
1. REPORT DATE (DD-MM-YYYY) 31-08-2015		2. REPORT TYPE Final Report (Phase III)		3. DATES COVERED (From - To) 06/01/13-08/31/15	
4. TITLE AND SUBTITLE Measurement and Modeling of Ecosystem Risk and Recovery for In Situ Treatment of Contaminated Sediments. Phase III.				5a. CONTRACT NUMBER W912HQ-10-C-0079	
				5b. GRANT NUMBER	
				5c. PROGRAM ELEMENT NUMBER	
6. AUTHOR(S) Luthy, Richard G. Cho, YeoMyoung Choi, YongJu				5d. PROJECT NUMBER ER-1552	
				5e. TASK NUMBER ER-1552	
				5f. WORK UNIT NUMBER	
7. PERFORMING ORGANIZATION NAME(S) AND ADDRESS(ES) Stanford University Yang & Yamazaki Environment & Energy Bldg, 473 Via Ortega Stanford University, Stanford, California 94305-4020				8. PERFORMING ORGANIZATION REPORT NUMBER	
9. SPONSORING / MONITORING AGENCY NAME(S) AND ADDRESS(ES) Strategic Environmental Research and Development Program 4800 Mark Center Drive, Suite 17D08, Alexandria, VA 22350-				10. SPONSOR/MONITOR'S ACRONYM(S) SERDP	
				11. SPONSOR/MONITOR'S REPORT NUMBER(S)	
12. DISTRIBUTION / AVAILABILITY STATEMENT Approved for public release; distribution is unlimited.					
13. SUPPLEMENTARY NOTES					
14. ABSTRACT The last phase of the ER-1552 project further expanded the project scope by enhancing the usability of the project outcomes from Phases I and II. The objectives were 1) to investigate the potential repartitioning of contaminants in sediment following the removal of AC after stabilization treatment, 2) to standardize field monitoring methods using polyethylene passive samplers, and 3) to develop a user-friendly, standalone program for HOC mass transfer model to predict sequestration and pore water concentrations. The experimental results showed that when sorbent is selectively lost from the sorbent-treated sediment by winnowing, the repartitioning of contaminants may occur to some degree, but the repartitioning process is neither prolonged nor substantial to cause significant loss of the treatment effectiveness. Our close examination on the PRC-based PE sampling method indicated that the PRC method can provide reliable predictions at certain conditions, but more studies are needed to further investigate the PRC method for varying conditions. A standalone HOC mass transfer model was successfully developed, which is equipped with an I/O excel file, GUI, and detailed user manual, so to enhance its user-friendliness in a great extend. A separate standalone program for sediment desorption kinetic model and the modeling case study booklet will also enhance the usability and accessibility of the HOC mass transfer model to DoD users.					
15. SUBJECT TERMS in-situ activated carbon amendment, mass transfer modeling, passive sampling method, sediment remediation					
16. SECURITY CLASSIFICATION OF:			17. LIMITATION OF ABSTRACT N/A	18. NUMBER OF PAGES	19a. NAME OF RESPONSIBLE PERSON Richard G. Luthy
a. REPORT	b. ABSTRACT	c. THIS PAGE			19b. TELEPHONE NUMBER (include area code) 650-721-2615

Table of Contents

List of Acronyms	iii
List of Tables	iv
List of Figures	v
Keywords	vii
Acknowledgements	viii
I. Abstract.....	1
II. Objectives.....	4
III. Background.....	6
1. Mechanisms of <i>in-situ</i> stabilization and reduction of bioavailability.....	6
2. Previous Studies of AC Amendment for <i>In-situ</i> Treatment.....	8
3. HOC Mass Transfer Model.....	8
4. Passive Sampling Technique.	10
IV. Materials and Methods	1
1. Prolonged effect of AC amendment (Task 9).....	1
1.1. Prepare fully sequestered sediment by MAC amendment (Task 9.1)	1
1.1.1. Test with carbon-coated magnetic particles.....	1
1.1.2. Test with Tenax bead as a model sorbent	2
1.2. PCB repartitioning test with sorbent-removed sediment (Task 9.2).....	3
2. Standardization of field monitoring method using PE samplers (Task 10).....	3
2.1. Assess potential anisotropic exchange kinetics in PE (Task 10.1)	3
2.2. Investigate alternative PE kinetic method (Task 10.2).....	4
2.2.1. Concept of an alternative non-equilibrium passive sampling method.....	4
2.2.2. Experimental design for method development.	6
3. Develop user-friendly standalone program for HOC mass transfer model (Task 11).....	8
3.1. Standalone program beta version development (Task 11.1).....	8
3.2. Improve user friendliness of HOC mass transfer model (Task 11.2)	8
3.3. Develop booklet for exemplary modeling results.....	8
3.3.1. Study sites and model input parameters.....	8
3.3.2. Model assumptions and execution	9
3.3.3. Developing booklet for modeling results for the case study sites	9
V. Results and Discussion.....	10

1. Prolonged effect of AC amendment (Task 9).....	10
1.1. Prepare fully sequestrated sediment by MAC amendment (Task 9.1)	10
1.1.1. Test with carbon-coated magnetic particles.....	10
1.1.2. Test with Tenax bead as a model sorbent.	10
1.2. PCB repartitioning test with sorbent-removed sediment (Task 9.2).....	10
2. Standardization of field monitoring method using PE samplers (Task 10).....	13
2.1. Assess potential anisotropic exchange kinetics in PE (Task 10.1).....	13
2.2. Investigate alternative PE kinetic method (Task 10.2).....	15
2.2.1. PE-water partitioning coefficients for different types of PEs.....	15
2.2.2. PCB uptake kinetics in quiescent sediment	18
2.2.3. Modeling PCB uptake kinetics in quiescent sediment.....	20
2.2.4. Applying PRC method for non-equilibrium PE sampling.....	25
3. Develop user-friendly standalone program for HOC mass transfer model (Task 11).....	28
3.1. Standalone program beta version development (Task 11.1).....	28
3.2. Improve user friendliness of HOC mass transfer model (Task 11.2)	29
3.3. Develop booklet for exemplary modeling results (Task 11.3)	33
VI. Conclusions and Implications for Future Research/Implementation.....	34
1. Prolonged effect of AC amendment (Task 9).....	34
2. Standardization of field monitoring method using PE samplers (Task 10).....	34
3. Develop user-friendly standalone program for HOC mass transfer model (Task 11).....	34
VII. Literature Cited.....	36
Appendix A. List of Scientific/Technical Publication.....	39
Appendix B. Other Supporting Materials	40
1. User Manual for the Standalone HOC Mass Transfer Model.....	40
2. User Manual for the Standalone HOC Sediment Desorption Model.....	50
3. Booklet for Exemplary Results of HOC Mass Transfer Model for the Effectiveness of Activated Carbon Amendment	55
Appendix C. Numerical Data for Figures	77
Appendix D. Electronic Files.....	82

List of Acronyms

AC	Activated carbon
ANOVA	Analysis of variance
BC	Black carbon
DOM	Dissolved organic matter
DI	Deionized
GC	Gas chromatography
HOC	Hydrophobic organic compound
HP	Hunters Point
LOQ	Limit of quantification
MDL	Method detection limit
PAH	Polycyclic aromatic hydrocarbon
PCB	Polychlorinated biphenyl
PE	Polyethylene
POM	Polyoxymethylene
PRC	Performance reference compound
SPMD	Semipermeable membrane devices
TOC	Total organic carbon

List of Tables

Table 1. Properties of the CCMPs provided by United Science Corporation.	1
Table 2. Fraction of model PCB congeners sequestered (i.e., removed) from sediment slurries after treatment by Tenax beads ($n=15$, average \pm standard deviation).	10
Table 3. First-order kinetics constants for PCB uptake and release in PE.	15
Table 4. Logarithm of K_{PE} values determined for different types of PEs used in this study.....	18
Table 5. The ratio of $C_{PE}(t)/C_{PE,eq}$ values for 17 μm PE to the value for the corresponding PE (i.e., $[C_{PE}(t)/C_{PE,eq}]_{17 \mu m}/[C_{PE}(t)/C_{PE,eq}]_x \mu m$, x =thickness for the corresponding PE) for the PCB uptake kinetics in quiescent sediment.	20
Table 6. The equilibrium PE concentrations ($C_{PE,eq}$) determined by the PRC method using data at various contact times and PE thicknesses for model congeners 43, 101, 153, and 180.	27
Table 7. Acceptable ranges for model input parameters.....	30

List of Figures

Figure 1. Absorption efficiency results for various particle types for the marine clam <i>Macoma balthica</i>	7
Figure 2. Schematic of the mechanisms involved with application of AC amendment to sediment in reducing exposure and environmental risk by lowering HOC release to water and bio-uptake by benthic biota, either by filter feeding or deposit feeding.	7
Figure 3. Model simulation of reductions in PCB pore-water concentrations for a continuously well-mixed system and for a system having randomly distributed AC particles and no advective pore-water movement by tides or wave action.	9
Figure 4. The conceptual framework for a model of HOC transport for a minimally mixed sediment system.	9
Figure 5. Separation of CCMPs from sediment slurry.	2
Figure 6. General temporal trend of contaminant uptake into passive samplers and its observation using passive sampling using a certain sampler thickness with three time points and using three sampler thicknesses with a certain time point.....	5
Figure 7. Preparation of the PE kinetic experiments in quiescent sediment:.....	7
Figure 8. Comparison of (a) 1-d and (b) 28-d Tenax uptake immediately after the PCB sequestration (0 month contact) to the untreated cases.....	11
Figure 9. One-day (1-d) Tenax uptake shown as relative amount to the total PCB mass for the model PCBs applying different times of mixing after PCB sequestration.	12
Figure 10. Twenty-eight-day (28-d) Tenax uptake shown as relative amount to the total PCB mass for the model PCBs applying different times of mixing after PCB sequestration.....	13
Figure 11. Uptake and release kinetics of five PCB congeners for PE in water.....	14

Figure 12. Concentrations of PCB PRCs, congeners 29, 69, 103, 155, and 192 in different types of PEs after equilibrating in a single batch of 80:20 (v:v) methanol:water solution.	16
Figure 13. Concentrations of PCB model congeners, 43, 101, 153, and 180 in different types of PEs after equilibrating in a single batch of Hunters Point sediment in a slurry phase.	17
Figure 14. PCB uptake kinetics for model PCB congeners 43, 101, 153, and 180 measured in experiments under quiescent contact between sediment and PE.	19
Figure 15. Comparison of the simulation results using first-order kinetic model and the experimental results for the uptake kinetics in PE for PCB 43 in quiescent sediment.	21
Figure 16. Comparison of the simulation results using 1-D diffusion model and the experimental results for the uptake kinetics in 17 μm PE for PCB 43 in quiescent sediment.	23
Figure 17. Comparison of the simulation results using a modified 1-D diffusion model and the experimental results for the uptake kinetics in PE for PCB 43 in quiescent sediment.	24
Figure 18. Release kinetics for PCB PRCs, congeners 29, 69, 103, 155, and 192, from PE in quiescent sediment.	26
Figure 19. Screenshot of the splash screen of the standalone HOC mass transfer model (alpha version).	28
Figure 20. Screenshot of the beta version standalone HOC mass transfer model GUI (input UI, message bar, and progress bar)	29
Figure 21. An example error message for an invalid input parameter.	31
Figure 22. An example error message for pre-existed simulation data in “Data Output” worksheet.	31
Figure 23. GUI of the standalone HOC sediment desorption parameter fitting program.	32

Keywords

In-situ treatment
Activated carbon amendment
Hydrophobic organic contaminants
Sediment
Mass transfer model
Long-term effectiveness
Polychlorinated biphenyls
Polycyclic aromatic hydrocarbons
Polyethylene passive sampler
User-friendly standalone program

Acknowledgements

Funding for this research was provided by the Department of Defense Strategic Environmental Research and Development Program (SERDP), project ER-1552 Phases III. Additional support was provided by the Chevron Energy Technology Company under Contract No. CW786669. YongJu Choi was supported in part by a Samsung Scholarship. Collaboration with Newcastle University was facilitated by the Leverhulme Trust, grant FOO 125/AA.

I. Abstract

Project Overview

Many Department of Defense (DoD) sediment sites are contaminated with polychlorinated biphenyls (PCBs) and polycyclic aromatic hydrocarbons (PAHs). PCBs and PAHs are persistent and toxic; and PCBs are bioaccumulative. Over the past decade, various laboratory and field trials have shown that *in-situ* sediment treatment technologies using activated carbon (AC) sorbents will reduce ecological and health risk from PCBs and PAHs. While several lines of evidence have demonstrated the AC treatment effectiveness, there is a need for further investigation of ecosystem recovery after AC sorbent amendment, assessment of secondary effects of AC on ecosystem health, development of mechanistic mass transfer modeling frameworks, and the design and testing of rapid, yet reliable, performance monitoring tools. The overarching goal of this project is to advance sediment *in-situ* AC treatment technologies by studying these considerations. This project was comprised of three phases.

In Phase I work was performed in three areas: 1. A passive sampling technique using polyethylene devices (PEDs) was developed as an inexpensive and easy method to determine pore-water hydrophobic organic compound (HOC) concentrations. 2. A biodynamic modeling approach was used successfully to predict the contaminant burden at the base of the food web. And, 3. A method was developed to estimate pore-water advection and dispersion using a theoretical heat transport model, which may improve the performance of the HOC mass transfer model.

In Phase II, the HOC mass transfer model and the passive sampling techniques developed and studied in Phase I were used to achieve several goals: 1. Improve the mechanistic understanding of the *in-situ* AC amendment, 2. Verify the benefit of the treatment to reduce the risk of HOCs in sediments, and 3. Develop a predictive tool for assessment of the long-term effectiveness of the treatment. The possible adverse effects of AC amendment on local invertebrates, which had been investigated in Phase I, were comprehensively studied with emphasis on secondary effects.

Lastly, Phase III of the project studied the changes in contaminant risk after loss or retrieval of AC from treated sediment, standardized the *in-situ* PE sampling technique, and developed a user-friendly standalone program for HOC mass transfer modeling. This final report details the accomplishments of Phase III.

Objectives of the Current Work

This phase of the work (Phase III) further expands the scope of the current project by enhancing the usability of the outcomes from the project. The objectives are to investigate the potential repartitioning of contaminants in sediment following the removal of AC after a full stabilization, to standardize field monitoring methods using polyethylene passive samplers, and to develop a user-friendly, standalone program for the HOC mass transfer model to predict HOC contaminant sequestration by AC and pore water concentrations.

Technical Approach

A series of sediment slurry experiments simulated the field situation wherein the maximum benefit from *in-situ* AC amendment is obtained and then the AC particles are removed, as might happen by erosion or intentional retrieval from a sediment site. Tenax beads were selected as a surrogate of AC to mimic this field situation, and PE sampling was used as a monitoring device for contaminant availability. For the PE sampling method, the use of performance reference compounds (PRC) was evaluated to consider kinetic effects of HOC sampling, to standardize the method, and to investigate possible anisotropic exchange kinetics in the field. Lastly, the current HOC mass transfer model developed in Phase II was modified for an executable version without the need to purchase MATLAB software. A booklet with case study modeling results was prepared and submitted together with the program.

Results

The experimental results showed that when sorbent is selectively lost from the sorbent-treated sediment by winnowing, the repartitioning of contaminants may occur to some degree, but the repartitioning process is neither prolonged nor substantial to cause significant loss of the treatment effectiveness. Even with an extensive period of mixing of sorbent-deprived sediment in a slurry phase following sorbent treatment and removal, the available fraction of PCBs in the sediment was substantially lower than that for the untreated sediment.

Our close examination on the PRC-based PE sampling method indicated that PE might show anisotropic exchange kinetics, which could limit the application of the PRC-based method. Still the PRC method can provide good predictions of equilibrium PE concentrations for less chlorinated PCB congeners and for PE with thinner thicknesses, while it can significantly underestimate the equilibrium PE concentrations for highly chlorinated congeners (i.e., more than 5 chlorine substitutions) and for relatively thick PE. Although our conclusions are based on a relatively small set of data, they clearly showed that more studies are needed to investigate the accuracy of the PRC method for different PCB congeners and PEs with different thicknesses.

The HOC mass transfer model MATLAB codes were successfully developed into a standalone program. The standalone program is equipped with an I/O excel file, GUI, and detailed user manual to enhance its user-friendliness. An additional standalone program for sediment desorption kinetic modeling was developed to easily determine model parameters. Furthermore, the modeling case study booklet will serve as an exemplary and introductory material of *in-situ* AC amendment and its effectiveness to DoD users.

Benefits

A situation that might result in of complete removal of AC amendment after treatment is not likely to occur, but regulators, site managers, and DoD users would want assurance that risk reduction is still maintained even if the AC were removed. Our study addressed these concerns and raises the confidence level for the *in-situ* AC amendment technology. Our effort with PED field method standardization helps to advance the understanding of PED passive sampling technique as a reliable monitoring tool for site investigation and remedy assessment. Development of the standalone program for the HOC mass transfer modeling improves the usability and accessibility of the model for remedial project managers and DoD users.

II. Objectives

Many Department of Defense (DoD) sediment sites are contaminated with polychlorinated biphenyls (PCBs) and polycyclic aromatic hydrocarbons (PAHs), which are persistent and toxic. Over the past decade, various laboratory and field trials have shown that *in-situ* sediment treatment technologies using activated carbon (AC) sorbents can reduce ecological risk and biouptake from PCBs and PAHs, as well as from persistent chlorinated pesticides. While several lines of evidence have shown the treatment effectiveness, there is need for further investigation of ecosystem recovery after sorbent amendment, study of secondary effects of AC on ecosystem health, development of mechanistic mass transfer modeling frameworks, and design and testing of rapid, yet reliable, monitoring tools. The overarching goal of this project is to advance the AC *in-situ* treatment technology by studying these considerations. This project was comprised of three phases.

Phase I: Conventional ecosystem health determinants, such as benthic organism bioassays and community surveys, are time-consuming and expensive. No fast, inexpensive field methods currently exist to predict the bio-uptake of contaminants and explain post-treatment ecological effects. The objectives of the first phase was to incorporate rapid, inexpensive assessment tools to measure contaminant concentrations in the sediment pore water, to use a biodynamic modeling approach to predict contaminant burden at the base of the food web, and to develop a general model to predict the ecological characteristics of recovery.

Phase II: With the current understanding, some concerns exist as to whether the AC itself may cause adverse effects in benthic invertebrates inhabiting the remediated area. Comprehensive studies targeting the causes and effects of carbon on organisms' health and habitat quality have to be investigated. Furthermore, predictive models are needed to assess long-term trends in PCB-pore water concentrations and (bio)availability under field conditions. Our previous ESTCP field project (ER-0510) showed the need for predictive models to assess the long-term performance of AC amendment under quiescent field conditions with slow mass transfer compared to well-mixed conditions in the laboratory. The objectives of the Phase II was to evaluate possible adverse effects of AC amendment on local invertebrates and to develop a mass transfer model to predict PCB mass transfer under conditions relevant to field application of AC-amendment, and assess the long-term sequestration ability of field-aged AC.

Phase III: This phase of the work further expanded the scope of the current project by enhancing the usability of the outcomes from the project. The objectives were to investigate the potential repartitioning of contaminants in sediment following the removal of AC after stabilization treatment, to standardize field monitoring methods using polyethylene passive samplers, and to develop a user-friendly, standalone program for HOC mass transfer model to predict sequestration and pore water concentrations.

This final report details the accomplishments of Phase III. Below are the corresponding subtasks for each objective of the Phase III.

1. Investigate prolonged effect of AC amendment (Task 9)

Subtask 9.1 Prepare fully sequestered sediment

Subtask 9.2 PCB repartitioning test with sorbent-removed sediment

2. Standardize field monitoring method using PE samplers (Task 10)

Subtask 10.1 Assess potential anisotropic exchange kinetics in PE

Subtask 10.2 Investigate alternative PE kinetic method

3. Develop standalone program for HOC mass transfer model (Task 11)

Subtask 11.1 Develop a beta version standalone program for the model

Subtask 11.2 Improve user friendliness of HOC mass transfer model

Subtask 11.3 Develop booklet for exemplary modeling results

III. Background

1. Mechanisms of *in-situ* stabilization and reduction of bioavailability.

The concept of activated carbon (AC) amendment for *in-situ* stabilization of hydrophobic organic contaminants (HOCs) builds on prior studies that describe the role of black carbon, e.g., soot, chars, and soot-like materials such as coal, to affect the transport, uptake, and biomagnification of HOCs in sediments (Ghosh, Gillette et al. 2000). Particle-scale analyses of sediment from the general study area at a field site in San Francisco Bay showed that the majority of HOCs were associated with black carbon-derived materials such as chars and were not as readily released to water (Ghosh, Gillette et al. 2000; Ghosh, Zimmerman et al. 2003). These black carbonaceous particles strongly affect the partitioning of HOCs due to their large surface area and adsorption affinity. Furthermore, several studies showed that strong sorption onto such particles is responsible for slower HOC release rates and reduction in HOC bioavailability (Kraaij, Ciarelli et al. 2001; Talley, Ghosh et al. 2002).

These observations led to the idea of using strong carbonaceous sorbent to shift contaminant sorption from a readily-available state to a strongly-sorbed state. This would significantly enhance a process that was occurring naturally, albeit slowly. Zimmerman et al. tested coke and activated carbon as such sorbents, and found that AC showed significantly greater performance to reduce polychlorinated biphenyl (PCB) availability to the aqueous phase than coke (Zimmerman, Ghosh et al. 2004). The much greater specific surface area and the pore structure of AC appeared to account for the greater effectiveness. Strong sorption to AC would reduce the absorption (i.e., the bio-uptake) of HOCs to sediment biota. This was confirmed by McLeod et al. who showed significantly lower absorption efficiency of radio-labeled benzo(a)pyrene and a PCB congener by a marine clam from AC compared to other carbonaceous particle types (McLeod, Van Den Heuvel-Greve et al. 2004). As shown in Figure 1, the bivalve absorption efficiency is the highest for wood and diatoms and the lowest for AC.

A conceptual schematic of the *in-situ* stabilization of HOCs by AC amendment is shown in Figure 2. Incorporation of AC into sediment particle promotes repartitioning of contaminants from the more readily-available sorbed fraction onto AC particles. In consequence, the strongly sorbed contaminants become much less available to biota either via contact with water or by particle ingestion.

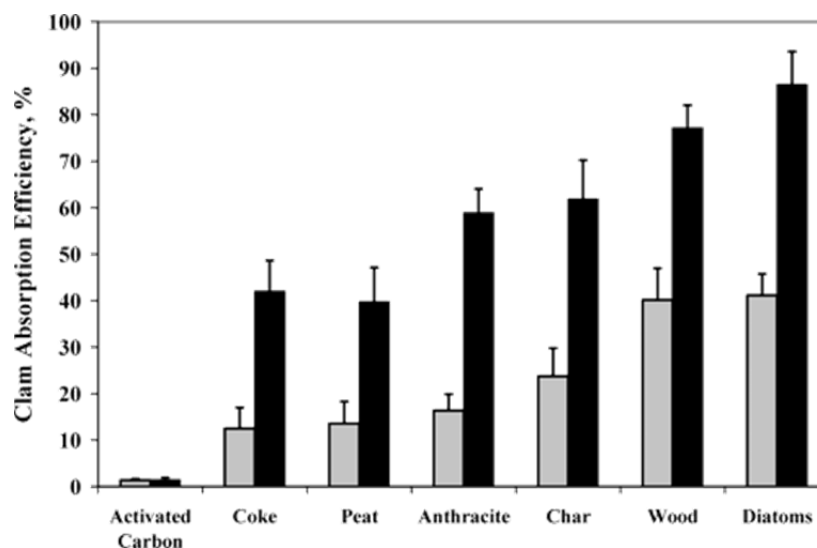


Figure 1. Absorption efficiency results for various particle types for the marine clam *Macoma balthica*. Light columns represent the polycyclic aromatic hydrocarbon benzo(a)pyrene; dark columns represent PCB-52. Error bars show 95% confidence intervals. For the particles tested, absorption efficiency for either compound is the lowest for activated carbon and the greatest for wood and diatoms (McLeod, Van Den Heuvel-Greve et al. 2004).

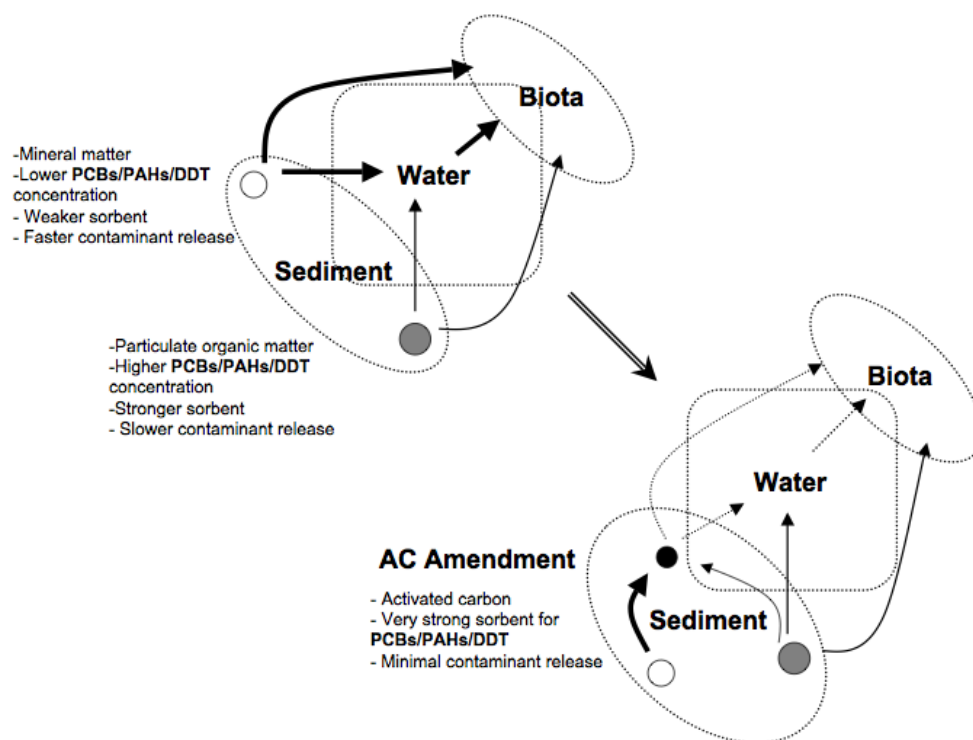


Figure 2. Schematic of the mechanisms involved with application of AC amendment to sediment in reducing exposure and environmental risk by lowering HOC release to water and bio-uptake by benthic biota, either by filter feeding or deposit feeding.

2. Previous Studies of AC Amendment for *In-situ* Treatment.

Various studies showed that incorporating AC into HOC-contaminated sediment would re-partition the HOCs, making them less available to pore-water and biota (Zimmerman, Ghosh et al. 2004; Millward, Bridges et al. 2005; Zimmerman, Werner et al. 2005; Cho, Smithenry et al. 2007; Tomaszewski, Werner et al. 2007; Cho, Ghosh et al. 2009; Hale, Tomaszewski et al. 2009). For instance, introducing 3.4 dry wt% of AC into well-mixed sediment-water slurries in the laboratory showed about 90% reductions of PCBs, PAHs and DDT in water and benthic organisms (Zimmerman, Ghosh et al. 2004; Millward, Bridges et al. 2005; Zimmerman, Werner et al. 2005; McLeod, Luoma et al. 2007; McLeod, van den Heuvel-Greve et al. 2007; Sun and Ghosh 2007; Tomaszewski, Werner et al. 2007). Mixing about 2% AC into the top 30-cm sediment layer at a mud flat in San Francisco Bay gave 50-70% reduction in PCBs in pore-water, passive samplers, and benthic test organisms (Cho, Smithenry et al. 2007; Cho, Ghosh et al. 2009).

3. HOC Mass Transfer Model.

Models are needed to explain the laboratory results with well-mixed systems, field results with minimally mixed systems, and furthermore the differences between them. From both engineering management and regulatory decision-making perspectives, models are the only means for making longer-term predictions about performance and estimating the time required to achieve an eventual quasi-equilibrium state, as illustrated in Figure 3. Such models must consider: 1. diffusive mass transfer under quiescent conditions, 2. advective pore-water movement in intertidal and sub-tidal regions, 3. effects of dissolved organic matter on reducing the mass transfer and/or sorption capacity of the AC, and 4. the distribution of AC particles within the sediment, e.g., uniformly distributed as in a well-mixed laboratory test or heterogeneously distributed as in a field test, or possibly layered.

Mass transfer under field conditions may occur quiescently, where diffusion processes limit HOC mass transfer. To explain HOC mass transfer in a stagnant system, Werner, Ghosh & Luthy developed a mass transfer model of an unmixed system with sorption-retarded molecular diffusion (Werner, Ghosh et al. 2006). An example of this model (Hale and Werner 2010) is shown in Figure 3, which shows that HOC mass transfer to AC in a quiescent system is greatly retarded and the full effect of AC on reducing HOC pore-water concentrations could be delayed for several years to approach near equilibrium.

The HOC mass transfer model was further advanced and validated by Cho et al. (Cho, Werner et al. 2012) and Choi et al. (Choi, Cho et al. 2014) for a stagnant sediment layer, which was major accomplishment in the previous phase of this SERDP project (Phase II). Overall, this model embraces the concept of intra-particle diffusion of contaminants by different particle types, distinguishing between two different sediment particles types (or sorption domains): one with slow intra-particle diffusion and slow desorption of contaminants ($rate_{slow}$), and the other with relatively faster intra-particle diffusion and desorption ($rate_{fast}$) (Figure 4). The third particle domain in the model is AC, which has the slowest diffusion/sorption kinetics because of its very strong sorption ability for PCBs (Figure 4). The model can simulate a series of different mixing regimes either for a well-mixed system or for a quiescent system.

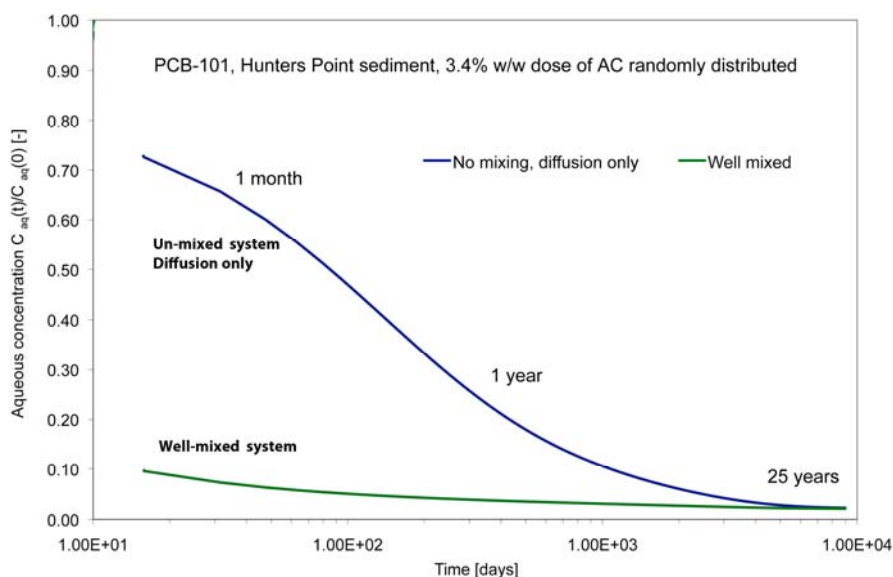


Figure 3. Model simulation of reductions in PCB pore-water concentrations for a continuously well-mixed system and for a system having randomly distributed AC particles and no advective pore-water movement by tides or wave action. After an initial decline, systems with no pore-water movement require several years to approach near equilibrium. The approach towards equilibrium depends on the extent of pore-water movement, e.g., by tides or wave action, and the distribution and size of the AC.

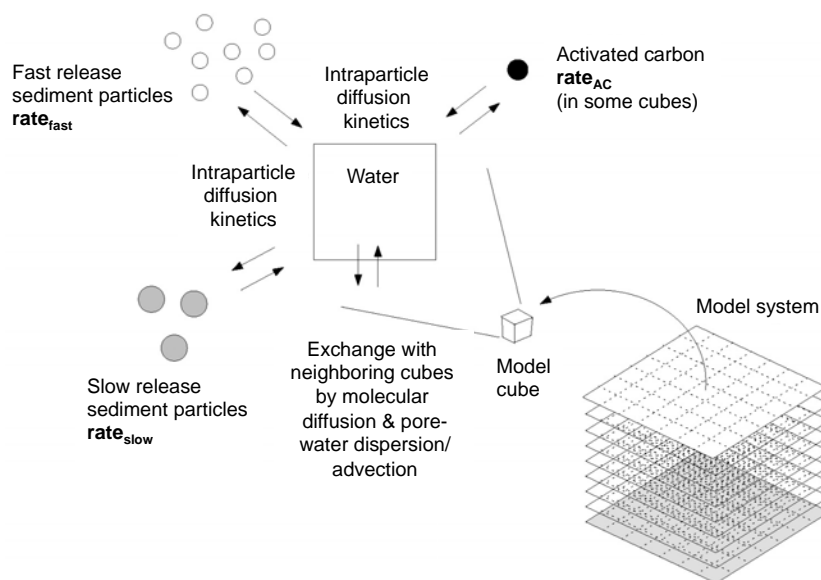


Figure 4. The conceptual framework for a model of HOC transport for a minimally mixed sediment system. Movement of contaminants between neighboring cubes can occur by molecular diffusion in pore-water, pore-water dispersion, or advective flow. There are three model system compartments: domains of fast release sediment particles, domains of slow release sediment particles, and AC, respectively. The parameters $rate_{fast}$, $rate_{slow}$, and $rate_{AC}$ are the PCB congener release rates (for slow and fast release sediment particles, s^{-1}) or uptake rate (for AC, s^{-1}).

The basic mass balance equation of the numerical model is shown below:

$$\begin{aligned} \frac{dS_{aq}(x, y, z, t)}{dt} = & D_{disp} \left[\frac{\partial^2 S_{aq}(x, y, z, t)}{\partial x^2} + \frac{\partial^2 S_{aq}(x, y, z, t)}{\partial y^2} + \frac{\partial^2 S_{aq}(x, y, z, t)}{\partial z^2} \right] \\ & - \frac{V_{sed}(x, y, z)}{V_{aq}} \cdot \frac{d}{dt} \left[3 \int_0^1 q^2 S_{sed_fast}(x, y, z, q, t) dq + 3 \int_0^1 q^2 S_{sed_slow}(x, y, z, q, t) dq \right] \\ & - \frac{V_{AC}(x, y, z)}{V_{aq}} \cdot \frac{d}{dt} \left[3 \int_0^1 q^2 S_{AC}(x, y, z, q, t) dq \right] - u_z \frac{\partial S_{aq}(x, y, z, t)}{\partial z} \end{aligned}$$

where V_j (cm^3) and S_j (g cm^{-3}) denote the total volume of each phase component in the cube and the volumetric pollutant concentration in that phase respectively, and q (-) the radial distance from the particle center divided by the particle radius. S_{sed_fast} (g cm^{-3}) is the amount of contaminant associated with rate_{fast} per total volume of sediment and S_{sed_slow} (g cm^{-3}) is the amount of contaminant associated with rate_{slow} per total volume of sediment. D_{disp} ($\text{cm}^2 \text{s}^{-1}$) denotes the dispersion coefficient, and u_z (cm d^{-1}) the pore-water velocity in z direction. The implementation of the intraparticle diffusion part of this model is based on the explicit numerical scheme described by Wu and Gschwend (1988).

Further expansion of the HOC mass transfer model framework is possible, which includes passive sapler phase (Choi, Cho et al. 2014), biouptake (Sun and Ghosh 2008), bioturbation (Lin, Cho et al. 2014), biodegradation (Werner, Ghosh et al. 2006), and sediment deposition and reworking (Lin, Cho et al. 2014).

4. Passive Sampling Technique.

Passive samplers are now widely accepted among researchers as a means to measure the freely dissolved aqueous concentration (C_{free}) of HOCs in a water body or sediment pore-water (Lohmann 2012). The passive sampling technique is generally less labor-intensive, more sensitive, and takes less amount of sample than direct measurement of aqueous concentration and maybe much more accurate than applying equilibrium partitioning approach using sediment concentration for the determination of C_{free} (ter Laak, Barendregt et al. 2006, Fernandez, MacFarlane et al. 2009, Lohmann and Muir 2010). Passive samplers preferentially accumulate hydrophobic contaminants from the aqueous phase they are put in contact, enabling highly sensitive detection of the contaminants in water (Hawthorne, Miller et al. 2009, Lohmann and Muir 2010, Hawthorne, Jonker et al. 2011). Initially, semi-permeable membrane devices (SPMDs) were proposed to mimic the bioconcentration of HOCs in aquatic environments (Huckins, Tubergen et al. 1990). More recently, single polymeric materials have become more popular because they are easier to prepare and analyze (Lohmann and Muir 2010). Low-density polyethylene (PE) is one of the most frequently used material as passive samplers because it is relatively inexpensive, readily available, robust, and easy to deploy in the field (Tomaszewski and Luthy 2008, Lohmann 2012).

At equilibrium, HOCs are believed to show linear partitioning between polymeric passive samplers and water (Adams 2002). Accordingly, the freely dissolved concentration of an HOC in water (C_{free} , ng L^{-1}) equilibrated with a PE sampler can be simply calculated as

$$C_{free} = C_{PE} / K_{PE} \quad (2.1)$$

where C_{PE} (ng kg⁻¹) is the concentration of an HOC in PE and K_{PE} (L kg⁻¹) is the PE-water partitioning coefficient.

In many cases, however, non-equilibrium sampling of HOCs may be needed because it is not always possible or practical to deploy a passive sampler until it attains equilibrium (Adams, Lohmann et al. 2007). For the non-equilibrium sampling, the kinetics of HOC uptake into PE should be taken account for the calculation of C_{free} . Under typical deployments in the water body or laboratory mixing, it is likely that the overall kinetics of compound uptake into PE is controlled by an aqueous boundary layer (Lohmann 2012). For the aqueous boundary layer-controlled uptake, the kinetics of HOC mass transfer between PE and water is described as (Huckins, Petty et al. 2006, Hale, Martin et al. 2010).

$$\frac{dC_{PE}}{dt} = \frac{2k_o}{x_{PE}} \left(C_{free} - \frac{C_{PE}}{K_{PE}} \right) \quad (2.2)$$

where k_o is the mass transfer coefficient (cm s⁻¹) for the aqueous boundary layer and x_{PE} is the PE thickness (cm).

For passive samplers deployed in the sediment bed, the HOC uptake kinetics is also a function of the compound desorption from sediments (Fernandez, MacFarlane et al. 2009). In this case, more complicated models may be needed to describe the HOC uptake kinetics over time. Several methods have been suggested to calculate C_{free} of the target compound by non-equilibrium sampling of the pore-water in sediment beds using performance reference compounds (PRCs) (Adams, Lohmann et al. 2007, Tomaszewski and Luthy 2008, Fernandez, MacFarlane et al. 2009). PRCs are analytically non-interfering compounds that are spiked into the passive sampler prior to deployment (Huckins, Petty et al. 2002). The PRC residual in a passive sampler is analyzed after deployment to deduce how close the system is towards equilibrium (Huckins, Petty et al. 2002). However, to date, researchers have not come into consensus which method is the most suited for the estimation of C_{free} in the sediment pore-water using the PRC approach.

IV. Materials and Methods

1. Prolonged effect of AC amendment (Task 9)

1.1. Prepare fully sequestered sediment by MAC amendment (Task 9.1)

1.1.1. Test with carbon-coated magnetic particles

The goal of task 9.1 was to contact sediment with carbonaceous sorbents or equivalent and then separate out the sorbent from the sediment to prepare sediment samples that is deprived of the readily available fraction of PCBs. For an initial attempt, carbonaceous materials with magnetic properties were used as sorbents. These materials are referred to as carbon-coated magnetic particles (CCMPs) instead of magnetic activated carbon (MAC) in this report, because the materials were produced by coating carbon onto magnetic particles.

Six different types of CCMPs were obtained from United Science Corporation (Center City, MN). The properties of the CCMPs are summarized in Table 1. The carbon contents were measured using a Carlo Erba NA-1500 elemental analyzer, and the specific surface area was either provided by the manufacturer or measured in the laboratory by a BET method. The magnetic response of the particles was tested by an electromagnet in the laboratory. Based on the properties, COIF1, the carbon covered iron filings, was selected as the most appropriate material for the study.

Table 1. Properties of the CCMPs provided by United Science Corporation.

Material ID	Description	Carbon content (%)	Specific surface area (m ² /g)	Magnetic response
IAIO	Carbon covered on a porous 10% iron oxide/90% alumina compact	18.2	165.3	Weak
COIO2	Carbon covered on iron oxide particles	0.9	0.69	Strong
IA5SD1	Carbon covered on a porous 5% iron oxide/95% alumina compact	20.9	179.7	Weak
COIF1	Carbon covered on iron filings	13.9	13.7	Strong
BFCoA7	Carbon covered on porous alumina	9.6	102.4	Weak
NBFCoA1	Carbon and nitrogen deposited on porous alumina	4.2	147.6	Weak

Preliminary tests to check the recovery of the selected CCMP from sediment was conducted by adding the particles into sediment slurry and i) vigorously shaking the slurry for one minute for a brief check and then ii) mixing the slurry on a horizontal shaker at 150 rpm for one month for recovery after a longer time period. After the mixing, the magnetic particles were separated from the slurries using an electromagnet as shown in Figure 1. The collected magnetic particles were weighed to determine the weight recovery with respect to the CCMP initially added.



Figure 5. Separation of CCMPs from sediment slurry. Left: collection from the sediment slurry, center: washing the collected particles with deionized water, right: collection of washed particles.

1.1.2. Test with Tenax bead as a model sorbent

As will be described in Results and Discussion (section 1.1.1), the CCMPs did not qualify for preparing PCB-sequestered sediment because of their poor recovery from sediment slurry. Instead, Tenax beads (60-80 mesh; Supelco, Bellefonte, PA) were selected as a model sorbent to remove readily available PCB fraction from the sediment. In 40 mL vials, 1 g of dry wt. sediment collected from Hunters Point Shipyard and 1 g of Tenax beads were mixed together. The vials were filled with water with 30 ppt salinity containing 1 g/L NaN_3 to inhibit microbial activity, and mixed at 100 rpm. After 1 day, the Tenax beads were collected and replenished with new beads to ensure that the beads were not overloaded with PCBs released from sediment. After 28 days of mixing, the Tenax beads were collected, and the vials containing the remaining sediment slurry were used for further treatment as described in section 1.2. The collected Tenax beads were analyzed to determine the amount of PCBs removed from the sediment. Considering the number of samples needed for the PCB repartitioning test, a total of 15 vials containing Tenax bead-treated (i.e., PCB sequestered) sediment slurry were prepared. Additional 15 vials containing sediment slurry that is not treated with Tenax beads was also prepared. The untreated slurries were mixed at 100 rpm for 28 days.

1.2. PCB repartitioning test with sorbent-removed sediment (Task 9.2)

The goal of task 9.2 was to study whether significant repartitioning of PCBs occur in the PCB sequestered sediment. Here, PCB repartitioning refers to the movement or shift of PCBs from slow releasing fraction, which will remain in sediment after sorbent treatment, to fast releasing fraction because of the PCB mass transfer that occur following selective sorbent removal. Significant PCB repartitioning will result in recovery of PCB bioavailability, which can be an unfavorable outcome due to the loss of sorbent from sediment after the sorbent treatment showed effectiveness.

The vials containing PCB sequestered or untreated sediment slurry were continuously shaken up to 12 months to allow contact among sediment particles and water. After 0, 1, 3, 6, and 12 months, triplicate vials each of the PCB sequestered and untreated samples were retrieved. One gram of Tenax beads was added to each vial, and shaken at 100 rpm for 1 day. The vials were then retrieved again and the Tenax beads were collected to determine 1-day Tenax bead uptake for PCBs. One-day Tenax uptake is frequently used to determine the availability of hydrophobic organic contaminants in sediments (Mackenbach, Jing et al. 2012, Harwood, Landrum et al. 2013). The remaining sediment slurry was added with 1 g of clean Tenax beads, and shaken for additional 27 days. The Tenax beads were collected after the mixing, the amount of PCBs in the beads was analyzed, and this amount was added to the 1-day Tenax uptake to determine 28-day Tenax uptake. The 28-d Tenax uptake was used as a supplementary indicator of PCB availability.

At the end of the test, the PCBs remaining in the sediment were determined to complete the PCB mass balance in each sample.

2. Standardization of field monitoring method using PE samplers (Task 10)

2.1. Assess potential anisotropic exchange kinetics in PE (Task 10.1)

Laboratory tests were conducted to compare the PCB exchange kinetics for PE in water for both directions, water to PE (i.e., PCB uptake in PE) and PE to water (i.e., PCB release from PE).

For the PCB PE release kinetic study, PCB-preloaded PEs were prepared by the following procedure. A cocktail solution of PCBs in hexane (9 µg of PCB 29, 69, 103 and 155, and 3 µg PCB 192) was spiked into a bottle containing 100 mL 80/20 methanol/water solution. After adding ten pieces of PE (51 µm thickness, Brentwood Plastics (St. Louis, MO)) cut in 2.5 cm × 2.5 cm, the bottle was rolled at 2 rpm for 7 days. The PCB-preloaded PEs were then retrieved, wiped clean, and collected in a 40 mL vial containing 30 mL deionized water. The vials was mixed for 24 hours to allow any residual methanol in PE to release out into the water.

The PCB-preloaded PEs were then contacted with Tenax beads (60-80 mesh; Supelco, Bellefonte, PA) to study the PCB release kinetics from PE. In triplicate 40 mL vials filled with

DI water containing 0.1 g/L sodium azide, one piece of PE (approximately 0.04 g) and 0.5 g of Tenax beads were added. The vials were shaken on a horizontal shaker at 100 rpm. The beads were sampled and replenished by new beads 5 hours, and 1, 5, 29, 50, and 80 days after the initial contact. After 125 days, both the Tenax beads and the PE were collected. The amount of PCBs in the Tenax beads collected at different times and the remaining amount of PCBs in PE were analyzed.

To study the PCB uptake kinetics into PE in water, 9 g of PE preloaded with the nine PCB congeners (PCB 29, 69, 103, 155, and 192) was prepared. In triplicate 40 mL vials, five small strips of clean PE (0.015 g each, 0.075 g total) were contacted with a sufficiently large amount (3 g) of the preloaded PE such that the preloaded PE can act an infinite source of the five PCB congeners for the clean PE strips. The small PE strips were collected at 5 hours, and 1, 5, 25, 50, 80, and 125 days to measure the uptake of PCBs.

2.2. Investigate alternative PE kinetic method (Task 10.2)

The performance reference compound (PRC)-based method is most frequently used to apply non-equilibrium method using polymeric passive samplers to assess the pore-water HOC concentrations in sediments. Recognizing the potential anisotropic PCB exchange kinetics in PE-water system in section 2.1 in Results in Discussion, efforts were undertaken to investigate a non-equilibrium passive sampling method using PE as an alternative to the PRC-based method.

The alternative non-equilibrium passive sampling method used PE with different thicknesses to assess the kinetic state of the PE either deployed in the field or applied in laboratory experiments. The idea of using passive samplers with different thicknesses for non-equilibrium passive sampling was suggested by Dr. Danny Reible at Texas Tech University as briefly introduced in Reible and Lotufo (2012) for polydimethylsiloxane (PDMS) fibers. However, no peer-reviewed articles are yet published in the literature to demonstrate the detailed concept and application methods.

2.2.1. Concept of an alternative non-equilibrium passive sampling method.

The underlying concept of the alternative non-equilibrium passive sampling method is that the compound uptake data for passive samplers with n different thicknesses at a certain time point will provide the same information on the kinetic approach to equilibrium as the data for passive samplers with a certain thickness at n time points provide. This is illustrated in Figure 3. At the linear phase, the contaminant uptake is proportional to the mass flux of the contaminant into the passive sampler (Flux) and time, but not a function of sampler thickness (θ). This can be observed by either linear contaminant uptake over time or constant contaminant uptake with different sampler thicknesses. At the stationary phase, the contaminant uptake is proportional to the sampler mass or volume (V), but not a function of time. This can be observed by either constant contaminant uptake over time or contaminant uptake proportional to sampler thicknesses. At the transition phase, the sampler uptake is a non-linear function of time, sampler surface area (A), and sampler thickness (θ), which can be observed by a non-linear increase in contaminant uptake with time or sampler thickness.

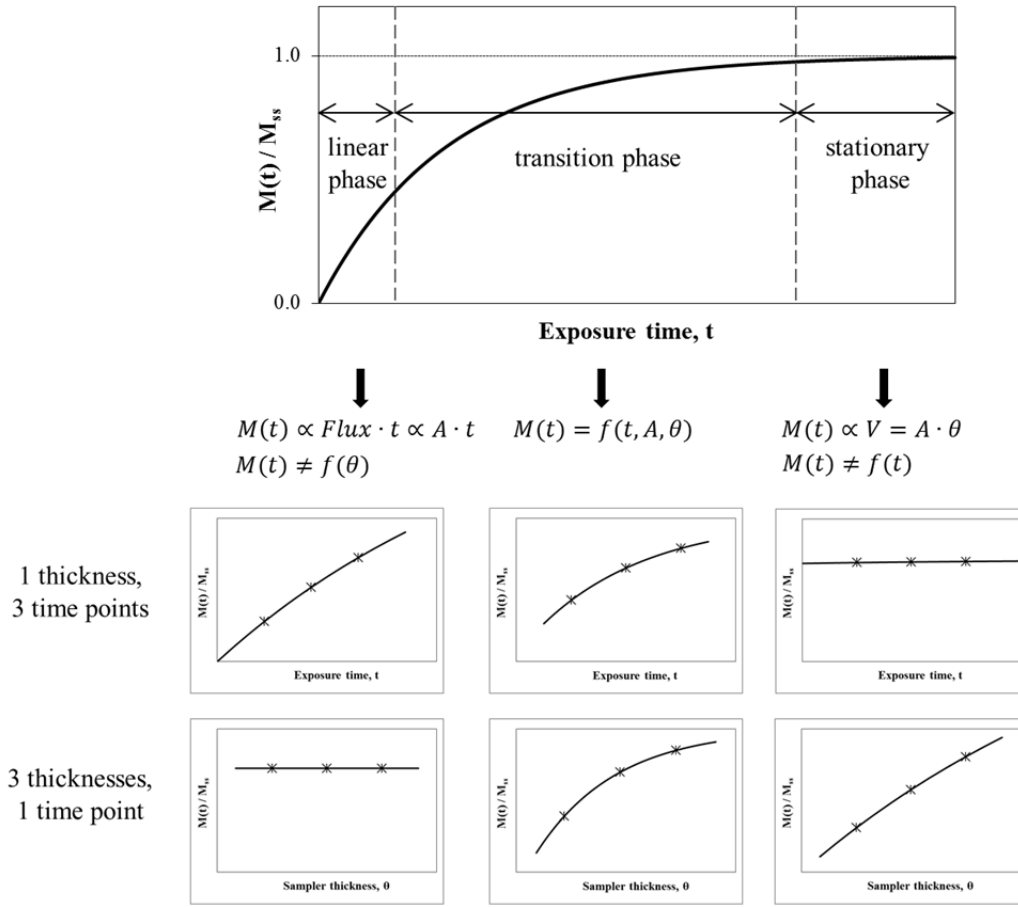


Figure 6. General temporal trend of contaminant uptake into passive samplers and its observation using passive sampling using a certain sampler thickness with three time points and using three sampler thicknesses with a certain time point.

If the contaminant uptake kinetics into passive samplers is expressed as a function of sampler thickness, time, and a kinetic constant, then the sampler uptake data for multiple sampler thicknesses at a certain exposure time can be used to derive the kinetic constant. Then the equilibrium passive sampler concentration can be calculated by the derived kinetic constant and the sampler uptake data. With the equilibrium passive sampler concentration and the passive sampler-water partitioning coefficient for the target contaminant, the equilibrium aqueous concentration can be determined. Therefore, the development of the alternative non-equilibrium passive sampler method involves the development of a kinetic model that best reproduces the compound uptake kinetics for passive samplers deployed in sediment.

2.2.2. Experimental design for method development.

To support the development and experimentally validate the alternative passive sampling method, PE kinetic experiments in quiescent sediment were conducted. PEs with different thicknesses (17, 51, and 102 μm) were obtained from Husky Plastics (Thornhill, ON). The PEs with different thicknesses were preloaded with PCB 29, 69, 103, 155, and 192 in a single batch of 80/20 (v/v) methanol/water solution. These are the PCB congeners used as PRCs in a previous study (Tomaszewski and Luthy 2008) because they are not frequently detected in PCB-contaminated sediment. PE with 51 μm thickness obtained from Brentwood Plastics (St. Louis, MO) was also added in the batch to compare the PCB concentrations loaded in the PE to those loaded in Husky PEs. The K_{PES} for the 51 μm Brentwood PE are available in Choi, Cho et al. (2013) for 100 PCB congeners. An extended preloading time of 17 days was applied for the current test (cf. 2 days in Tomaszewski and Luthy (2008)) to ensure equilibrium for the thickest PE used. Then, the PRC-spiked PEs were collected, wiped to remove solvent, and stored at 4°C until use. Triplicate 2.5 cm \times 2.5 cm pieces of the PRC-spiked PEs for each type of PE were sampled to determine the PRC concentrations initially spiked to PE.

For the sediment contact with PE in quiescent condition, 60 mL jars were half-filled with Hunters Point sediment (see Figure 7). One piece of the PRC-spiked PE cut in 2.5 cm \times 2.5 cm was carefully applied on the sediment so as not to cause any significant agitation of the sediment directly, and to promote contact with PE and remove air pockets at the same time. After PE was placed, the sediment was carefully added to fill the jar. The tests were prepared in triplicate for each contact time and PE thickness. The jars were stored at 20°C until sampling. At sediment-PE contact times of 1, 4, 16, 64, 132, and 264 days, triplicate jars for PE with each thickness were retrieved and the PEs embedded in sediment were collected for PCB analysis. In addition to the PRCs (i.e., PCB 29, 69, 103, 155, and 192), PCB 43, 101, 153, and 180, representing tetra-, penta-, hexa-, and hepta-chlorinated PCB homolog groups, respectively, were analyzed and used as model compounds because of the relative abundance of these congeners in Hunters Point sediment.

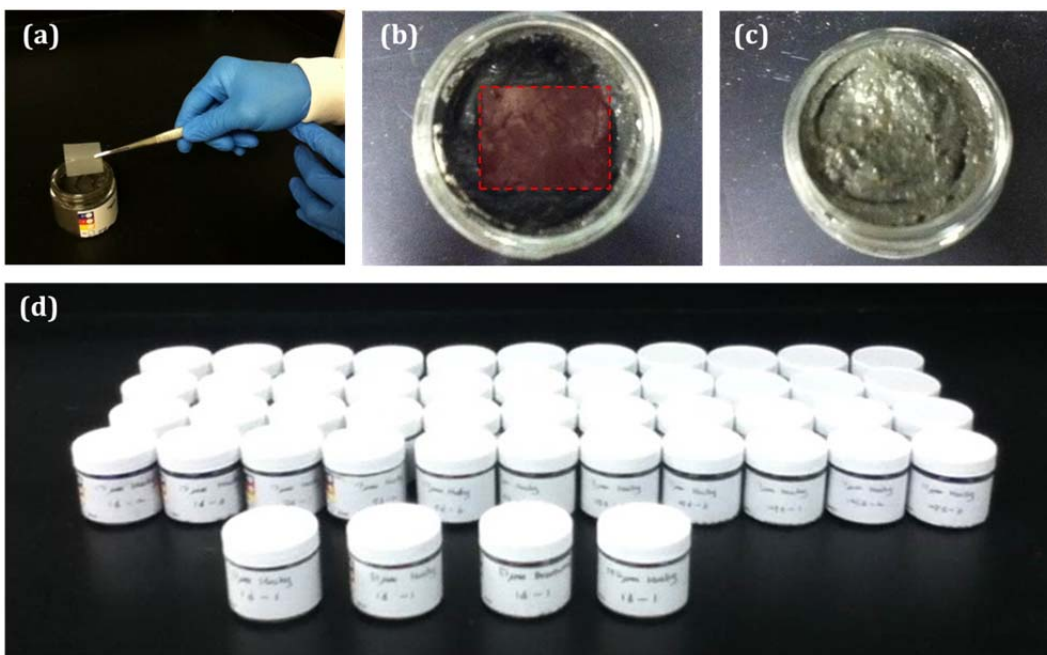


Figure 7. Preparation of the PE kinetic experiments in quiescent sediment: (a)(b) addition of a PE sampler in a 60 mL-jar half-filled with sediment collected from Hunters Point (PE is highlighted in red in (b) for visualization), (c) the 60 mL-jar filled to the top with the sediment, and (d) the whole test set-up with triplicate jars for each time point and type of PE.

To determine the PE concentrations of the model PCB congeners 43, 101, 153, and 180 in equilibrium with sediment, a slurry phase experiment was conducted. In a 250 mL jar, 120 g dry wt. sediment was placed, and artificial seawater with 30 ppt salinity was added to have a final sediment to water ratio of 1:1.5. Sodium azide was added to prevent microbial activity. Approximately 15 mg each of the different types of PEs (i.e., 17, 51, and 102 μm Husky PEs and 51 μm Brentwood PE) spiked with PRCs were added. The jars were prepared in triplicate. The jars were hand-mixed vigorously to disperse the sediment and placed in a shaker. The samples were shaken for 125 days at 100 rpm. After the shaking, the PEs were collected from the jars and analyzed for concentrations for the five PRCs and four model congeners. The residual amount of the PRCs after the shaking was less than 10% of the initial amount spiked for all combinations of PCB congeners and PE types. From the PE kinetic experiments conducted in Task 10.1, it was shown that the PCB release kinetics are somewhat slower than the uptake kinetics, so disappearance of PRCs from PE to near completeness ensures that the PCB uptake from sediment to PE approached close to equilibrium.

3. Develop user-friendly standalone program for HOC mass transfer model (Task 11)

3.1. Standalone program beta version development (Task 11.1)

Upon the request from the SERDP office, a standalone tool for the HOC mass transfer model was developed in subtask 11.1. The current model written in MATLAB[®] codes requires the MATLAB[®] software for execution, which will generate additional cost for the users. Therefore, we develop an executable program of the HOC mass transfer model using MATLAB Compiler[™] (<http://www.mathworks.com/products/compiler/?refresh=true>). The compiled application created with MATLAB Compiler[™] can be run on a royalty-free software called MATLAB Compiler Runtime[™].

3.2. Improve user friendliness of HOC mass transfer model (Task 11.2)

Along with standalone program development, we put efforts on the enhancement of user friendliness of the HOC mass transfer model. Enhancement and newly added features are below.

- I/O data file was revised so that model parameter input is minimal and intuitive for users.
- a graphic user interphase (GUI) was built for I/O data file loading, so users can avoid working directly with complex MATLAB codes.
- a progress bar was added, and combined into GUI to monitor simulation progress. This feature is important for long-term simulation (e.g. 10 years simulation)
- a error/exception handling systems was included in the model code, so to detect and prevent adverse system parameters and invalid inputs.
- User manual for the standalone program was prepared to give step-by-step instructions for installation, running, and trouble shooting

On the standalone HOC mass transfer model program, we asked for feedback from collaborators who were involved in the model development, and volunteer testers who generally have minimal knowledge of MATLAB and in-situ AC work. The beta version program was tested for user-friendliness as well as performance. Any reported bugs were fixed, and suggestions on the user-friendliness were considered for the program updates.

3.3. Develop booklet for exemplary modeling results

3.3.1. Study sites and model input parameters.

Ten sediment sites in the U.S. and Europe were selected to study the effectiveness of in-situ AC amendment using the HOC mass transfer model. These sites were selected based on the availability of site- and HOC-specific model input parameters. The site characteristics, contaminant information, and the model input parameters were obtained from previous reports in the literature for each site (Jonker and Koelmans 2002, Zimmerman, Ghosh et al. 2004, Werner, Higgins et al. 2005, Werner, Ghosh et al. 2006, Tomaszewski, Werner et al. 2007, You, Landrum et al. 2007, Sun and Ghosh 2008, Hale, Tomaszewski et al. 2009, Hale, Kwon et al. 2010, Hale and Werner 2010, Werner, Hale et al. 2010, Choi, Cho et al. 2013, Choi, Cho et al. 2014, Lin, Cho et al. 2014). The study sites exhibited a range of sediment total organic carbon (TOC) and black carbon (BC) contents, types of major HOCs of concern (PCBs, PAHs, and DDTs), HOC

release rates, and other sediment characteristics. Two or three representative HOCs were selected from each site based on their relative abundance and the availability of the HOC mass transfer model input parameters from the literature.

3.3.2. Model assumptions and execution

Using the model input parameters obtained from the literature, the HOC mass transfer model was run for the representative model HOCs for each site. It was assumed that the AC with a particle size range of 75-300 μm (geometric mean radius of 75 μm) was used for all sites. The average AC dose for the whole model system was set at 1.5 times the sediment TOC with an upper limit of 5% sediment dry weight. A well-mixed AC dose of 1-2 x TOC was shown to be effective for controlling HOC bioavailability in laboratory experiments (Zimmerman, Werner et al. 2005, Choi, Cho et al. 2013). Although still not completely understood as to mechanisms, several studies reported adverse effects of AC amendments on sediment biota at high AC dose (Jonker, Suijkerbuijk et al. 2009, Kupryianchyk, Reichman et al. 2011, Janssen, Choi et al. 2012, Meynet, Hale et al. 2012, Janssen and Beckingham 2013). Based on approximate AC doses at which adverse effects are not observed in those studies, 5% sediment dry weight was chosen as a maximum AC dose for assessment in this work.

For the unmixed module, the cube side-lengths were specified as 225 μm , which were three times the geometric mean radius of AC. The three-dimensional model system had a depth of 15 cm and a horizontal dimension of 0.225 cm x 0.225 cm (10 x 10 cubes). The vertical dimension represented the potential mixing depth of AC with sediment, which encompasses the bioactive layer of sediment (Beckingham and Ghosh 2011). The horizontal dimension was minimized to save computation time while not affecting the model outputs. The AC distribution in the model system was assumed to follow the characteristic AC distribution found in a pilot study at Hunters Point Shipyard, CA (Cho, Werner et al. 2012).

The mass transfer model was run for a simulation time of 1 min for brief mechanical mixing using the mixed module followed by a simulation time of 15 years using the unmixed module for AC-sediment contact during a prolonged stagnant phase. Average pore-water HOC concentration in the model system was obtained as an indicator of the effectiveness of AC amendment from the model.

3.3.3. Developing booklet for modeling results for the case study sites

The booklet was organized to show general site characteristics and contaminant information, model input parameters, and modeling results in a site-by-site manner. This allows readers to select the site that is most similar to the site of their interest, review the model input parameters for details, and then check the modeling results.

V. Results and Discussion

1. Prolonged effect of AC amendment (Task 9)

1.1. Prepare fully sequestered sediment by MAC amendment (Task 9.1)

1.1.1. Test with carbon-coated magnetic particles

The recovery of the selected CCMPs (ID: COIF1) after a brief, one-minute mixing was approximately 90%. However, after one month contact, the recovery was reduced to 75% of the initial amount added to the sediment slurry, suggesting that the magnetic responsiveness of the particles got weaker. The possible explanations for the weak magnetic response after the one month contact are that i) the surface of the particles was covered by colloids and macromolecules and ii) the magnetic property was reduced or lost by redox reactions. Based on the preliminary tests, it was determined that the CCMPs were not appropriate to be used as a test material.

1.1.2. Test with Tenax bead as a model sorbent.

Tenax beads were finally selected as a model sorbent to prepare fully sequestered sediment owing to their easiness to separate from sediment slurries by flotation. By the contact between the Tenax beads and the sediment in a slurry phase and subsequent removal of the Tenax, a total of 15 PCB-sequestered sediment slurries were prepared. The fraction of PCBs sequestered by this process (i.e., removed from the sediment slurries by sorption to the Tenax) for three model PCB congeners, 101, 153, and 180, ranged from 14 to 23% of the total amount in the original sediment (Table 2). Significant amounts of the model PCB congeners were found to still remain in the sediment after the PCB sequestration process.

Table 2. Fraction of model PCB congeners sequestered (i.e., removed) from sediment slurries after treatment by Tenax beads ($n=15$, average \pm standard deviation).

Model PCB congeners	PCB 101	PCB 153	PCB 180
Fraction sequestered by Tenax treatment	0.23 \pm 0.08	0.20 \pm 0.07	0.14 \pm 0.05

1.2. PCB repartitioning test with sorbent-removed sediment (Task 9.2)

While only fractions of 14-23% of the model PCB congeners were removed from the PCB-contaminated sediment by the PCB sequestration process, a substantial reduction in the PCB availability, determined by 1-d and 28-d Tenax uptake was immediately after the PCB sequestration (i.e., 0 month contact). The results shown in Figure 8 indicate that the 1-d Tenax uptakes were reduced by 95-97% for the model congeners by the PCB sequestration compared to the untreated cases. The 28-d Tenax uptakes were reduced by 83-87%. These data show that the sorbent treatment effectively controls the PCB availability by selectively removing the relatively easily available fraction of the PCB congeners from sediment.

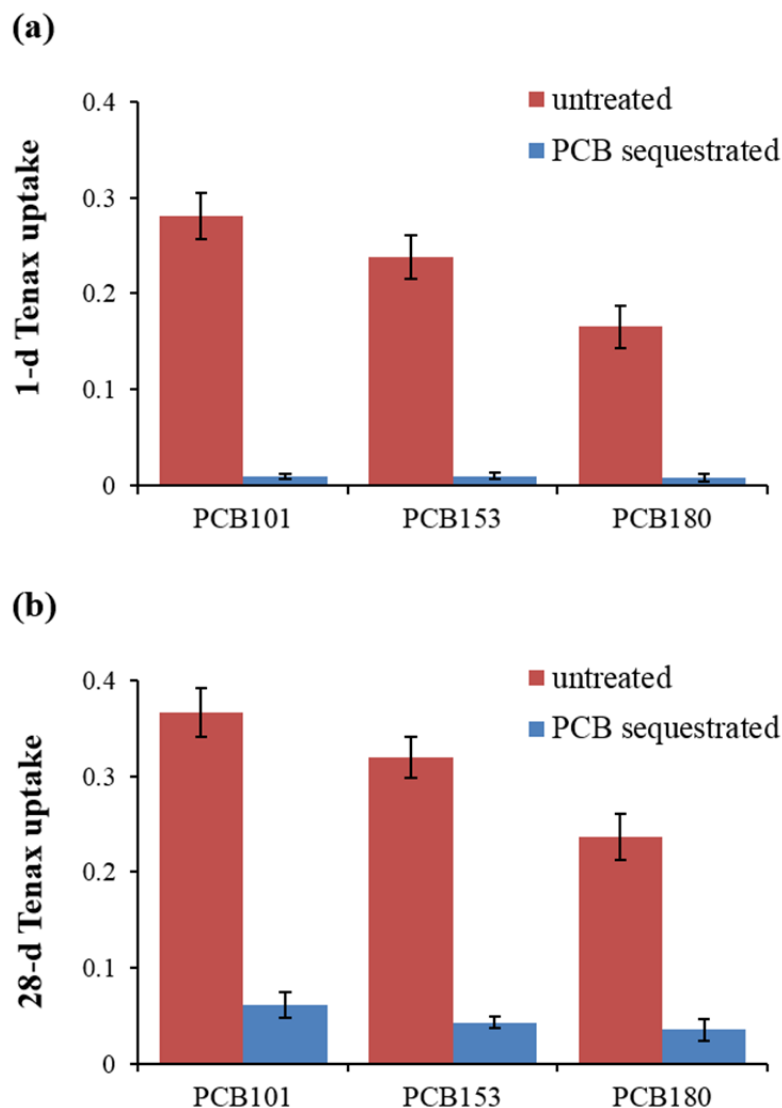


Figure 8. Comparison of (a) 1-d and (b) 28-d Tenax uptake immediately after the PCB sequestration (0 month contact) to the untreated cases.

The fractions of the 1- and 28-d Tenax uptakes relative to the total amount of PCBs in the initial sediment is plotted against the mixing time of the PCB sequestered sediment in Figure 9 and Figure 10. The results showed that the 1- and 28-d Tenax uptakes for the sorbent-treated samples somewhat increased after mixing in a slurry phase for 1 month (Two-way ANOVA for 0 month and 1 month mixing, three model compounds, $p < 0.05$). The fraction of 1-d Tenax uptakes for 0 month mixing were 0.008-0.009 while those for 1 month mixing were 0.034-0.037 for the three model compounds. However, the Tenax uptakes did not show further increase by more extensive period of mixing. After 12 months of mixing, the fraction of 1-d Tenax bead uptakes were in the range of 0.023-0.036, which were 88-92% lower than those for the untreated controls. Similarly, the fraction of 28-d Tenax bead uptakes after 12 months of mixing were considerably lower (by 79-87%) than those for the untreated controls.

These results showed that when sorbent is selectively lost from the sorbent-treated sediment by winnowing, the repartitioning of contaminants may occur to some degree, but the repartitioning process is neither prolonged nor substantial to cause significant loss of the treatment effectiveness. Even with an extensive period of mixing of sorbent-deprived sediment in a slurry phase after sorbent treatment and removal, the available fraction of PCBs in the sediment, as estimated by 1- and 28-d Tenax bead uptakes, maintained to be substantially lower than those for the untreated sediment.

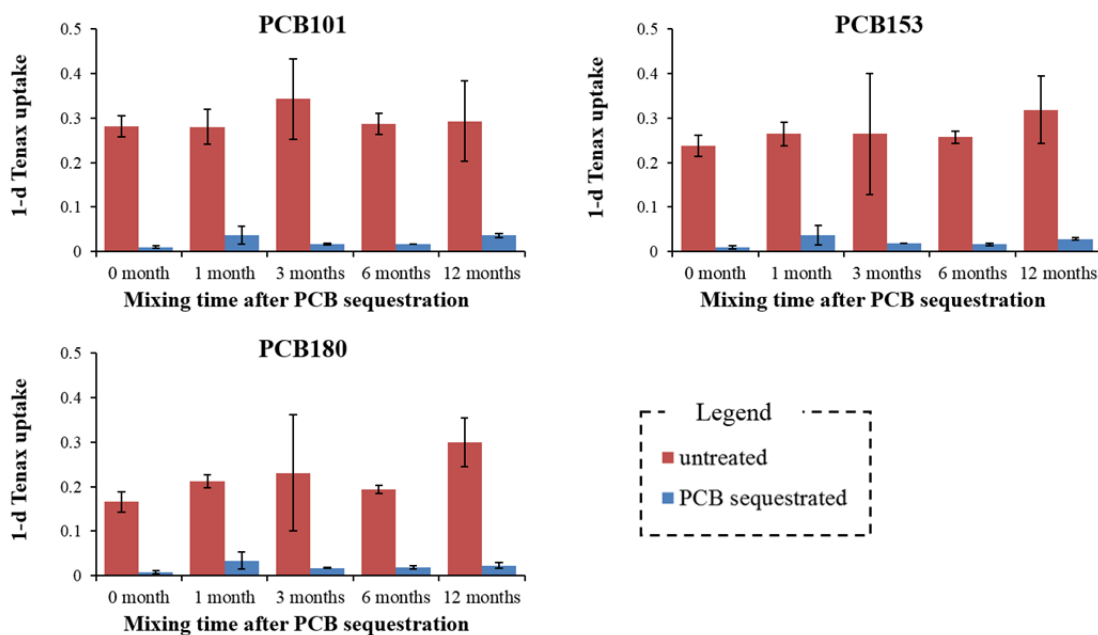


Figure 9. One-day (1-d) Tenax uptake shown as relative amount to the total PCB mass for the model PCBs applying different times of mixing after PCB sequestration.

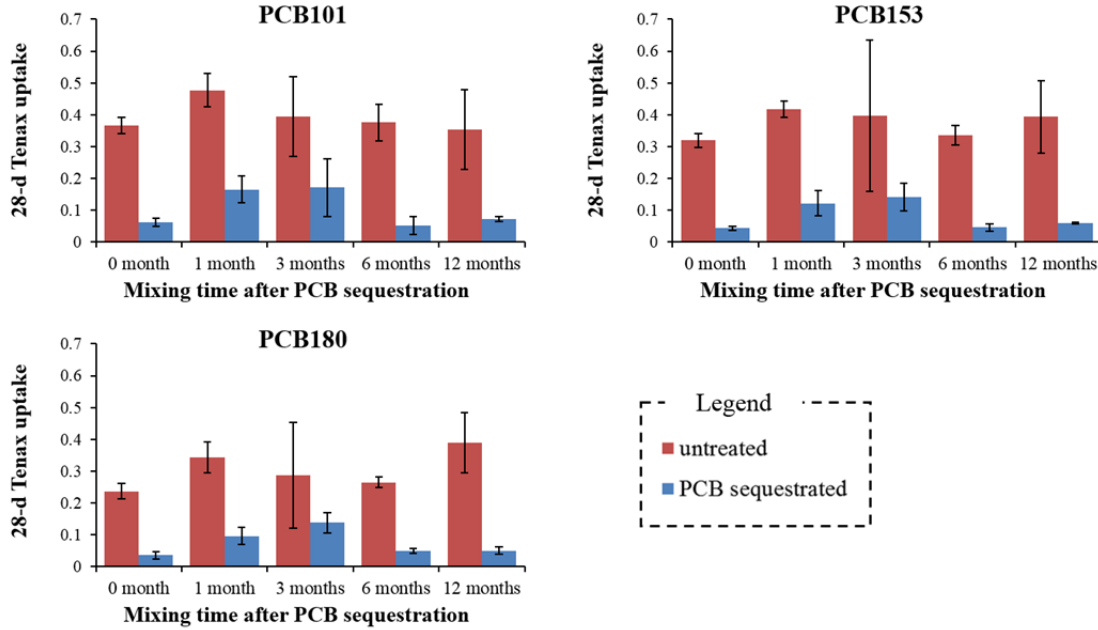


Figure 10. Twenty-eight-day (28-d) Tenax uptake shown as relative amount to the total PCB mass for the model PCBs applying different times of mixing after PCB sequestration.

2. Standardization of field monitoring method using PE samplers (Task 10)

2.1. Assess potential anisotropic exchange kinetics in PE (Task 10.1)

The experimental results for PCB uptake and release kinetics of PE in water are plotted in Figure 11 for five PCB congeners, PCB 29 (tri-), 69 (tetra-), 103 (penta-), 155 (hexa-), and 192 (hepta-chlorinated). As expected, the experimental results showed that less-chlorinated PCB congeners exhibited faster kinetics than higher-chlorinated congeners. In the current experiment, which was a well-mixed system with no external mass transfer resistance (i.e., kinetics depend only on PCB exchange between water and PE), the tri-chlorinated congener PCB 29 reached 95% of equilibrium within two days. On the other hand, for the hepta-chlorinated congener PCB 192, it took more than 100 days to reach 95% of equilibrium.

The kinetic test results were fitted to the following first-order model that is generally used to describe the compound exchange kinetics between water and passive samplers (Booij, Hofmans et al. 2003, Huckins, Petty et al. 2006, Adams, Lohmann et al. 2007):

Uptake kinetics:

$$C_{PE,t} = C_{PE,eq}[1 - \exp(-k_e t)] \quad (1)$$

Release kinetics:

$$C_{PE,t} = C_{PE,0} \exp(-k_e t)$$

where $C_{PE,t}$ (ng/g) is the PCB concentration in PE at time t (hr); $C_{PE,eq}$ (ng/cm³) is the equilibrium PCB concentration in PE at equilibrium, which is equivalent to the concentration in the excessive amount of preloaded PE added in the uptake kinetic experiment; C_{PE0} is the initial PCB concentration in PE, which is equivalent to the preloaded PE PCB concentration initially added in the release kinetic experiment, and k_e (1/hr) is the first-order exchange rate constant. As shown in Figure 11, the results for the PCB uptake and release kinetic experiments fitted well with the first-order model.

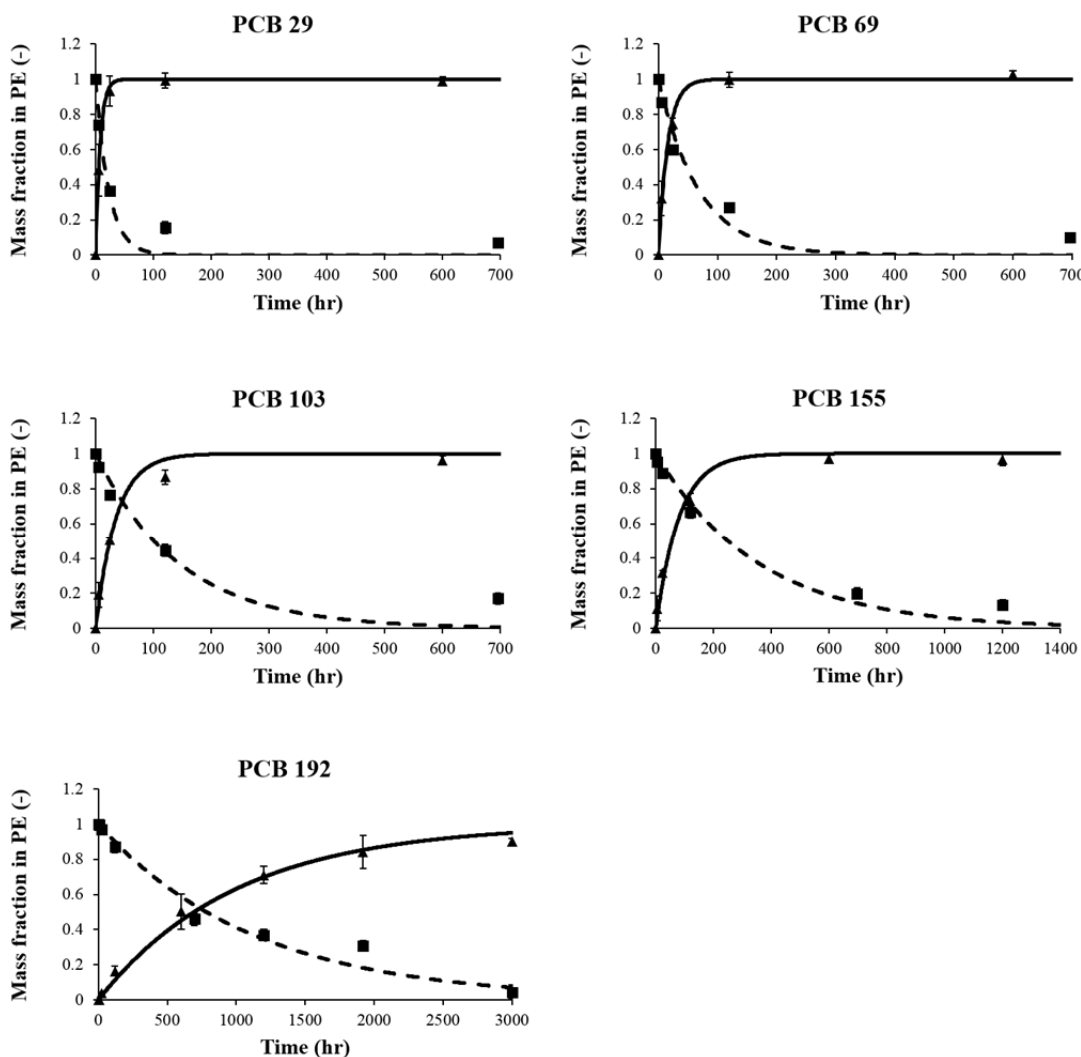


Figure 11. Uptake and release kinetics of five PCB congeners for PE in water. The triangles and squares are experimental results for uptake and release kinetics, respectively. The solid and dashed lines are fitted data using first-order model for uptake and release kinetics, respectively. Note the different scales in x-axis for different PCB congeners.

The first-order uptake and release rate constants for the five PCB congeners from the best-fit regression curves in Figure 11 are shown in Table 3. Comparison of the uptake and release rate constants determined in this study suggested that the uptake of PCBs into PE was

somewhat faster than the release from PE. The uptake rate constants were consistently greater than the release constants by an average factor of two (Table 3). These results indicated that there is a possibility of anisotropic exchange kinetics in PE (i.e., non-identical kinetics for compound uptake into and release from PE). This casted doubts on the performance reference compound (PRC)-based methods for non-equilibrium sampling of PCBs whose underlying assumption is the isotropic exchange kinetics in PE.

Table 3. First-order kinetics constants for PCB uptake and release in PE.

Model Compound	First-order kinetic constant (hr⁻¹)		Constant ratio (A/B)
	uptake (A)	release (B)	
PCB 29	0.129	0.044	2.92
PCB 69	0.0631	0.0146	4.32
PCB 103	0.0285	0.0069	4.14
PCB 155	0.0125	0.00028	4.48
PCB 192	0.00114	0.00089	1.13

2.2. Investigate alternative PE kinetic method (Task 10.2)

2.2.1. PE-water partitioning coefficients for different types of PEs.

The concentrations of the PRCs preloaded in PEs from 80:20 (v:v) methanol:water solution showed slight difference among the PEs with different thicknesses and from different manufacturers. The PRC concentrations for 51 μm and 102 μm Husky PEs were not significantly different from each other (Two-way ANOVA, $p>0.1$; see Figure 12). The concentrations for 17 μm Husky PE were slightly lower than those for other Husky PEs (Two-way ANOVA, $p<0.01$), presumably because of the slight difference in the additives applied or plastic structure. The concentrations for 51 μm Brentwood PE were slightly lower than those for 51 μm Husky PE (Two-way ANOVA, $p<0.01$).

The concentrations of the model PCB congeners after equilibrating with Hunters Point sediment in a slurry phase showed similar results (Figure 13). The model congener concentrations for 51 μm and 102 μm Husky PEs were not significantly different (Two-way ANOVA, $p>0.1$), while those were different from 17 μm Husky PE (Two-way ANOVA, $p<0.05$). The model PCB congener concentrations for 51 μm Brentwood PE were slightly lower than those for 51 μm Husky PE (Two-way ANOVA, $p<0.05$).

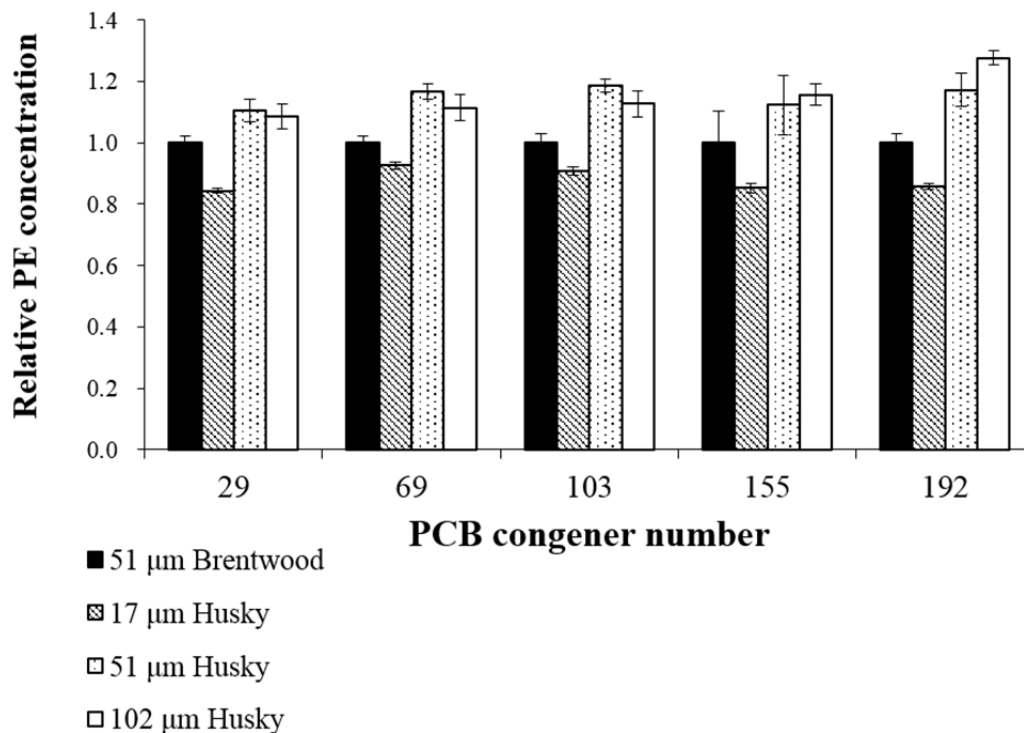


Figure 12. Concentrations of PCB PRCs, congeners 29, 69, 103, 155, and 192 in different types of PEs after equilibrating in a single batch of 80:20 (v:v) methanol:water solution. The data are shown as the concentration in each type of PE relative to that in 51 μ m Brentwood PE.

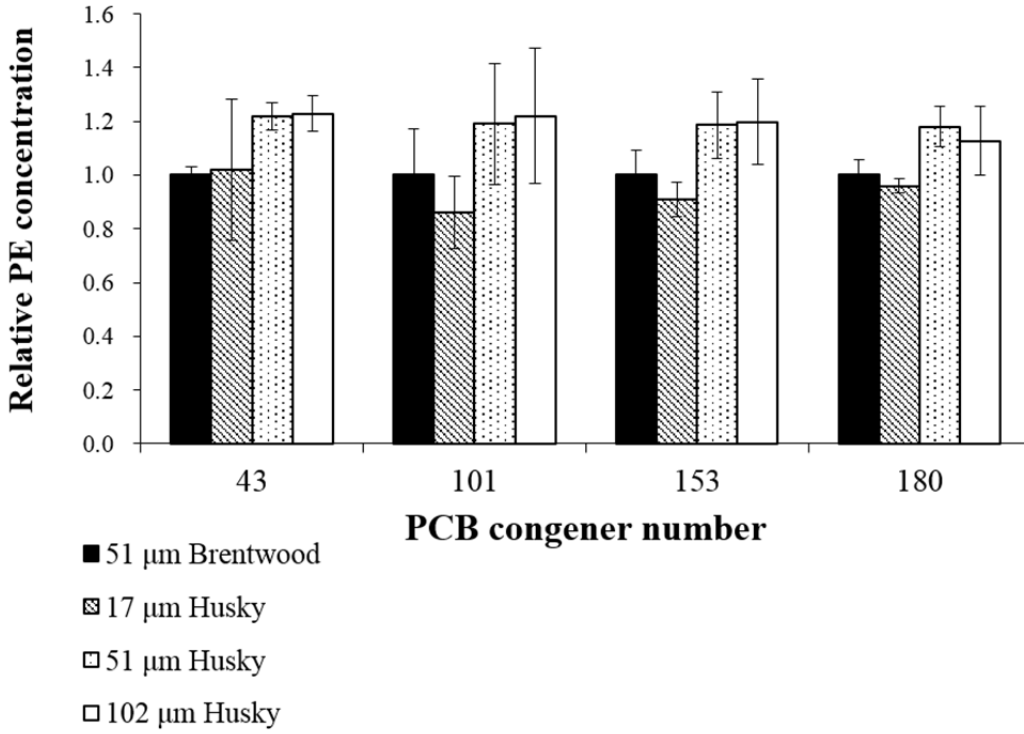


Figure 13. Concentrations of PCB model congeners, 43, 101, 153, and 180 in different types of PEs after equilibrating in a single batch of Hunters Point sediment in a slurry phase. The data are shown as the concentration in each type of PE relative to that in 51 μm Brentwood PE.

The PE-water partitioning coefficients (K_{PE}) for the PRCs and model congeners are available at a salinity of 30 ppt only for 51 μm Brentwood PE in Choi, Cho et al. (2013). Using the literature values as a reference, the K_{PE-w} values for 17, 51, and 102 μm Husky PEs were determined by the following relationship:

$$\frac{K_{PE,i}}{K_{PE,ref}} = \frac{C_{PE,eq,i}}{C_{PE,eq,ref}} = \frac{C_{PE(mw),eq,i}}{C_{PE(mw),eq,ref}} \quad (2)$$

where i and ref represent the type of PE of interest (i.e., 17, 51, and 102 μm Husky PEs) and that used as a reference (i.e., 51 μm Brentwood PE), respectively, and $C_{PE,eq}$ and $C_{PE(mw),eq}$ are the PE concentration at equilibrium in aqueous and methanol:water solution, respectively. By the calculation, the K_{PE} values for 17, 51, and 102 μm Husky PEs were determined as shown in Table 4.

Table 4. Logarithm of K_{PE} values determined for different types of PEs used in this study.

PCB congener#	51 μm Brentwood ¹	17 μm Husky	51 μm Husky	102 μm Husky
29	5.44 \pm 0.06	5.37 \pm 0.05	5.48 \pm 0.05	5.48 \pm 0.05
69	5.78 \pm 0.08	5.75 \pm 0.07	5.85 \pm 0.07	5.83 \pm 0.07
103	6.19 \pm 0.10	6.16 \pm 0.09	6.27 \pm 0.09	6.25 \pm 0.09
155	6.61 \pm 0.24	6.58 \pm 0.19	6.70 \pm 0.19	6.71 \pm 0.19
192	6.98 \pm 0.06	6.92 \pm 0.06	7.05 \pm 0.06	7.09 \pm 0.06
43	5.69 \pm 0.05	5.70 \pm 0.11	5.78 \pm 0.05	5.78 \pm 0.06
101	6.19 \pm 0.06	6.12 \pm 0.08	6.27 \pm 0.09	6.28 \pm 0.10
153	6.73 \pm 0.01	6.69 \pm 0.03	6.81 \pm 0.04	6.81 \pm 0.05
180	7.02 \pm 0.07	7.01 \pm 0.07	7.08 \pm 0.07	7.08 \pm 0.08

¹Determined by Choi, Cho et al. (2013).

2.2.2. PCB uptake kinetics in quiescent sediment

The PCB uptake kinetics for congeners 43, 101, 153, and 180 in quiescent sediment is plotted in Figure 14. The results are shown as the PE concentration at each contact time relative to the equilibrium PE concentration determined by the slurry phase experiments ($C_{PE}(t)/C_{PE,eq}$). The results suggested that it takes at least more than a year for the model congeners to approach close to equilibrium (e.g., $C_{PE}(t)/C_{PE,eq} > 0.95$) under quiescent conditions. Even for the least chlorinated congener (PCB 43, tetra-chlorinated) and the thinnest PE (17 μm), the $C_{PE}(t)/C_{PE,eq}$ value was 0.53 after 264 days of contact. This indicated that it is not practical to apply equilibrium PE sampling methods for in situ pore-water measurement for PCBs with more than three substituted chlorines. The PCB uptake kinetics was slower for the more chlorinated congeners. For PCB 180 (hepta-chlorinated), the $C_{PE}(t)/C_{PE,eq}$ value was 0.09 for 17 μm PE after 264 days of contact.

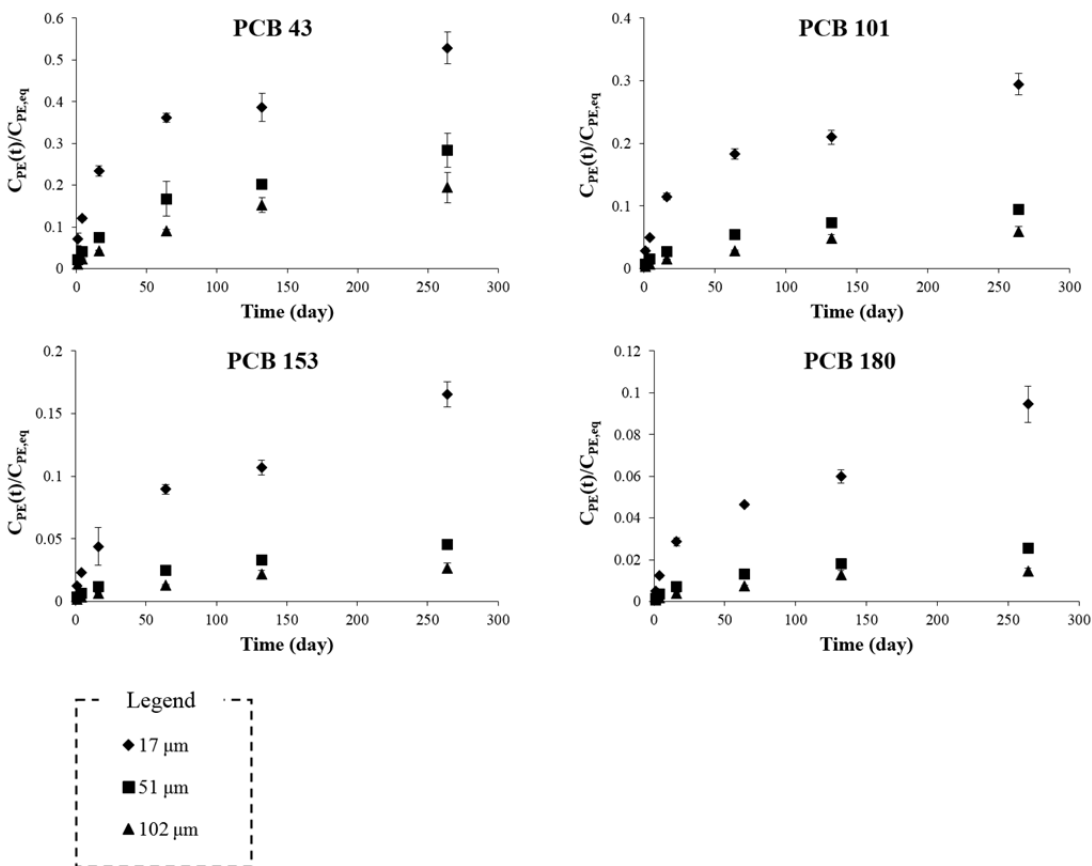


Figure 14. PCB uptake kinetics for model PCB congeners 43, 101, 153, and 180 measured in experiments under quiescent contact between sediment and PE.

As expected, the PCB uptake kinetics was a function of PE thickness. The thinner the PE was, the faster the PCB uptake kinetics was. The ratio of $C_{PE}(t)/C_{PE,eq}$ values for 17 μm PE to the values for 51 and 102 μm PE are shown in Table 5. The data showed that for congeners 153 and 180, the ratios maintained around 3 for 51 μm PE and 6 for 102 μm PE throughout the study. As the thickness ratios between 51 μm and 17 μm , and 102 μm and 17 μm are 3.0 and 6.0, respectively, this indicated that the uptake kinetics for congeners 153 and 180 were at linear state of uptake (see Figure 6 in section 2.2.1 in Materials and Methods) for a contact time of 264 days. As seen in Figure 6, the PE concentration should be inversely proportional to the PE thickness in the regions where the linear uptake kinetics applies. For PCB 43, the ratio of $C_{PE}(t)/C_{PE,eq}$ values for 17 μm PE to the values for 51 and 102 μm PE got significantly less than 3 and 6, respectively, after 64 days of contact. This indicated that the uptake kinetics was at transient state for PCB 43 between 64 and 264 days. For PCB 101, the ratio of $C_{PE}(t)/C_{PE,eq}$ values for 17 μm PE to the values for 102 μm PE got significantly less than 6 after 132 days, while the ratio for 17 μm and 51 μm PEs was around 3 for the entire contact time studied.

Table 5. The ratio of $C_{PE}(t)/C_{PE,eq}$ values for 17 μm PE to the value for the corresponding PE (i.e., $[C_{PE}(t)/C_{PE,eq}]_{17\mu\text{m}}/[C_{PE}(t)/C_{PE,eq}]_{x\mu\text{m}}$, x =thickness for the corresponding PE) for the PCB uptake kinetics in quiescent sediment.

Contact time (d)	PCB 43		PCB 101	
	51 μm	102 μm	51 μm	102 μm
1	3.35 \pm 0.75	6.31 \pm 1.45	4.12 \pm 0.83	7.74 \pm 1.66
4	2.99 \pm 0.20	5.32 \pm 0.45	3.33 \pm 0.27	6.97 \pm 1.02
16	3.15 \pm 0.17	5.42 \pm 0.30	4.25 \pm 0.21	7.65 \pm 0.43
64	2.16 \pm 0.54	3.97 \pm 0.20	3.39 \pm 0.40	6.47 \pm 0.44
132	1.92 \pm 0.17	2.53 \pm 0.36	2.86 \pm 0.22	4.32 \pm 0.56
264	1.86 \pm 0.30	2.72 \pm 0.54	3.11 \pm 0.32	4.95 \pm 0.74
Contact time (d)	PCB 153		PCB 180	
	51 μm	102 μm	51 μm	102 μm
1	3.64 \pm 0.69	6.34 \pm 1.26	3.72 \pm 0.99	6.74 \pm 1.73
4	3.42 \pm 0.30	6.64 \pm 0.86	3.46 \pm 0.40	6.81 \pm 0.98
16	3.64 \pm 1.25	6.56 \pm 2.28	4.12 \pm 0.28	7.32 \pm 0.74
64	3.65 \pm 0.39	6.92 \pm 0.49	3.54 \pm 0.30	6.33 \pm 0.42
132	3.26 \pm 0.24	4.92 \pm 0.69	3.35 \pm 0.21	4.68 \pm 0.77
264	3.63 \pm 0.32	6.20 \pm 1.03	3.70 \pm 0.38	6.44 \pm 0.81

The idea of using different thicknesses of PE for non-equilibrium passive sampling is to use the ratio of accumulated PE concentration at time t for thickness i and j ($C_{PE}(t)_i/C_{PE}(t)_j$) to assess the state of PCB uptake kinetics at time t , and then calculate the equilibrium PE concentration for PE with thickness of either i or j . At linear uptake state, the $C_{PE}(t)_i/C_{PE}(t)_j$ value reduces to the following trivial solution:

$$C_{PE}(t)_i/C_{PE}(t)_j = \frac{K_{PE,i}\theta_{PE,j}}{K_{PE,j}\theta_{PE,i}} \quad (3)$$

Therefore, the suggested non-equilibrium passive sampling method cannot be applied at linear uptake state.

2.2.3. Modeling PCB uptake kinetics in quiescent sediment.

The development of a non-equilibrium passive sampling method involves a development of a compound uptake kinetic model in a passive sampler. The compound uptake kinetic model is used to derive equilibrium aqueous concentrations from the passive sampler uptake data measured at a non-equilibrium state. To find a PCB uptake kinetic model in PE that most appropriately describe the uptake kinetics observed in the experiments, several models were tried.

Firstly, it was assumed that the PCB uptake kinetics follow a first-order model described in (Booij, Hofmans et al. 2003, Huckins, Petty et al. 2006):

$$C_{PE,t} = C_{PE,eq}[1 - \exp(-k_e \cdot t)] \quad (4)$$

where k_e (d^{-1}) is the exchange rate constant. This model was shown to match well with the experimental results for PCB uptake kinetics in PE from aqueous solutions in this study (section 2.1). The exchange rate constant can be further described as (Huckins, Petty et al. 2006)

$$k_e = \frac{A_{PE}k_o}{V_{PE}K_{PE}} = \frac{2k_o}{K_{PE}} \cdot \frac{1}{\theta_{PE}} \quad (5)$$

where A_{PE} and V_{PE} are the PE surface area (cm^2) and volume (cm^3), respectively; k_o is the mass transfer coefficient at the interface (cm/s); K_{PE} is the dimensionless PE-water partitioning coefficient (cm^3 water/ cm^3 PE); and θ_{PE} is the PE thickness (cm). According to Booij, Hofmans et al. (2003), k_o can be described as a function of K_{ow} , which is an inherent property of the target analyte.

For PCB 43, the experimental data for 17 μm PE was used to obtain the k_o value, and the value was used to obtain modeling results for all PE thicknesses. The modeling results are compared to the experimental results in Figure 15. The data showed that the first-order kinetic model did not appropriately predict the uptake kinetics for PCB 43 in quiescent sediment. The simulation results underestimated the rate of uptake for PCB 43 at earlier phase of the experiment and overestimated the rate at later phase for 17 μm PE. The simulation results for 51 and 102 μm PEs underestimated the rate of uptake for all contact times studied in the experiment.

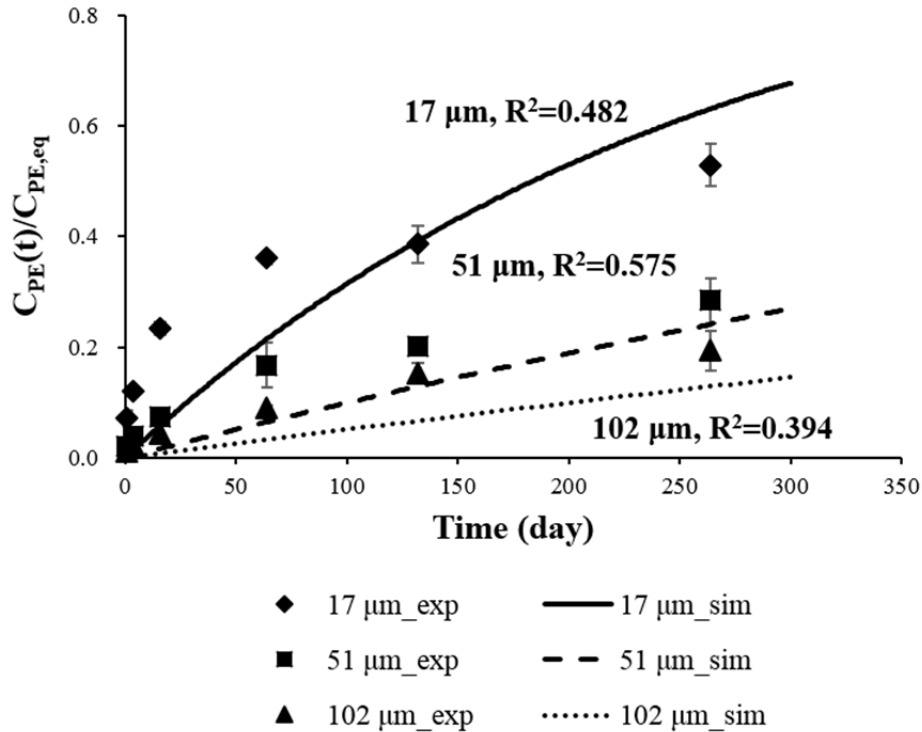


Figure 15. Comparison of the simulation results using first-order kinetic model and the experimental results for the uptake kinetics in PE for PCB 43 in quiescent sediment.

Secondly, a 1-D diffusion model developed by Fernandez, MacFarlane et al. (2009) was employed to simulate the uptake kinetics in PE for PCB 43 in quiescent sediment. For a PE of thickness $2l$ (cm) and semi-infinite sediment on both sides, the PCB mass transfer can be expressed as (Fernandez, MacFarlane et al. 2009)

$$\partial C_{PE}/\partial t = D_{PE} \partial^2 C_{PE}/\partial x^2, \quad -l < x < l \quad (6)$$

$$\partial C_{sed}/\partial t = D_{sed} \partial^2 C_{sed}/\partial x^2, \quad x < -l \text{ and } x > l \quad (7)$$

with the following boundary conditions:

$$C_{sed}/C_{PE} = K_{sed/PE} = K_d/K_{PE}, \quad x = -l \text{ and } x = l \quad (8)$$

$$D_{PE} \partial C_{PE}/\partial x = D_{sed} \partial C_{sed}/\partial x, \quad x = -l \text{ and } x = l \quad (9)$$

$$D_{PE} \partial C_{PE}/\partial x = 0, \quad x = 0 \quad (10)$$

where C_{PE} (ng/g) and C_{sed} (ng/g) are the concentrations in PE and sediment, respectively; D_{PE} (cm²/s) and D_{sed} (cm²/s) are the diffusivity within PE and sediment, respectively; $K_{sed/PE}$ (g PE/g sediment) is the sediment-PE partitioning coefficient; and K_d (cm³ water/g sediment) is the sediment-water distribution coefficient. The D_{PE} values for PCBs are available in the literature and the D_{sed} values can be determined as

$$D_{sed} = (1 + r_{sw} K_d)^{-1} D_w / \tau \quad (11)$$

where r_{sw} (g solid/cm³ water) is the solid-to-water ratio; D_w (cm²/s) is the aqueous diffusivity; and τ is tortuosity. The tortuosity is assumed to be equal to the porosity of the sediment.

Using the D_{sed} value obtained from eq. (11), eqs. (6)-(10) were numerically solved to simulate the uptake kinetics in 17 μ m PE for PCB 43. The modeling results in Figure 16 showed that the 1-D diffusion model significantly overestimated the uptake kinetics for PCB 43 observed in the experiment.

The overestimation of the uptake kinetics for PCB 43 in the 1-D diffusion model can be attributed to the overestimation of D_{sed} value by eq. (11). D_{sed} is a parameter that represents the PCB mass transfer kinetics in the sediment side. The modeling results suggested that the kinetics within PE did not affect the PCB uptake kinetics in PE. The simulation results for PE concentration at any position of the PE were within 1% at any time point. This indicated that once the compound entered the sediment-PE interphase, it was almost readily distributed throughout the PE thickness due to rapid mass transfer within PE. Therefore, the uptake kinetics for PCB 43 should be almost solely dependent on the mass transfer in the sediment side.

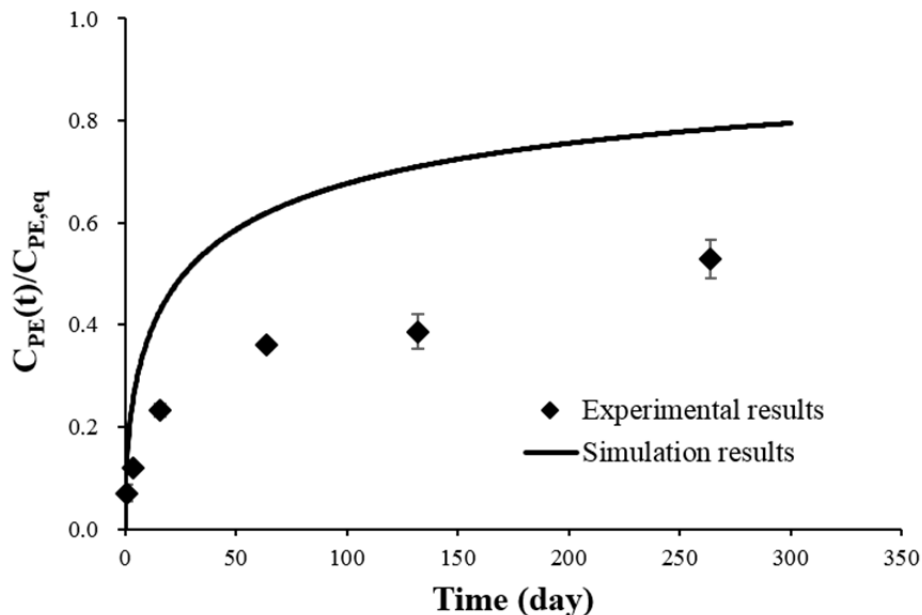


Figure 16. Comparison of the simulation results using 1-D diffusion model and the experimental results for the uptake kinetics in 17 μm PE for PCB 43 in quiescent sediment.

Lastly, a modified 1-D diffusion model was used to simulate the PCB uptake kinetics in PE. According to the results of the 1-D diffusion model that showed overestimation of the D_{sed} value by eq. (11), the D_{sed} value was determined using the best-fit numerical solution of eqs. (6)-(10). The D_{sed} value for PCB 43 obtained from the best-fit solution was $8.1 \times 10^{-12} \text{ cm}^2/\text{s}$, which was almost two orders of magnitude smaller than the value of $6.3 \times 10^{-10} \text{ cm}^2/\text{s}$ obtained by eq. (11). The best-fit numerical solution using the modified 1-D diffusion model matched very well with the experimental results for 17 μm PE ($R^2 = 0.969$). However, the modeling results somewhat underestimated the uptake kinetics in 51 and 102 μm PE. At 264 days of contact, the modeling results were 22% and 38% smaller than the experimental results for 51 and 102 μm PEs, respectively.

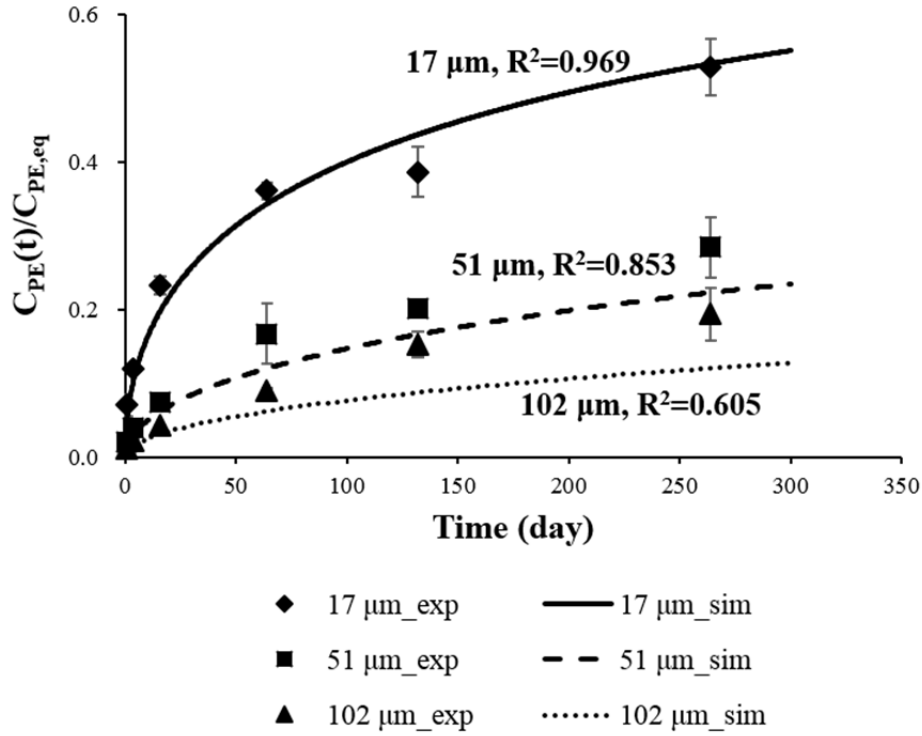


Figure 17. Comparison of the simulation results using a modified 1-D diffusion model and the experimental results for the uptake kinetics in PE for PCB 43 in quiescent sediment.

The PCB mass transfer process involved in PCB uptake kinetics in PE would be more complicated than that assumed in the 1-D diffusion model. Both the mass transfer kinetics within the sediment particles and the sediment pore-water should play roles in the amount of PCBs available at the PE-sediment interphase. The difference between the modeling results using the modified 1-D diffusion model and the experimental results suggested that modeling errors can be significant when the PCB mass transfer kinetics in sediment is represented by a single kinetic parameter, D_{sed} .

Despite the deviation of the modeling results from the experimental results observed in 51 and 102 μm PEs, the modified 1-D diffusion model matched closest to the experimental results among the three models studied. However, there is a limitation for the application of the modified 1-D diffusion model for non-equilibrium PE sampling using different PE thicknesses. To develop a simple method to calculate equilibrium PE concentrations from the non-equilibrium PE sampling method, the kinetic model is best described as an analytical solution. An analytical solution for the 1-D diffusion model is given in (Fernandez, Harvey et al. 2009), but it is applicable only when the following condition is valid

$$t \ll l^2/D_{PE} \quad (12)$$

For PCB 43 ($D_{PE}=1.0 \times 10^{-9} \text{ cm}^2/\text{s}$) and for 17 μm PE ($l=0.00085 \text{ cm}$), the l^2/D_{PE} value is only 12 minutes. Therefore, the analytical solution cannot be applied for PE exposure

conditions. For the numerical solution used in this study, each model run took approximately 10 days for PCB 43. It was estimated that at least 100 simulation runs are needed to apply the numerical solution to calculate equilibrium PE concentrations from the non-equilibrium PE sampling data. Therefore, it is not practical to use the numerical solution for the modified 1-D diffusion model for non-equilibrium PE sampling.

2.2.4. Applying PRC method for non-equilibrium PE sampling

Instead of the suggested alternative non-equilibrium PE sampling method, the currently available PRC-based method was used to estimate equilibrium PE concentrations in the quiescent sediment experiments. Assuming that the behavior of the target analyte and the PRC is identical and the isotropic exchange kinetics is valid in quiescent sediment, the equilibrium PE concentration for the target analyte i can be calculated as (Tomaszewski and Luthy 2008, Fernandez, Harvey et al. 2009)

$$C_{PE,eq,i} = \frac{C_{PE,i}(t)}{C_{PE0,PRC} - C_{PE,PRC}(t)} \cdot C_{PE0,PRC} \quad (13)$$

where $C_{PE,eq,i}$ (ng/g) is the equilibrium PE concentration for target analyte i ; $C_{PE0,PRC}$ (ng/g) is the initial PE concentration for PRC; and $C_{PE,i}(t)$ and $C_{PE,PRC}(t)$ (ng) are the concentrations in PE at time t for the target analyte and PRC, respectively.

The PRC release kinetics observed in the experiments are shown as the PE concentration at time t relative to the initial PE concentration for the PRCs ($C_{PE}(t)/C_{PE0}$) in Figure 18. As observed in the PCB uptake kinetics, the release kinetics was faster for the less chlorinated congeners and for the thinner PE.

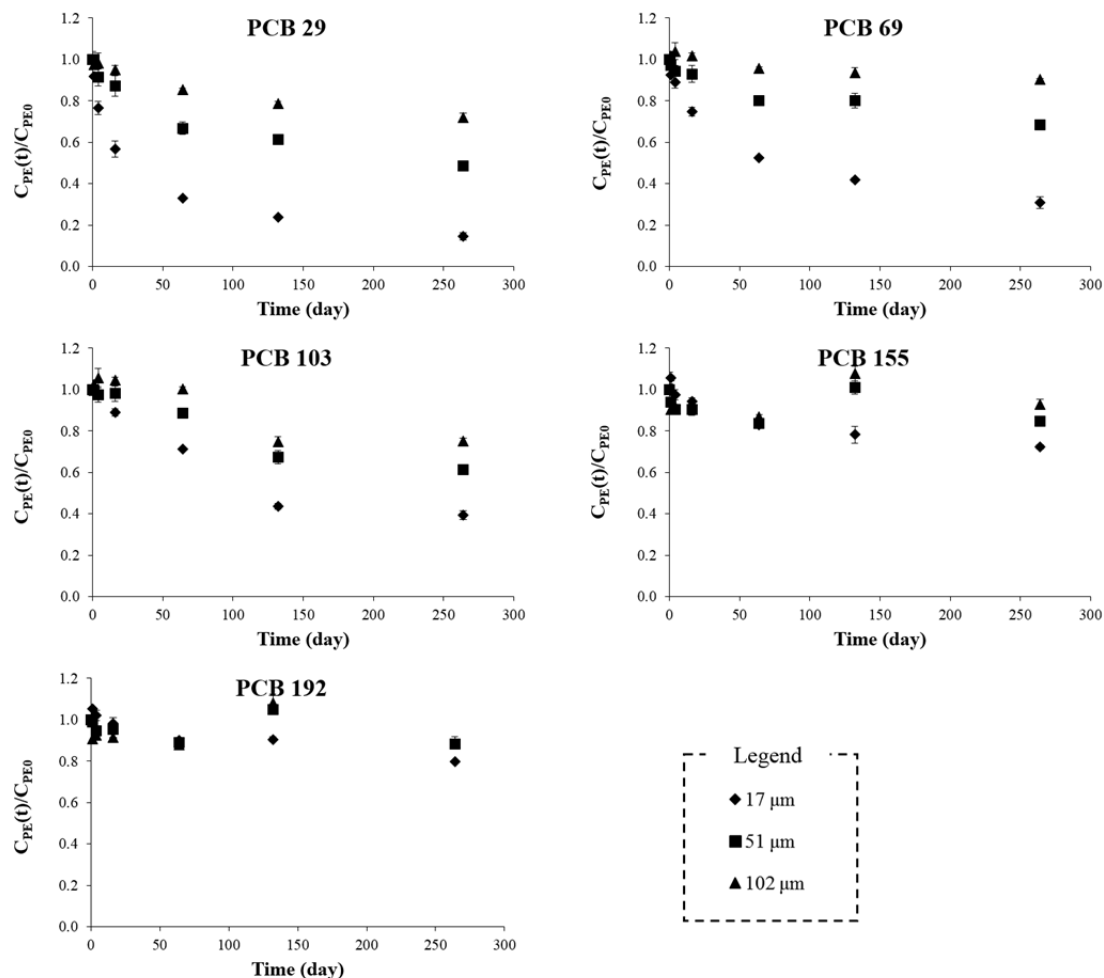


Figure 18. Release kinetics for PCB PRCs, congeners 29, 69, 103, 155, and 192, from PE in quiescent sediment.

The PRC data were used to calculate the equilibrium PE concentrations for model congeners 43, 101, 153, and 180. A PRC with the same chlorination level were used for each model congener (i.e., congener 69 for 43, 103 for 101, 155 for 153, and 192 for 180). From the entire data set for the quiescent sediment experiments, the standard error among replicates was determined to be 2.6%. By statistical analysis, it was calculated that the $C_{PE(t)PRC}/C_{PE0,PRC}$ should be less than 0.85 to ensure less than $\pm 50\%$ error at 95% confidence level. Therefore, only the cases showing $C_{PE(t)PRC}/C_{PE0,PRC}$ values of less than 0.85 were used for the calculation.

Table 6. The equilibrium PE concentrations ($C_{PE,eq}$) determined by the PRC method using data at various contact times and PE thicknesses for model congeners 43, 101, 153, and 180. The equilibrium PE concentrations directly measured by a slurry phase test are shown for comparison.

$C_{PE,eq}$ determination	Calculated by PRC method at each contact time				Measured by slurry phase test
Contact time (d)	16	64	132	264	
Target analyte: PCB 43					
17 μ m	75.5	62.0	54.2	62.5	81.7
51 μ m	NA	82.0	99.2	87.4	97.7
102 μ m	NA	NA	NA	NA	98.5
Target analyte: PCB 101					
17 μ m	NA	1560	917	1200	2470
51 μ m	NA	NA	769	674	3410
102 μ m	NA	NA	674	832	3500
Target analyte: PCB 153					
17 μ m	NA	4090	3830	4650	7790
51 μ m	NA	1530	NA	3056	10200
102 μ m	NA	NA	NA	NA	10300
Target analyte: PCB 180					
17 μ m	NA	NA	NA	4500	9620
51 μ m	NA	NA	NA	NA	11800
102 μ m	NA	NA	NA	NA	11300

NA: Not available because of $C_{PE(t)PRC}/C_{PE0,PRC}$ values equal to or greater than 0.85.

For PCB 43, the PRC method reasonably predicted the equilibrium PE concentrations. The equilibrium PE concentrations determined by the PRC method within 40% of the values directly measured by the slurry phase test (Table 6). However, for more chlorinated congeners, the equilibrium PE concentrations determined by the PRC method showed larger deviation from the directly measured values. In some cases, the PRC method predicted smaller values than the directly measured equilibrium PE concentrations by a factor of 5 or greater. Generally, the PRC method underestimated the equilibrium PE concentrations compared to the direct measurement.

For PCB 101, 153, and 180, the differences between the measured and calculated equilibrium PE concentrations were smaller for 17 μ m PE than 51 and 102 μ m PEs. For 17 μ m PE, the calculated concentrations were 37-63% of the measured values. For 51 and 102 μ m PEs, the calculated concentrations were only 15-30% of the measured values.

In sum, the comparison between the equilibrium PE concentrations determined by direct measurement and the PRC method suggested that better accuracy of the PRC-based prediction can be obtained for less chlorinated congeners and for PE with thinner thickness. For highly chlorinated congeners (more than 5 chlorine substitutions) and for relatively thick PE, the PRC-based prediction may significantly underestimate the equilibrium PE concentrations. It should be noted that these conclusions are based on relatively small set of data, and more studies should

be needed to investigate the accuracy of the PRC method for different PCB congeners and PEs with different thicknesses. This is because in quiescent sediment systems the desorption of very strongly hydrophobic compounds may proceed slower than the diffusion of PRCs from polyethylene.

3. Develop user-friendly standalone program for HOC mass transfer model (Task 11)

3.1. Standalone program beta version development (Task 11.1)

First, the MATLAB[®] source code of the HOC mass transfer model was transformed to an alpha version of a standalone executable file by MATLAB Compiler[™] on the Microsoft Windows platform (Figure 19). For short-term and long-term simulations, this alpha ver. program was proven to be functional without critical bugs. Major new features for upgrading to the beta version were identified as input UI (user interphase) and status bar.

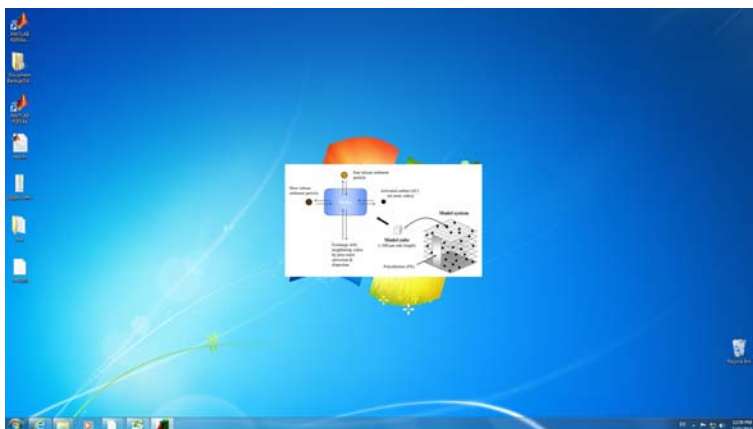


Figure 19. Screenshot of the splash screen of the standalone HOC mass transfer model (alpha version).

The beta version program is equipped with GUI (graphical user interphase), message boxes, and a status bar. The GUI enables users to choose their I/O spreadsheet, and run the program. Soon after, a message box will pop up indicating the simulation start and an estimated simulation time. A separate status bar will show the progress of the simulation. At completion of the simulation, another message box will notify the completion to the user. Users can edit their input parameters of a contaminant of their concern in the I/O spreadsheet, and view the simulation results after the simulation.

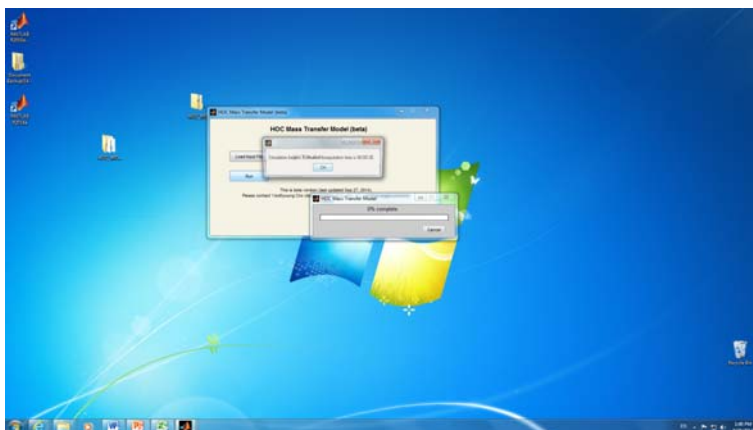


Figure 20. Screenshot of the beta version standalone HOC mass transfer model GUI (input UI, message bar, and progress bar)

3.2. Improve user friendliness of HOC mass transfer model (Task 11.2)

As planned in the Materials and Methods section, the user friendliness of the HOC mass transfer model was greatly improved by GUI and other features. Notable changes in I/O file, source code, and user manual are shown below.

I/O file

- Previously, the “Data Input” form required initial pore-water concentration of the model compound (C_{aq0}). Now, in the revised form, users will be asked to submit sediment concentration (C_{sed0}). For typical field sites, sediment concentration is expected to be more easily available than equilibrium aqueous concentration.
- Unit of pore-water velocity has been changes from cm/s to cm/d (more frequently used unit).

MATLAB source code

- The source code has been revised to detect invalid or unrealistic input parameters, and to suggest user-side correction on the I/O file (Figure 21). This will also prevent unstable or endless model runs. For the purpose, an acceptable range or a condition for each input parameter was defined (Table 7).
- The program will also check any existing data in ‘Data Output’ sheet of the I/O file, and ask users to initialize the output sheet (Figure 22).
- With any other unexpected errors during simulation will be reported in an error dialog.

Table 7. Acceptable ranges for model input parameters.

Parameters	Acceptable values/ranges	Comment
AC Amendment Application		
Initial mechanical mixing with sediment and AC [min]	≥ 0	
AC-sediment contact in stagnant system [month]	≥ 0	
Nominal mixing depth (in multiples of 5 cm) [cm]	>0 , multiples of 5	
Nominal AC dose [g/g]	$0 \leq \leq 0.2$	Overdose ($>20\%$) may cause ecological adverse impact.
Core-scale (5 cm) AC distribution heterogeneity (type 1 if homogeneous / 2 if heterogeneous)	1, 2	
MM-scale (2 mm) AC distribution heterogeneity (type 1 if homogeneous / 2 if heterogeneous)	1, 2	
Site-Specific Properties		
Sediment porosity [-]	$0 < < 1$	
Sediment particle density [g/cm ³]	$0 < < 3$	
Pore-water flow velocity [cm/d]	$0 \leq \leq 50$	

Table 7. Acceptable ranges for model input parameters (continued).

Activated Carbon (AC) Properties		
Mean radius [μ m]	$10 \leq \leq 500$	Too fine AC is not recommended due to potential ecological health issue. Too large AC will not be preferred because of low performance.
AC density [g/cm ³]	$1 \leq \leq 3$	
AC intraparticle porosity [-]	$0 < < 1$	
Mass Transfer Parameters		
initial sediment concentration [ng/g]	>0	
aqueous diffusivity [cm ² /s]	$0 < < 10^{-4}$	http://en.wikipedia.org/wiki/Mass_diffusivity
sediment-water distribution coefficient, Kd [cm ³ /g]	$>10^2$	for hydrophobic contaminants
fast release rate from sediment [1/s]	$0 < < 10^{-2}$	
slow release rate from sediment [1/s]	$0 < < 10^{-2}$	smaller than rate_fast
mass fraction associated with rate(slow) [-]	$0 < < 1$	
apparent AC-water partitioning coefficient [cm ³ /g]	$>Kd$	condition for benefits from AC amendment
apparent diffusion coefficient for intraparticle diffusion within AC [1/s]	>0	
mechanical dispersivity [longitudinal - for flow conditions only] [cm]	>0	

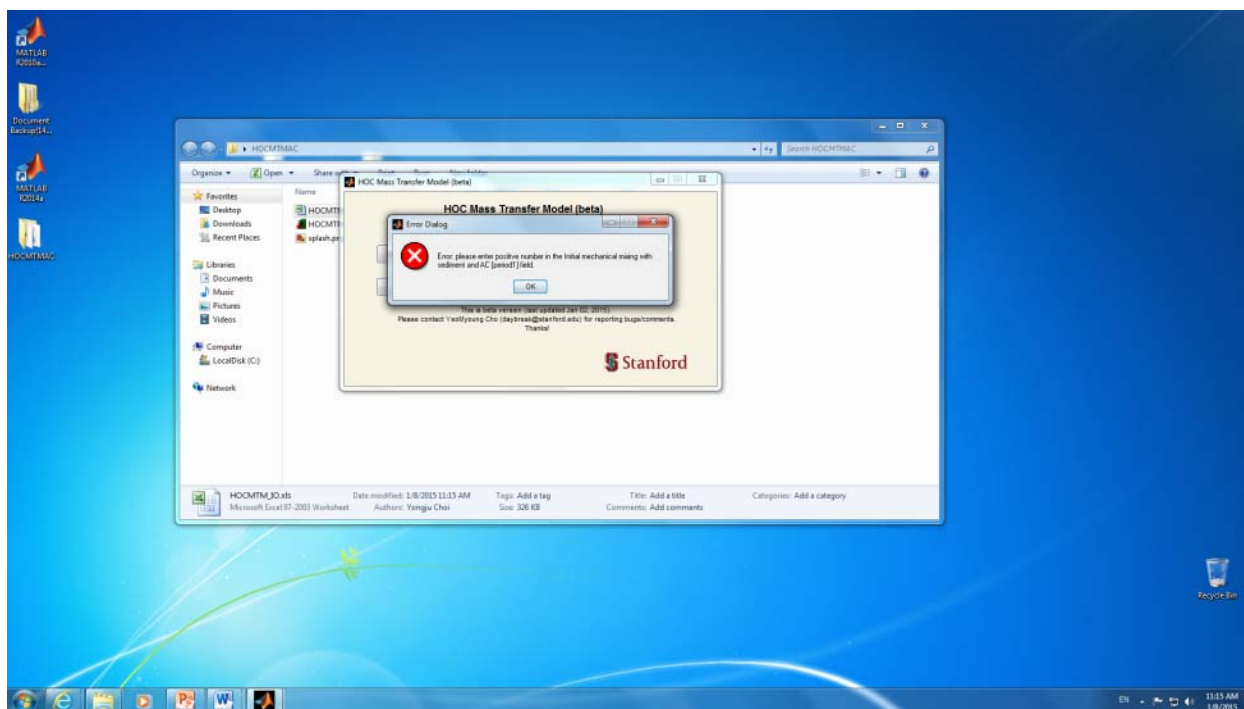


Figure 21. An example error message for an invalid input parameter.

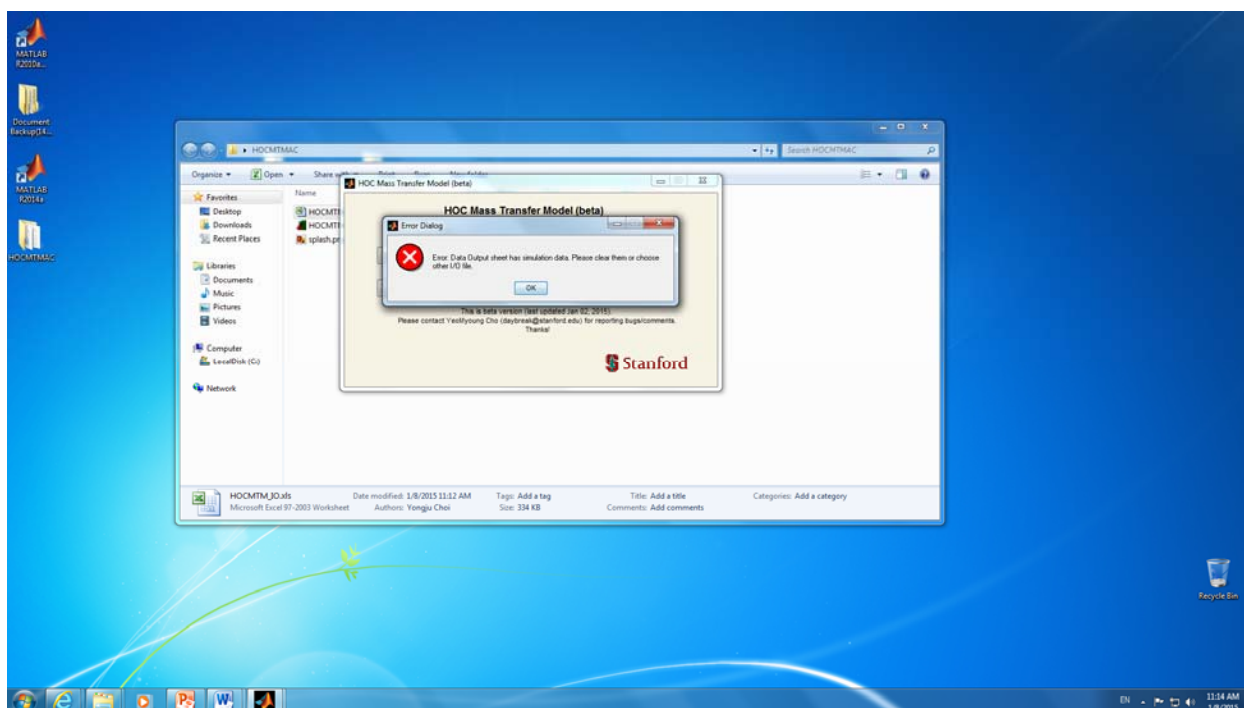


Figure 22. An example error message for pre-existed simulation data in “Data Output” worksheet.

- System requirements have been revised. From testing, it was found that 64-bit processor is required to run the program on MATLAB Compiler Runtime 2014a, 8.3 (64-bit).
- A trouble shooting section was included.

In this final report, we submit the most current beta version program with an I/O file and auxiliary files in one zip file. The user manual is attached in the Appendix B.

In addition to the accomplishments listed above, we further identified an independent modeling step during model parameterization phase, where is a room for user-friendliness enhancement. Sediment desorption test is one of key experiments determining three model parameters: fast release rate, slow release rate, and mass fraction associated with slow rate. Contaminant desorption kinetics are highly site-specific and have significant effect on the mass transfer model simulation results, so experimental determination is strongly required. To obtain the three desorption kinetic parameters, the experimental results from desorption test need to be fitted to a kinetic model (HOC sediment desorption model), which is also coded in MATLAB language. Therefore, in the same manner, the model usability can be greatly improved by compiling as a standalone program of the desorption model, which will consequently enhance user-friendliness of the HOC mass transfer model. So a self-executable program of the HOC sediment desorption model was developed with GUI installed. In Figure 23, a GUI for the standalone HOC sediment desorption model is shown. In the GUI window, users enter their desorption test data, and run the program. Then, the program provides the fitted graph with the three model parameters. The sediment desorption standalone program (zip file) and its user manual (Appendix B) are submitted with this final report.

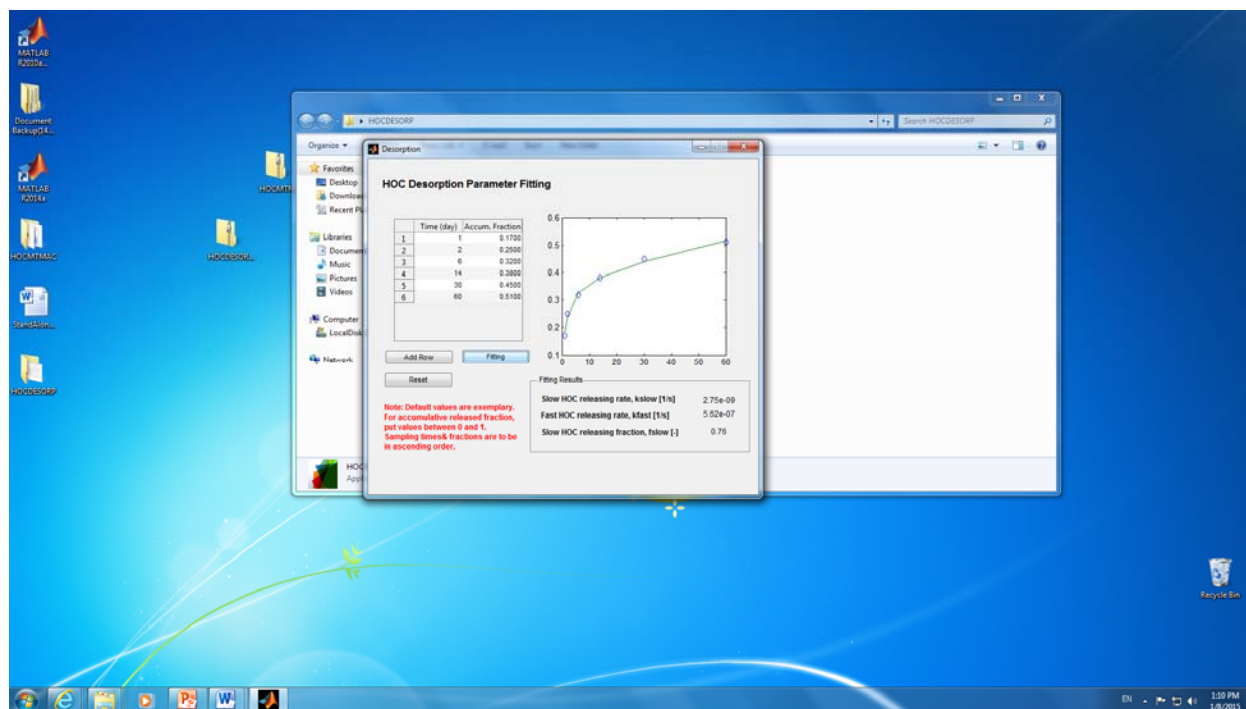


Figure 23. GUI of the standalone HOC sediment desorption parameter fitting program.

3.3. Develop booklet for exemplary modeling results (Task 11.3)

The booklet for exemplary modeling results developed in this work is attached in the Appendix B. The HOC mass transfer modeling results were further analyzed in conjunction with the site-specific properties at the ten case study sites. The outcome of the analysis was written as a paper entitled as “Predicted effectiveness of in-situ activated carbon for field sediment sites with variable site- and compound-specific characteristics” by Y. Choi, Y.-M. Cho, R.G. Luthy, and D. Werner and submitted to *Journal of Hazardous Materials*. The paper is currently in review. The manuscript and supporting document for the subject paper are attached in Appendix C.

VI. Conclusions and Implications for Future Research/Implementation

The research has been successfully completed in regards to the project milestones as summarized below. All of the project's objectives were met.

1. Prolonged effect of AC amendment (Task 9)

The experimental results showed that when sorbent is selectively lost from the sorbent-treated sediment by winnowing, the repartitioning of contaminants may occur to some degree, but the repartitioning process is neither prolonged nor substantial to cause significant loss of the treatment effectiveness. Even with an extensive period of mixing of sorbent-deprived sediment in a slurry phase after sorbent treatment and removal, the available fraction of PCBs in the sediment, as estimated by 1- and 28-d Tenax bead uptakes, was substantially less than those for the untreated sediment. The scenarios of complete removal of AC after amendment is not likely to occur, but regulators, site managers, and DoD users would want assurance that risk reduction is still maintained even if the AC were removed. In this task, we successfully addressed those concerns and raised confidence level for the in-situ AC amendment technology.

2. Standardization of field monitoring method using PE samplers (Task 10)

In this task, the current passive sampling technique based on performance reference compound (PRC) was closely examined. Firstly, we compared uptake and release rates of PCBs into/from PE samplers, and found that PE may show anisotropic exchange kinetics, which could limit the applicability of the PRC-based method. In this study, a non-equilibrium passive sampling method was proposed using different thickness of PEs. By comparing PCB uptakes into PEs with different thickness, the status of PCB uptake kinetics could be identified. Also, PE-water partitioning coefficients (K_{PE}) for several PCBs and PEs with varying thickness were determined in this study. Two frequently used PE uptake kinetic models: first order kinetic model and 1-D diffusion model were tested for their performance and limitation in a non-equilibrium passive sampling method scenario. Still the PRC method can provide good predictions of equilibrium PE concentrations for less chlorinated PCB congeners and for PEs with thinner thickness, while it can significantly underestimate the equilibrium PE concentrations for highly chlorinated congeners (more than 5 chlorine substitutions) and for relatively thick PE. This is because in quiescent sediment systems the desorption of very strongly hydrophobic compounds may proceed slower than the diffusion of PRCs from polyethylene. Although our conclusions are based on relatively small set of data, they clearly showed that more studies are needed to investigate the accuracy of the PRC method for different PCB congeners and PEs with different thicknesses.

3. Develop user-friendly standalone program for HOC mass transfer model (Task 11)

HOC mass transfer model MATLAB codes were successfully developed to a standalone program. The user-friendliness of the model was greatly enhanced by an I/O excel file, GUI, and detailed user manual. Furthermore, a separate standalone program for sediment desorption kinetic test and parameter determination was developed, so to easily obtain the most important

model parameters for HOC mass transfer model. With our achievements, potential users can simulate various in-situ AC application scenarios and predict their performance without comprehensive knowledge about coding or programming. Along with those efforts, we organized a case study booklet showing the effectiveness of in-situ AC amendment using the HOC mass transfer model. The study sites exhibited a range of site characteristics. This allows readers to refer a site that is most similar to the site of their interest for the model input parameters and corresponding modeling results. Above all, this booklet will serve as an intuitive introductory material about in-situ AC amendment and its effectiveness to users. Overall, our results from the Task 11 will greatly improve the usability and accessibility of the HOC mass transfer model for remedial project managers and DoD users.

VII. Literature Cited

- Adams, R. G. (2002). Polyethylene devices and the effects of sediment resuspension on the cycling of PAHs and PCBs in the lower Hudson Estuary. Ph.D. Dissertation Ph.D. Dissertation, Massachusetts Institute of Technology.
- Adams, R. G., R. Lohmann, L. A. Fernandez, J. K. MacFarlane and P. M. Gschwend (2007). "Polyethylene devices: passive samplers for measuring dissolved hydrophobic organic compounds in aquatic environments." Environ Sci Technol **41**(4): 1317-1323.
- Beckingham, B. and U. Ghosh (2011). "Field-scale reduction of PCB bioavailability with activated carbon amendment to river sediments." Environmental Science & Technology **45**(24): 10567-10574.
- Booij, K., H. E. Hofmans, C. V. Fischer and E. M. Van Weerlee (2003). "Temperature-dependent uptake rates of nonpolar organic compounds by semipermeable membrane devices and low-density polyethylene membranes." Environ Sci Technol **37**(2): 361-366.
- Cho, Y. M., D. Werner, Y. Choi and R. G. Luthy (2012). "Long-term monitoring and modeling of the mass transfer of polychlorinated biphenyls in sediment following pilot-scale in-situ amendment with activated carbon." J Contam Hydrol **129-130**: 25-37.
- Choi, Y., Y. M. Cho, W. R. Gala and R. G. Luthy (2013). "Measurement and modeling of activated carbon performance for the sequestration of parent- and alkylated-polycyclic aromatic hydrocarbons in petroleum-impacted sediments." Environmental Science & Technology **47**(2): 1024-1032.
- Choi, Y., Y. M. Cho and R. G. Luthy (2013). "Polyethylene-water partitioning coefficients for parent- and alkylated-polycyclic aromatic hydrocarbons and polychlorinated biphenyls." Environmental Science & Technology **47**(13): 6943-6950.
- Choi, Y., Y. M. Cho, D. Werner and R. G. Luthy (2014). "In situ sequestration of hydrophobic organic contaminants in sediments under stagnant contact with activated carbon. 2. mass transfer modeling." Environmental Science & Technology **48**(3): 1843-1850.
- Fernandez, L. A., C. F. Harvey and P. M. Gschwend (2009). "Using performance reference compounds in polyethylene passive samplers to deduce sediment porewater concentrations for numerous target chemicals." Environmental Science & Technology **43**(23): 8888-8894.
- Fernandez, L. A., J. K. MacFarlane, A. P. Tcaciuc and P. M. Gschwend (2009). "Measurement of freely dissolved PAH concentrations in sediment beds using passive sampling with low-density polyethylene strips." Environ Sci Technol **43**(5): 1430-1436.
- Hale, S. E., S. Kwon, U. Ghosh and D. Werner (2010). "Polychlorinated biphenyl sorption to activated carbon and the attenuation caused by sediment." Global NEST Journal **12**(3): 318-326.
- Hale, S. E., T. J. Martin, K. U. Goss, H. P. Arp and D. Werner (2010). "Partitioning of organochlorine pesticides from water to polyethylene passive samplers." Environmental Pollution **158**(7): 2511-2517.
- Hale, S. E., J. E. Tomaszewski, R. G. Luthy and D. Werner (2009). "Sorption of dichlorodiphenyltrichloroethane (DDT) and its metabolites by activated carbon in clean water and sediment slurries." Water Research **43**(17): 4336-4346.
- Hale, S. E. and D. Werner (2010). "Modeling the mass transfer of hydrophobic organic pollutants in briefly and continuously mixed sediment after amendment with activated carbon." Environmental Science & Technology **44**(9): 3381-3387.
- Harwood, A. D., P. F. Landrum and M. J. Lydy (2013). "Bioavailability-based toxicity endpoints of bifenthrin for *Hyalomma azteca* and *Chironomus dilutus*." Chemosphere **90**(3): 1117-1122.

Hawthorne, S. B., M. T. Jonker, S. A. van der Heijden, C. B. Grabanski, N. A. Azzolina and D. J. Miller (2011). "Measuring picogram per liter concentrations of freely dissolved parent and alkyl PAHs (PAH-34), using passive sampling with polyoxymethylene." Anal Chem **83**(17): 6754-6761.

Hawthorne, S. B., D. J. Miller and C. B. Grabanski (2009). "Measuring low picogram per liter concentrations of freely dissolved polychlorinated biphenyls in sediment pore water using passive sampling with polyoxymethylene." Anal Chem **81**(22): 9472-9480.

Huckins, J. N., J. D. Petty and K. Booij (2006). Monitors of Organic Chemicals in the Environment. New York, NY, Springer.

Huckins, J. N., J. D. Petty, J. A. Lebo, F. V. Almeida, K. Booij, D. A. Alvarez, W. L. Cranor, R. C. Clark and B. B. Mogensen (2002). "Development of the permeability/performance reference compound approach for in situ calibration of semipermeable membrane devices." Environ Sci Technol **36**(1): 85-91.

Huckins, J. N., M. W. Tubergen and G. K. Manuweera (1990). "Semipermeable membrane devices containing model lipid: A new approach to monitoring the bioavailability of lipophilic contaminants and estimating their bioconcentration potential." Chemosphere **20**(5): 533-552.

Janssen, E. M. and B. A. Beckingham (2013). "Biological responses to activated carbon amendments in sediment remediation." Environmental Science & Technology **47**(14): 7595-7607.

Janssen, E. M., Y. Choi and R. G. Luthy (2012). "Assessment of nontoxic, secondary effects of sorbent amendment to sediments on the deposit-feeding organism *Neanthes arenaceodentata*." Environmental Science & Technology **46**(7): 4134-4141.

Jonker, M. T., M. P. Suijkerbuijk, H. Schmitt and T. L. Sinnige (2009). "Ecotoxicological effects of activated carbon addition to sediments." Environmental Science & Technology **43**(15): 5959-5966.

Jonker, M. T. O. and A. A. Koelmans (2002). "Sorption of polycyclic aromatic hydrocarbons and polychlorinated biphenyls to soot and soot-like materials in the aqueous environment mechanistic considerations." Environmental Science & Technology **36**(17): 3725-3734.

Kupryianchyk, D., E. P. Reichman, M. I. Rakowska, E. T. H. M. Peeters, J. T. C. Grotenhuis and A. A. Koelmans (2011). "Ecotoxicological effects of activated carbon amendments on macroinvertebrates in nonpolluted and polluted sediments." Environmental Science & Technology **45**(19): 8567-8574.

Lin, D., Y. M. Cho, D. Werner and R. G. Luthy (2014). "Bioturbation delays attenuation of DDT by clean sediment cap but promotes sequestration by thin-layered activated carbon." Environmental Science & Technology **48**(2): 1175-1183.

Lohmann, R. (2012). "Critical review of low-density polyethylene's partitioning and diffusion coefficients for trace organic contaminants and implications for its use as a passive sampler." Environmental Science & Technology **46**(2): 606-618.

Lohmann, R. and D. Muir (2010). "Global Aquatic Passive Sampling (AQUA-GAPS): using passive samplers to monitor POPs in the waters of the world." Environmental Science & Technology **44**(3): 860-864.

Mackenbach, E. M., Y. Jing, M. A. Mills, P. F. Landrum and M. J. Lydy (2012). "Application of a Tenax model to assess bioavailability of PCBs in field sediments." Environ Toxicol Chem **31**(10): 2210-2216.

Meynet, P., S. E. Hale, R. J. Davenport, G. Cornelissen, G. D. Breedveld and D. Werner (2012). "Effect of activated carbon amendment on bacterial community structure and functions in a PAH impacted urban soil." Environmental Science & Technology **46**(9): 5057-5066.

Sun, X. and U. Ghosh (2008). "The effect of activated carbon on partitioning, desorption, and biouptake of native polychlorinated biphenyls in four freshwater sediments." Environmental Toxicology and Chemistry **27**(11): 2287-2295.

ter Laak, T. L., A. Barendregt and J. L. Hermens (2006). "Freely dissolved pore water concentrations and sorption coefficients of PAHs in spiked, aged, and field-contaminated soils." Environmental Science & Technology **40**(7): 2184-2190.

Tomaszewski, J. E. and R. G. Luthy (2008). "Field deployment of polyethylene devices to measure PCB concentrations in pore water of contaminated sediment." Environ Sci Technol **42**(16): 6086-6091.

Tomaszewski, J. E., D. Werner and R. G. Luthy (2007). "Activated carbon amendment as a treatment for residual DDT in sediment from a superfund site in San Francisco Bay, Richmond, California, USA." Environmental Toxicology and Chemistry **26**(10): 2143-2150.

Werner, D., U. Ghosh and R. G. Luthy (2006). "Modeling polychlorinated biphenyl mass transfer after amendment of contaminated sediment with activated carbon." Environ Sci Technol **40**(13): 4211-4218.

Werner, D., S. E. Hale, U. Ghosh and R. G. Luthy (2010). "Polychlorinated biphenyl sorption and availability in field-contaminated sediments." Environ Sci Technol **44**(8): 2809-2815.

Werner, D., C. P. Higgins and R. G. Luthy (2005). "The sequestration of PCBs in Lake Hartwell sediment with activated carbon." Water Research **39**(10): 2105-2113.

You, J., P. F. Landrum, T. A. Trimble and M. J. Lydy (2007). "Availability of polychlorinated biphenyls in field-contaminated sediment." Environmental Toxicology and Chemistry **26**(9): 1940-1948.

Zimmerman, J. R., U. Ghosh, R. N. Millward, T. S. Bridges and R. G. Luthy (2004). "Addition of carbon sorbents to reduce PCB and PAH bioavailability in marine sediments: Physicochemical tests." Environmental Science & Technology **38**(20): 5458-5464.

Zimmerman, J. R., D. Werner, U. Ghosh, R. N. Millward, T. S. Bridges and R. G. Luthy (2005). "Effects of dose and particle size on activated carbon treatment to sequester polychlorinated biphenyls and polycyclic aromatic hydrocarbons in marine sediments." Environmental Toxicology and Chemistry **24**(7): 1594-1601.

Appendix A. List of Scientific/Technical Publication

Articles in peer-reviewed journals

- Choi, Y., Y. M. Cho and R. G. Luthy (2014a). "In situ sequestration of hydrophobic organic contaminants in sediments under stagnant contact with activated carbon. 1. column studies." Environmental Science & Technology **48**(3): 1835-1842..
- Choi, Y., Y. M. Cho, D. Werner and R. G. Luthy (2014b). "In situ sequestration of hydrophobic organic contaminants in sediments under stagnant contact with activated carbon. 2. mass transfer modeling." Environmental Science & Technology **48**(3): 1843-1850.
- Choi, Y., Y. M. Cho, R. G. Luthy, and D. Werner. "Predicted effectiveness of in-situ activated carbon amendment for field sediment sites with variable site- and compound-specific characteristics" Journal of Hazardous Materials accepted with major revision, revised manuscript submitted on Aug 11 2015.
- Choi, Y., Y. M. Cho, W. R. Gala, T. P. Hoelen, D. Werner and R. G. Luthy. "Decision-making framework for the application of in-situ activated carbon amendment to sediment" Journal of Hazardous Materials submitted on Aug 23 2015.

Appendix B. Other Supporting Materials

1. User Manual for the Standalone HOC Mass Transfer Model

User Manual for the Standalone HOC Mass Transfer Model

last updated Aug 20 2015

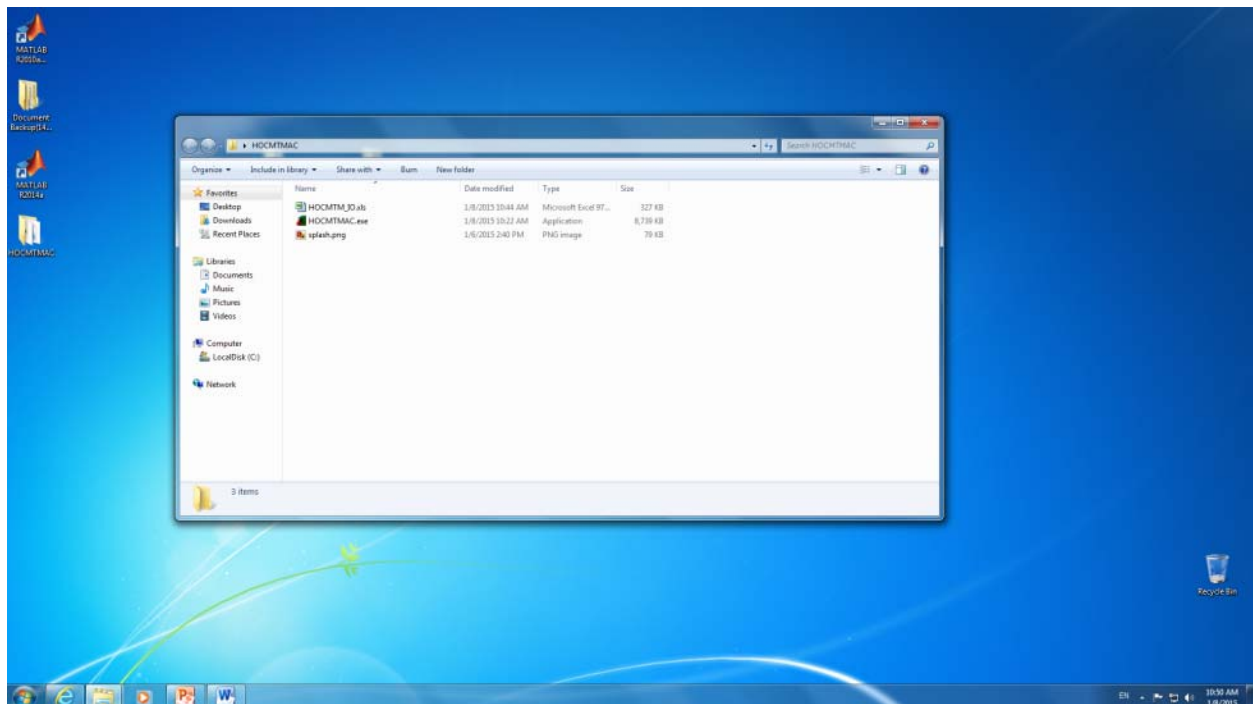
Contacts: YeoMyoung Cho (daybreak@stanford.edu) / Richard G. Luthy (luthy@stanford.edu)

1. System Requirements

- Windows machine (64-bit processor)
- MS Excel
- MATLAB Compiler Runtime (MCR, R2014a (8.3)) available on <http://www.mathworks.com/products/compiler/mcr/index.html>

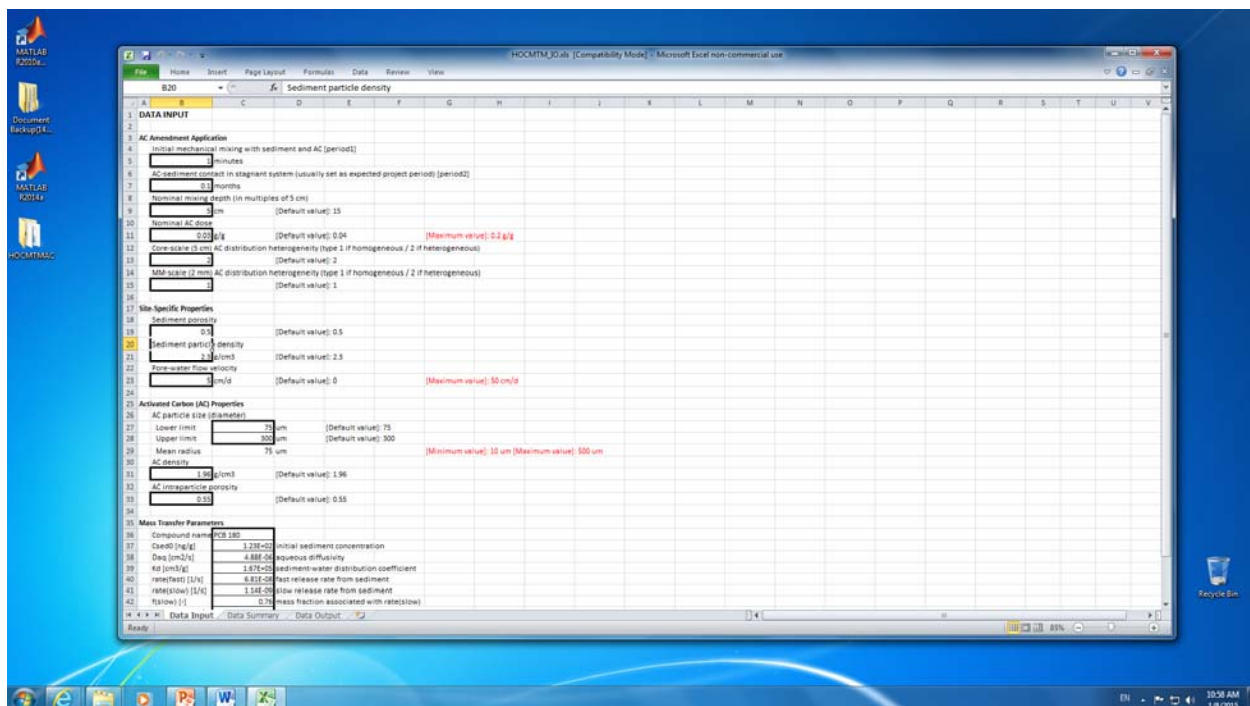
2. Operation

Step 1. Download and extract files from HOCMTMAC.zip

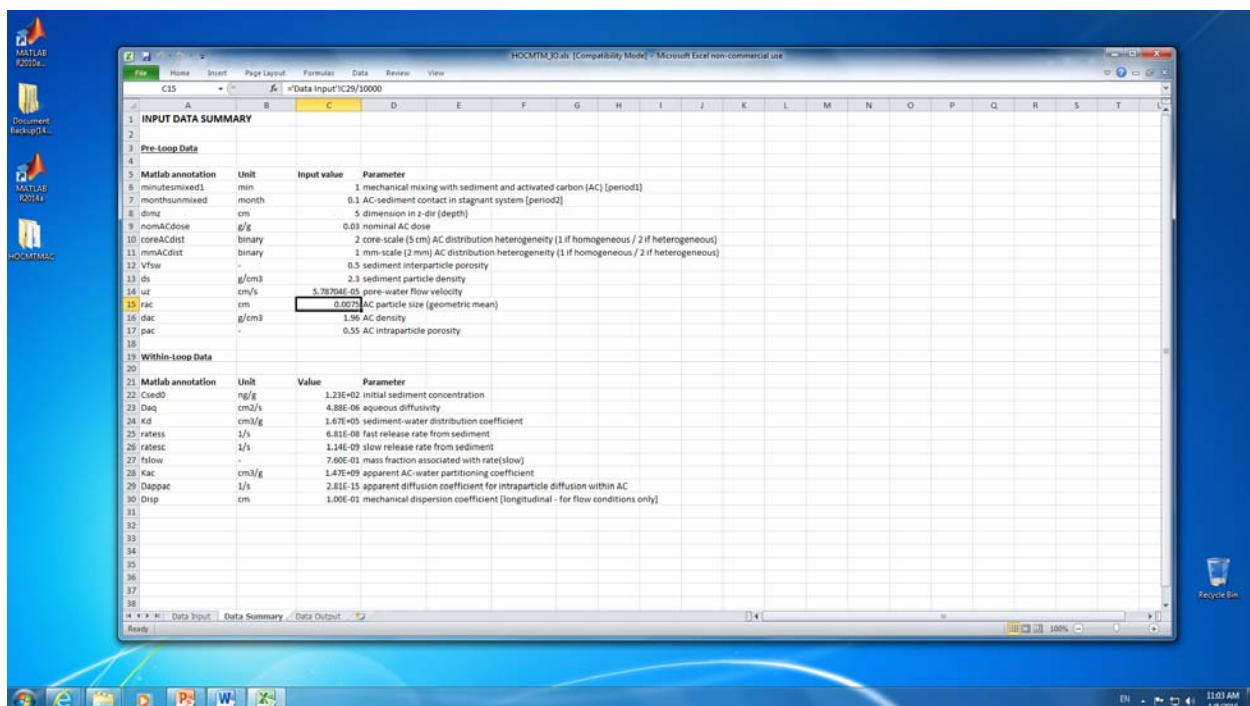


Three files are included. HOCMCMAC.exe (MATLAB standalone executable file), HOCMTM_IO.xls (IO MS office Excel file), and splash.png.

Step 2. Open the I/O file. The file contains three tabs: Data Input, Data Summary, and Data Output. Enter model parameters in 'Data Input' worksheet. **Only edit cells with thick borderlines in 'Data Input' sheet.** Modifications/renaming of other tabs can prohibit proper model runs. Also, please ensure to enter all parameters in a right format. At last, delete any previous data in 'Data Output' sheet. The file contains default values for PCB 180 in Hunters Point Shipyard, CA (Choi et al. 2014).

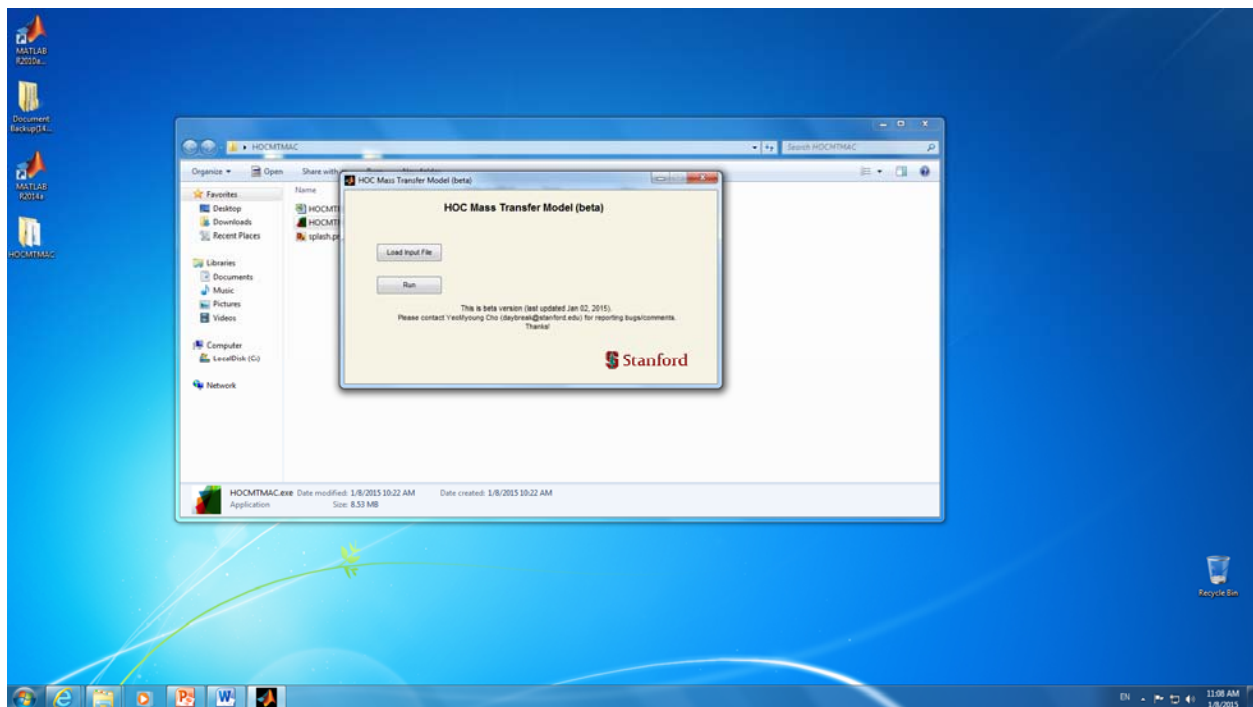
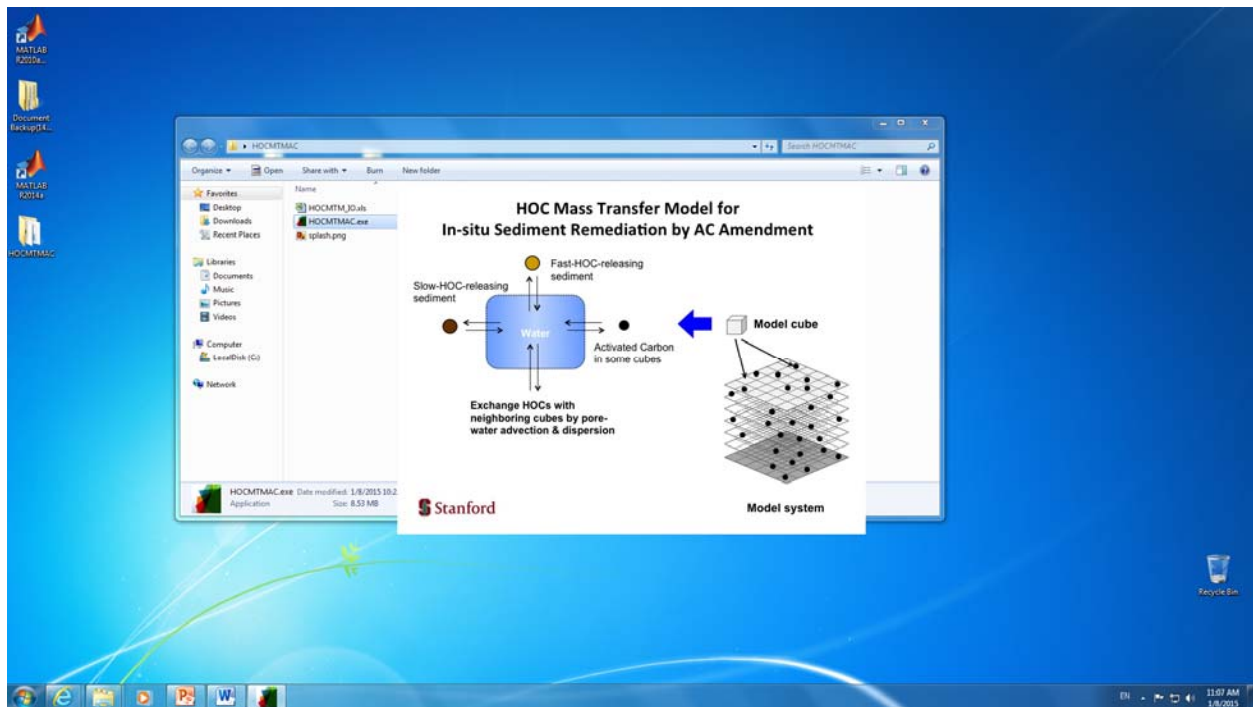


Step 3. Check 'Data Summary' worksheet for actual input parameters.

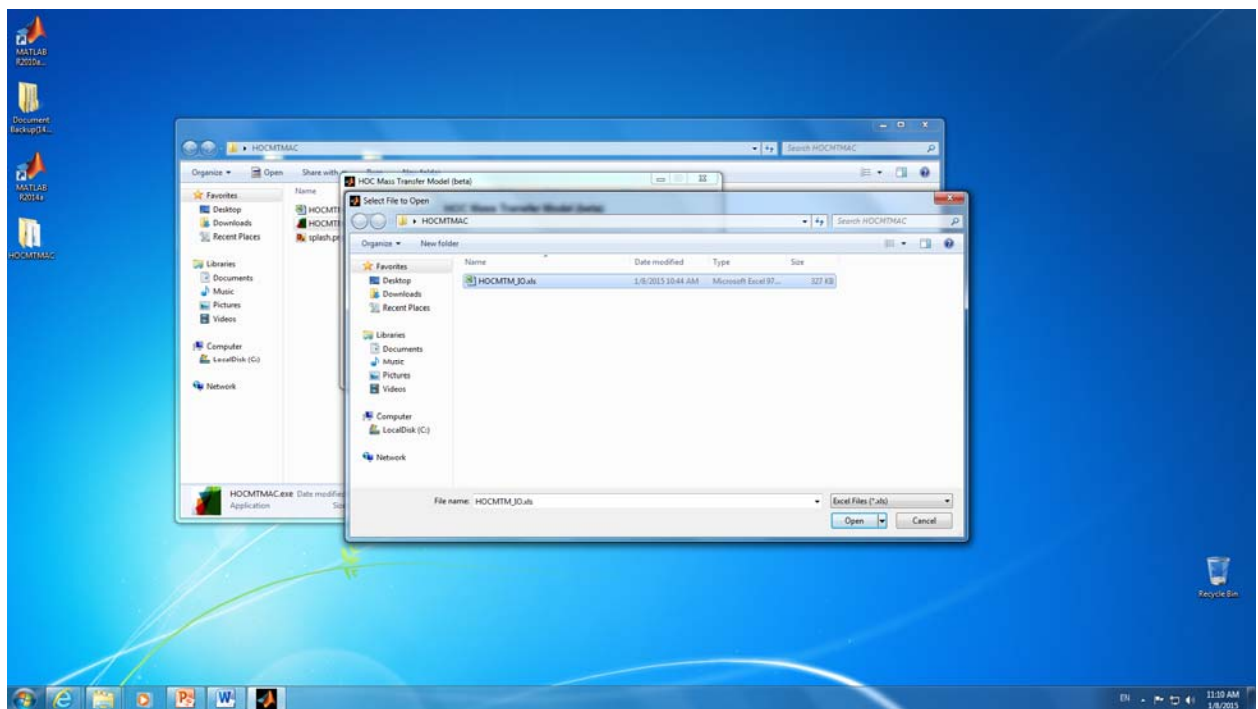
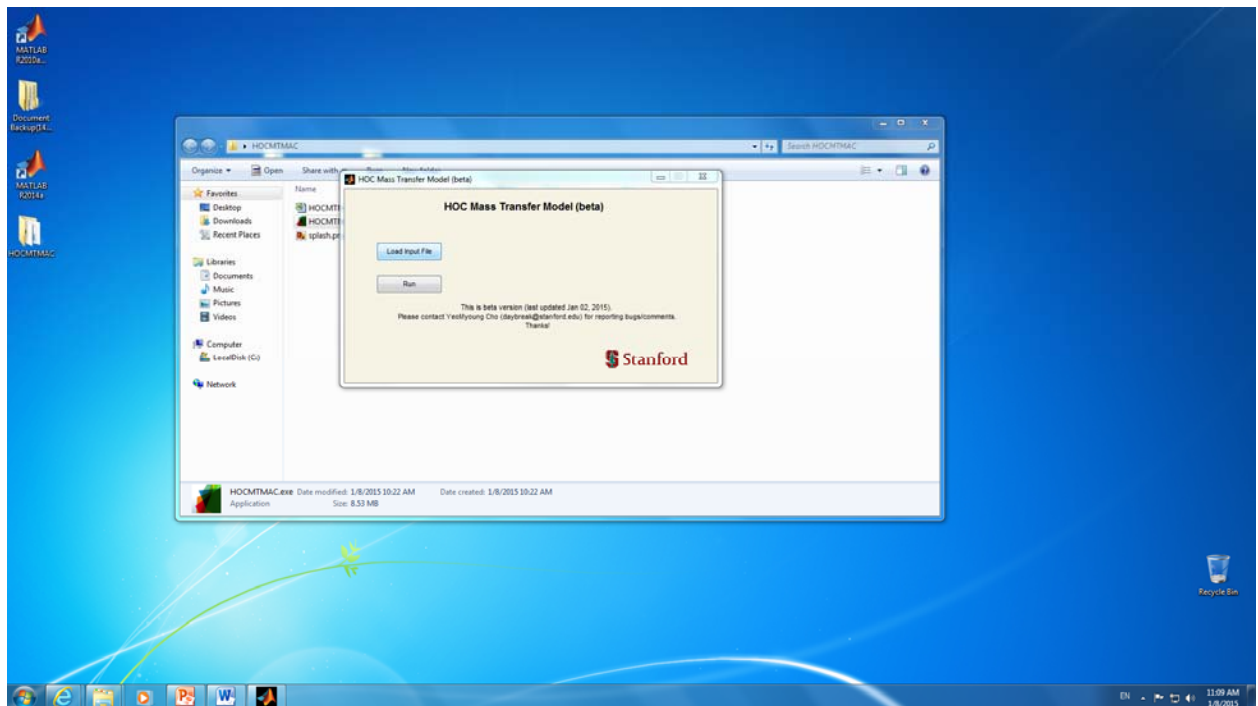


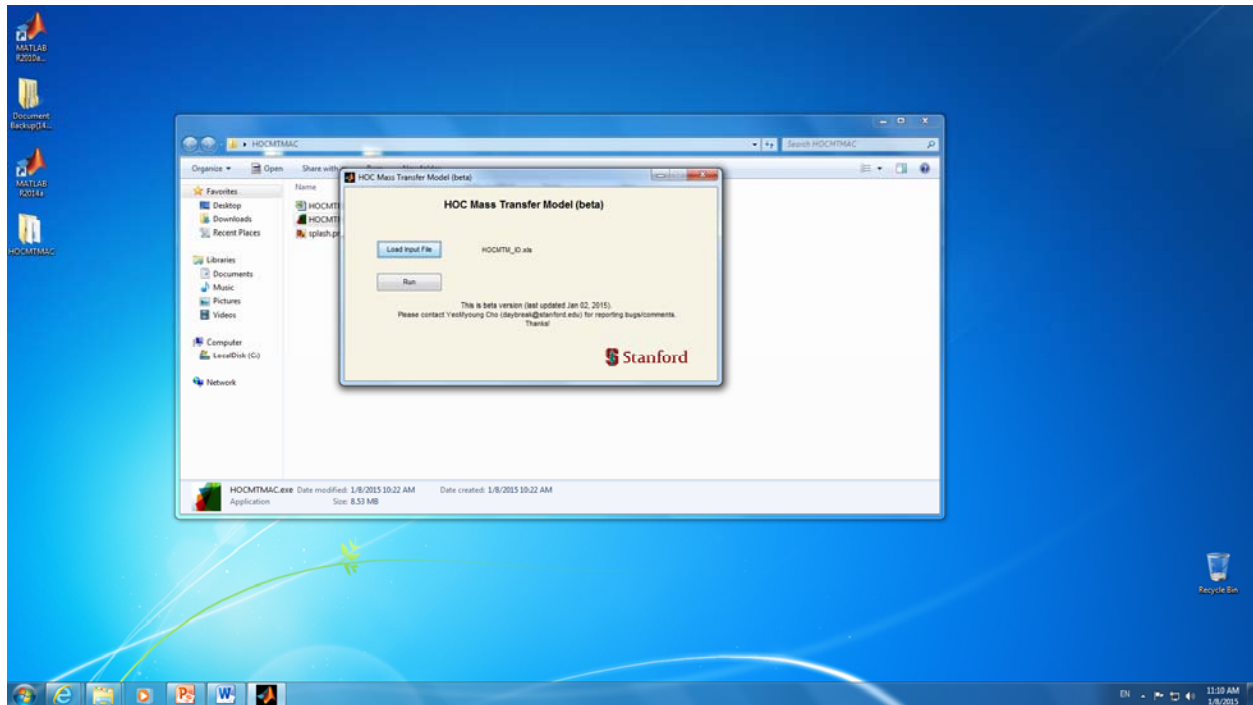
Step 4. Rename the I/O file as needed. Note that the I/O file should locate in the same folder where the model program (HOCMTMAC.exe) is. Save and **Close** the I/O file.

Step 5. Double click HOCMCMAC.exe. After a splash screen, a GUI (graphic user interphase) with a Stanford logo will pop up.

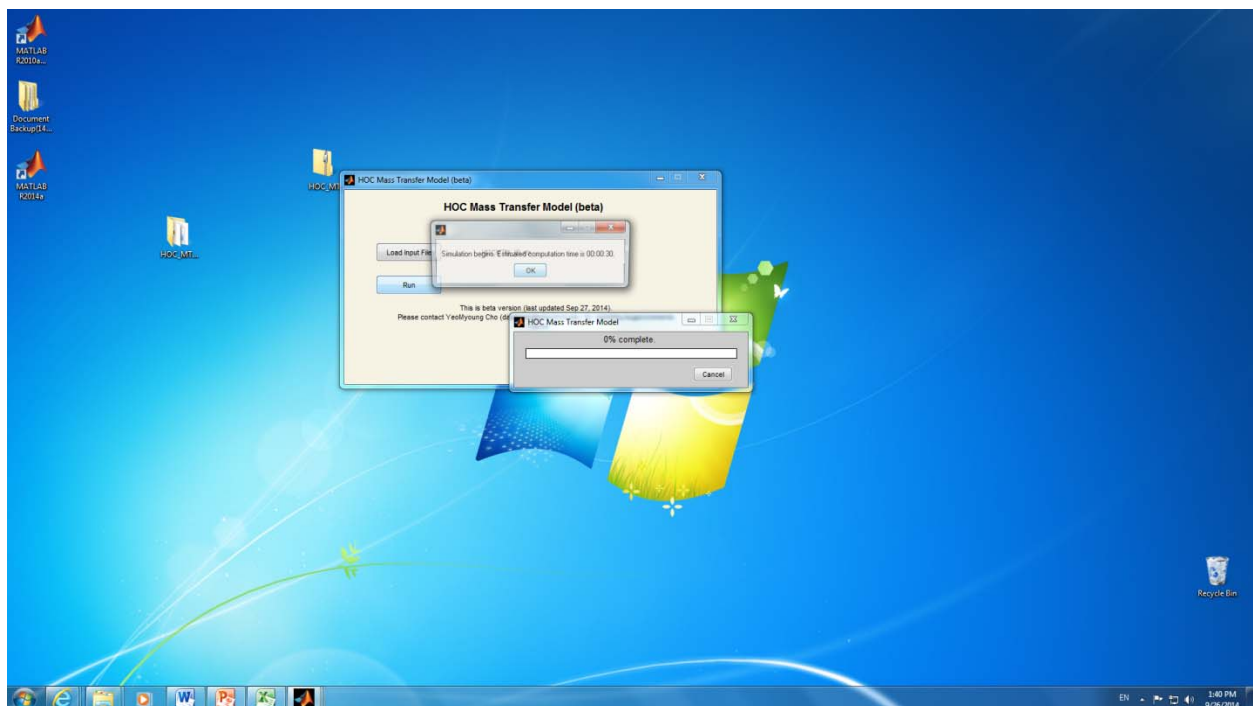


Step 6. Press the button 'Load Input File', and select the I/O file. The name of the I/O file will be shown in the GUI.

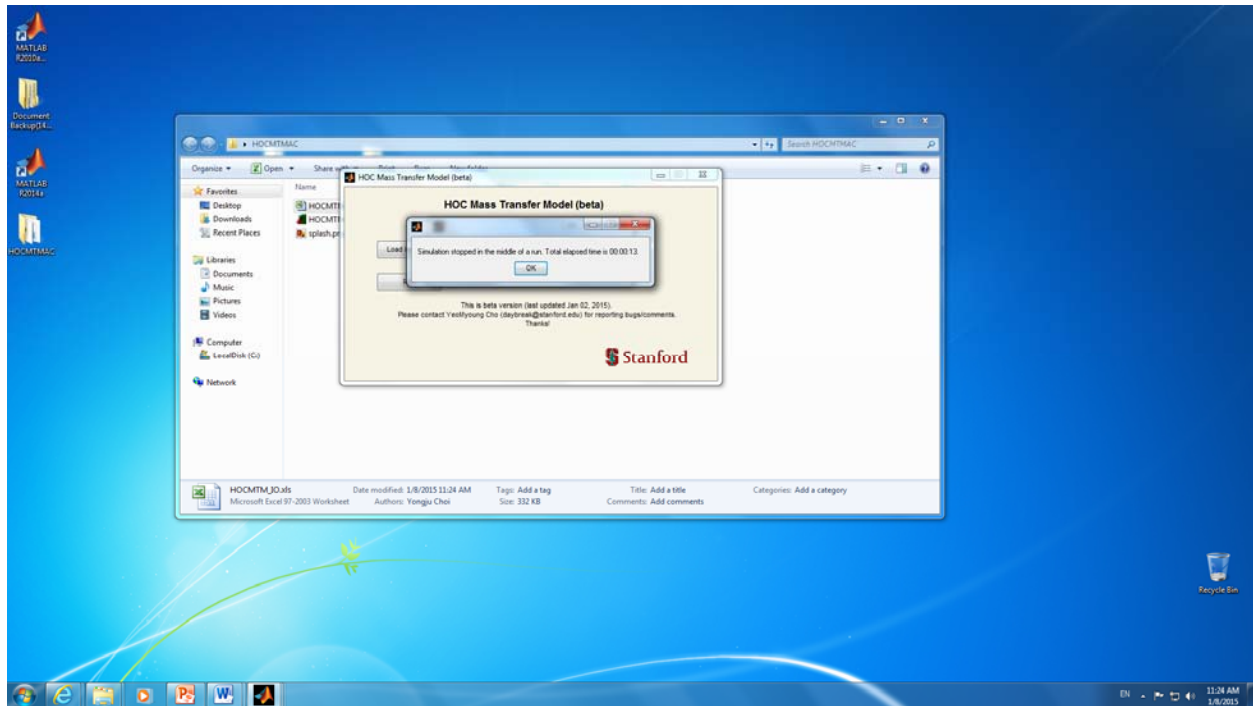




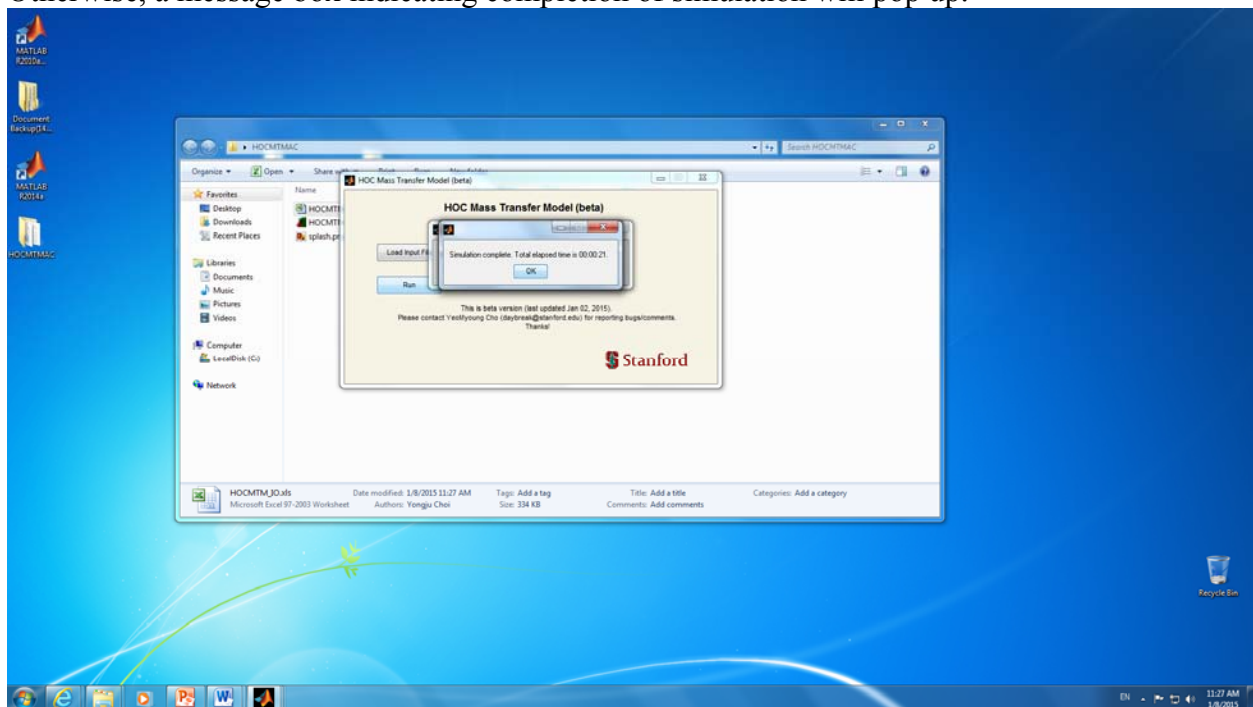
Step 7. Press 'Run'. A status bar and a message box will pop up. The message box will show the estimated time, and the status bar will show the simulation progress as %.



Step 8. If press the cancel button in the status bar in the middle of a run, simulation will stop, and partial data will be exported to the I/O file.

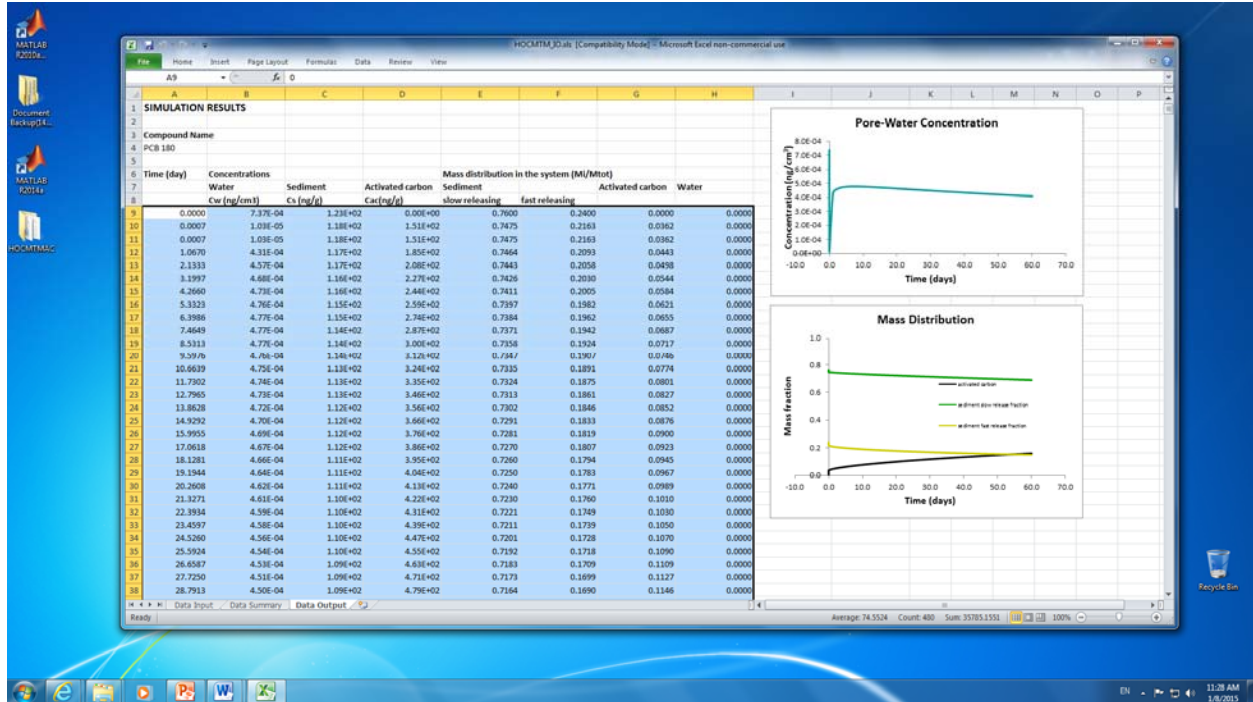


Otherwise, a message box indicating completion of simulation will pop up.



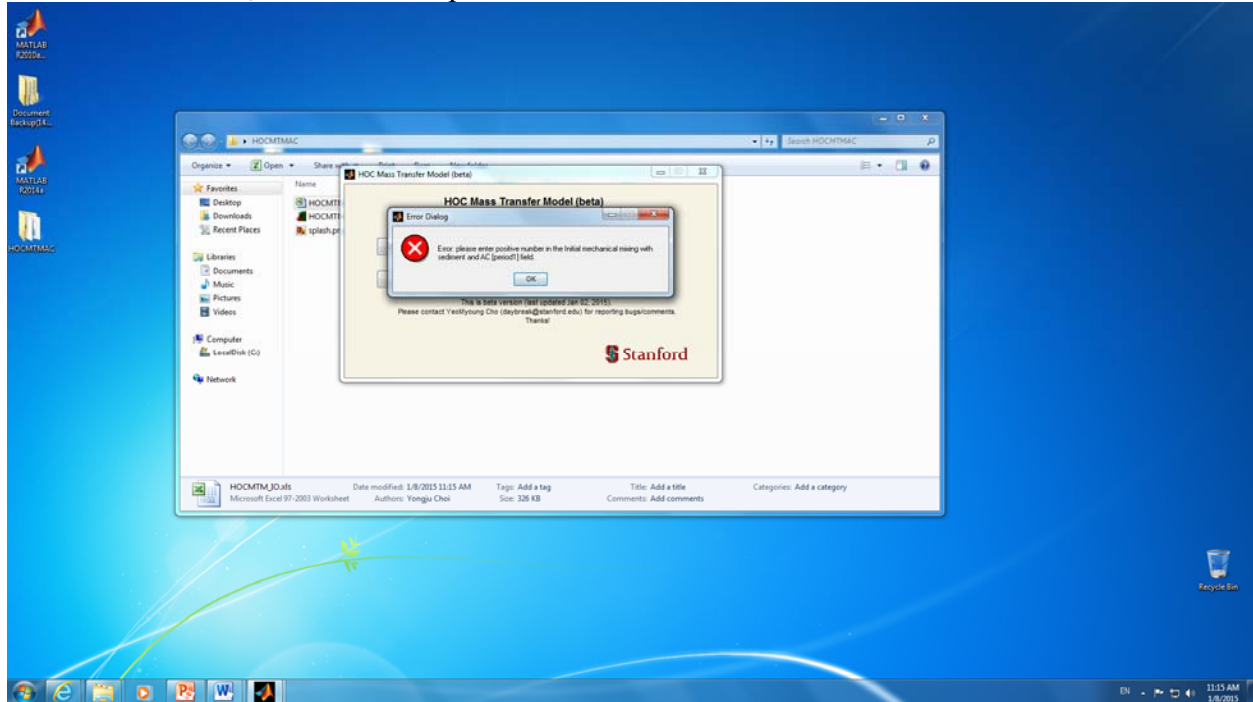
To exit the program, simply press the close button at the right top corner.

Step 9. Open the I/O file and check 'Data Output' worksheet for the results.

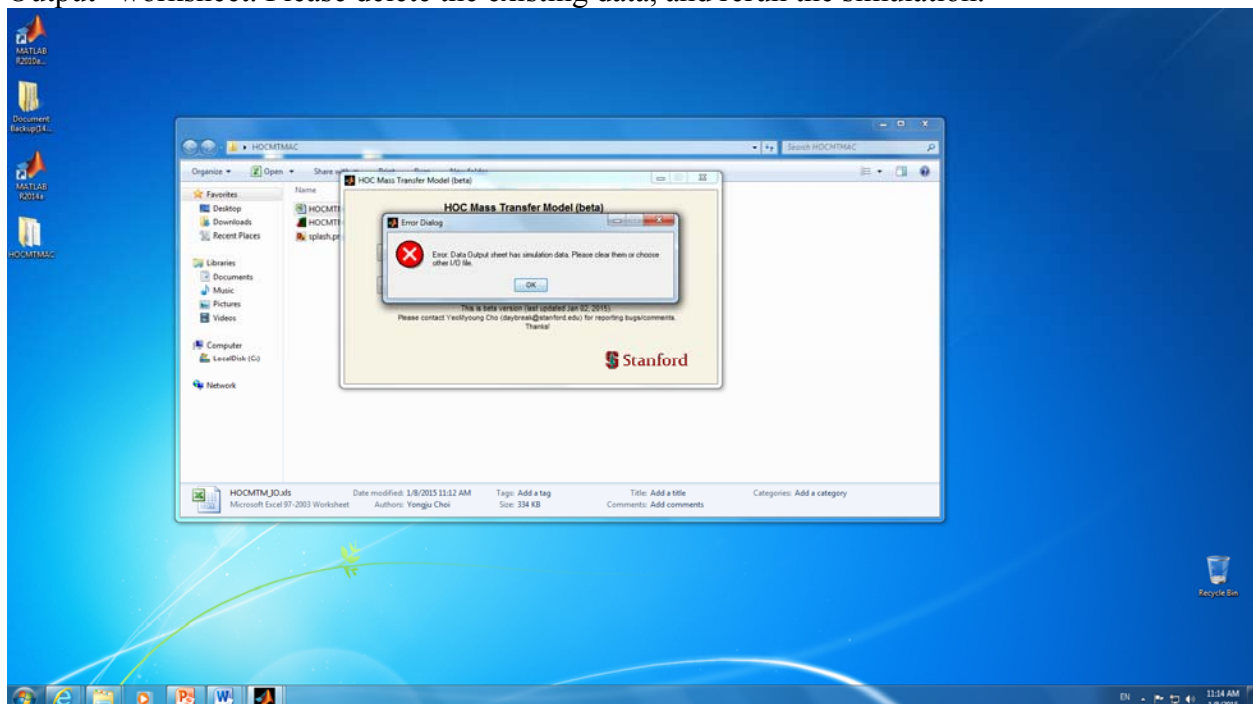


3. Troubleshooting

If the program encounters an error during simulation, simulation will abort, and pop up an error message window. Common errors would be invalid data input. In this case, an error message may provide an acceptable range or condition for the specific input parameter. The user can go back to the I/O file, and check the parameter.



Another major common error occurs when the I/O file contains previous simulation data in “Data Output” worksheet. Please delete the existing data, and rerun the simulation.



4. References

- Werner D, Ghosh U, Luthy RG. *Environ. Sci. Technol.*, **2006**, 40 (13), pp 4211–4218
- Cho Y-M, Werner D, Choi Y, and Luthy RG. *J. Cont. Hydrol.*, **2011**, 129, pp 25-37
- Choi Y, Cho Y-M, Werner D, and Luthy RG. *Environ. Sci. Technol.*, **2014**, 48 (3), pp 1843–1850

2. User Manual for the Standalone HOC Sediment Desorption Model

User Manual for the Standalone HOC Sediment Desorption Model

last updated Aug 20 2015

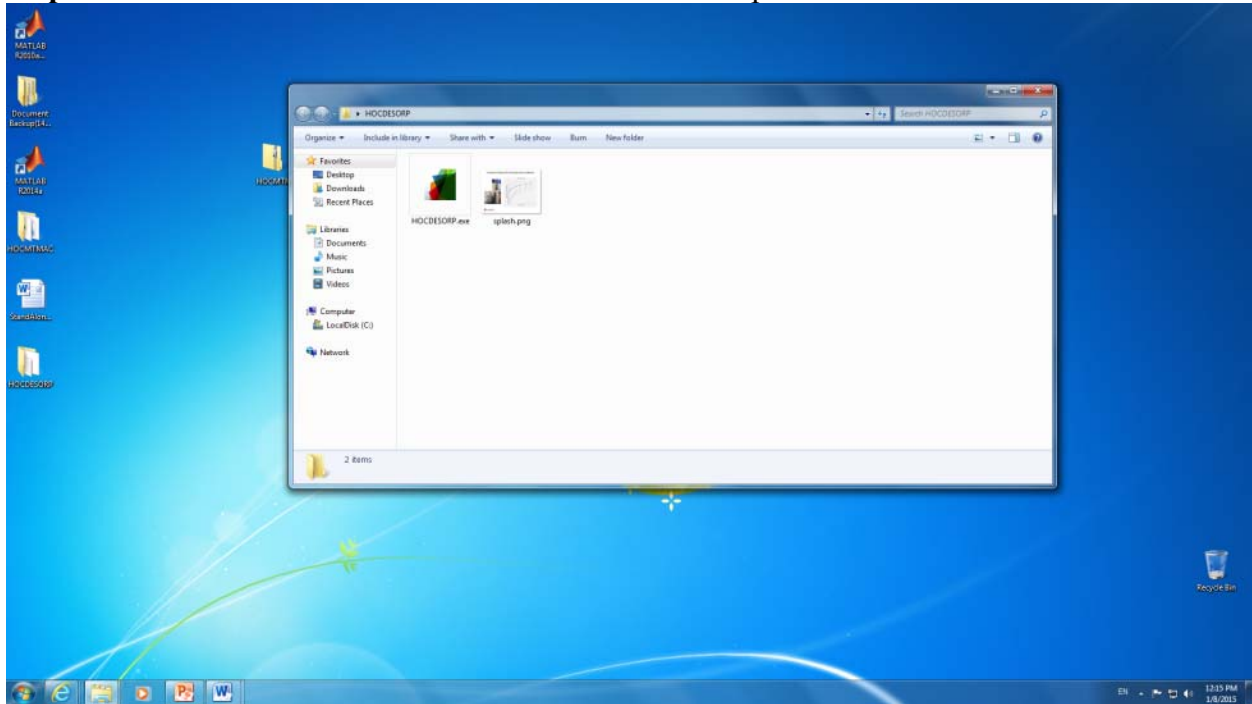
Contacts: YeoMyoung Cho (daybreak@stanford.edu) / Richard G. Luthy (luthy@stanford.edu)

5. System Requirements

- Windows machine (64-bit processor)
- MS Excel
- MATLAB Compiler Runtime (MCR, R2014a (8.3)) available on <http://www.mathworks.com/products/compiler/mcr/index.html>

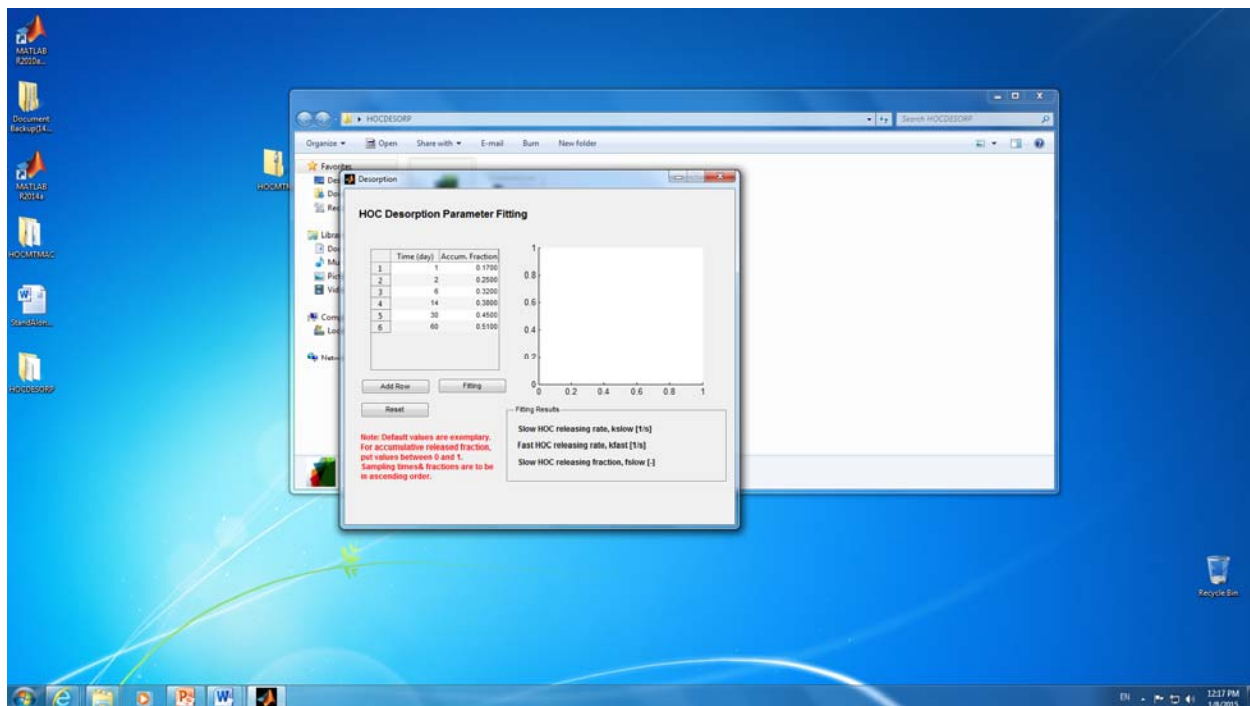
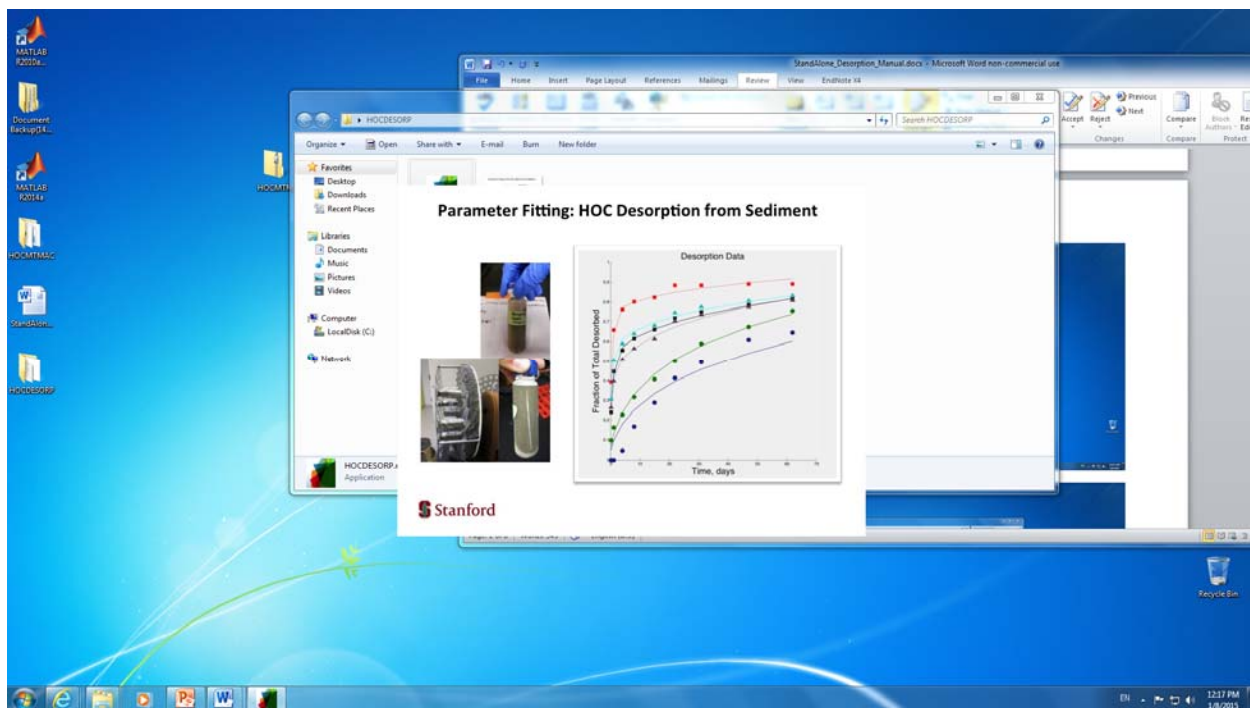
6. Operation

Step 1. Download and extract files from HOCDESORP.zip



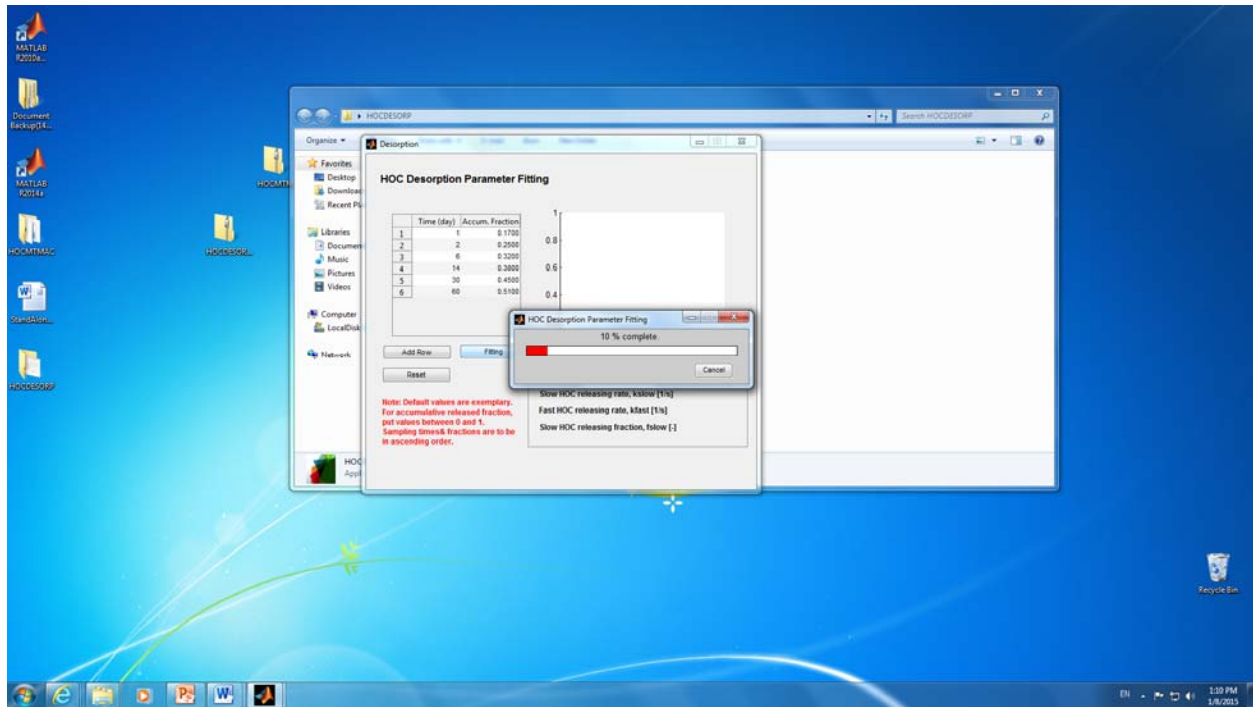
Two files are included. HOCDESORP.exe (MATLAB standalone executable file), and splash.png.

Step 2. Double click HOCDESORP.exe. After a splash screen, a GUI (graphic user interphase) will pop up.

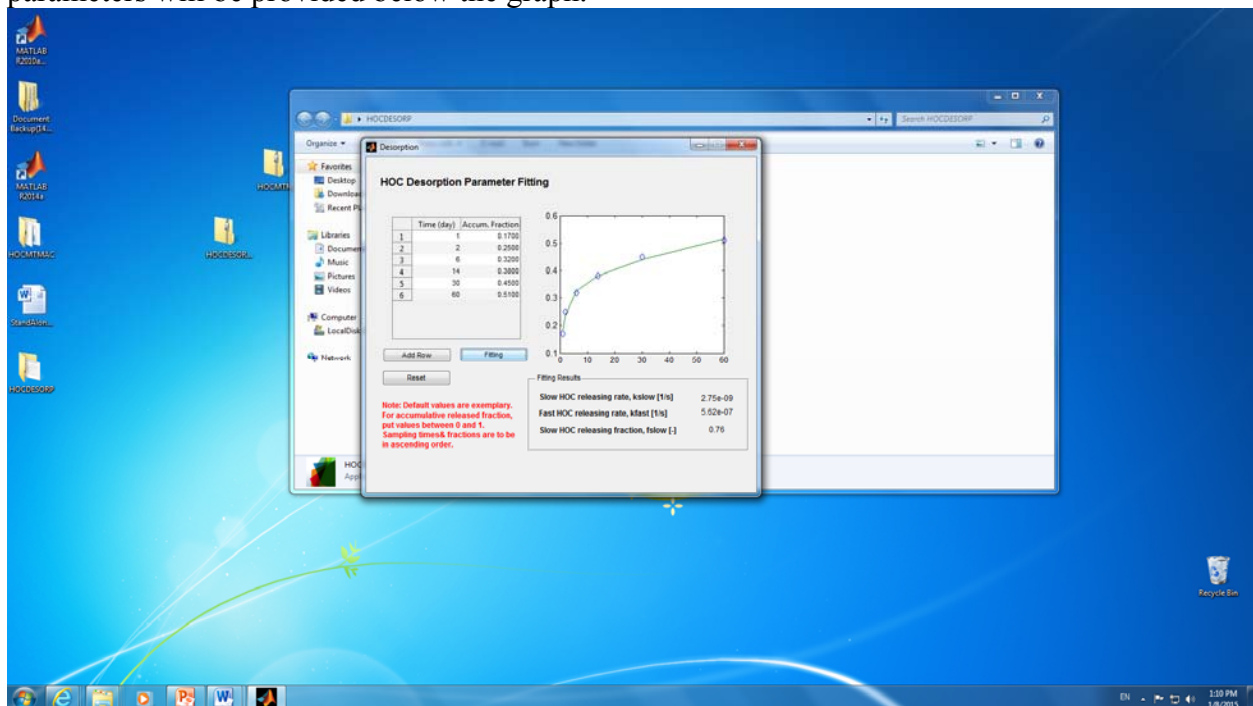


Step 3. On the left, there is a data entry form. The minimum number of data points is six. The data should be in ascending order for proper fitting. More rows can be added by clicking “Add Row” button.

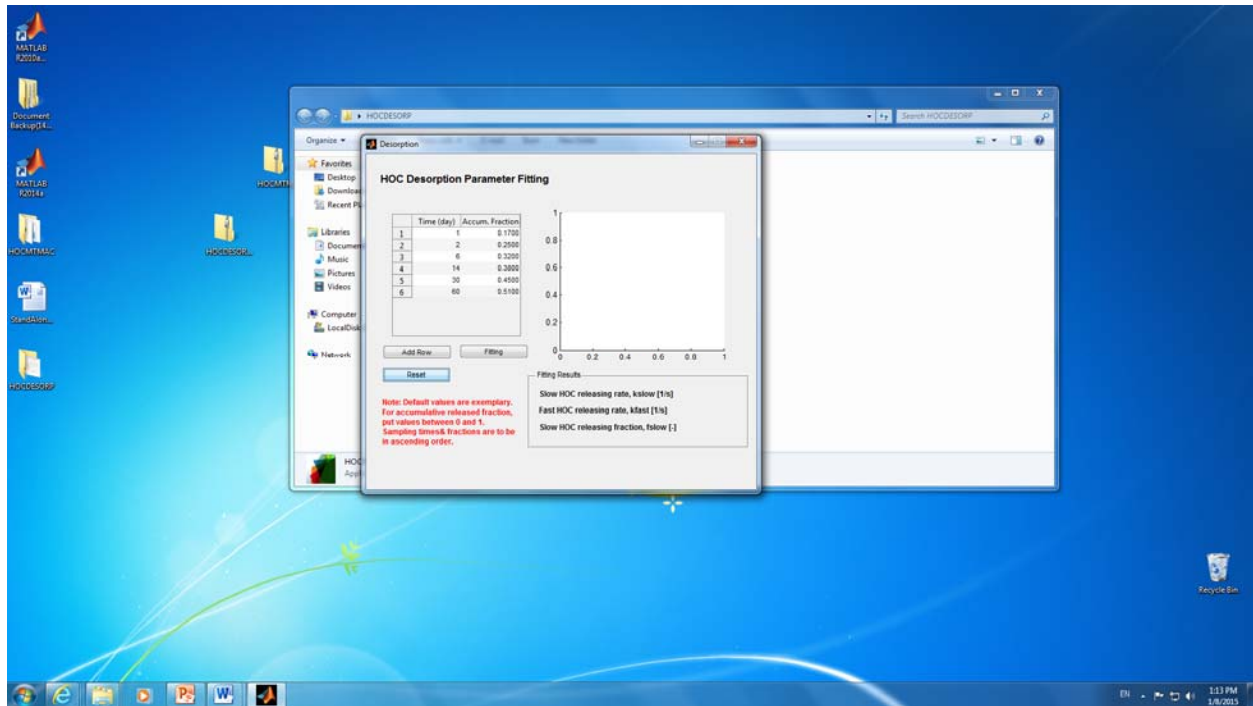
Step 4. Press 'Fitting' for desorption parameter fitting. A status bar will pop up and indicate the simulation progress.



Step 5. After simulation, fitting results will be shown in a graph on the right, and three parameters will be provided below the graph.



Step 6. Press “Reset” button to reset all fields for next fitting operations. To exit the program, simply press the close button at the right top corner.



7. References

- Werner D, Ghosh U, Luthy RG. *Environ. Sci. Technol.*, **2006**, 40 (13), pp 4211–4218
 Cho Y-M, Werner D, Choi Y, and Luthy RG. *J. Cont. Hydrol.*, **2011**, 129, pp 25-37
 Choi Y, Cho Y-M, Werner D, and Luthy RG. *Environ. Sci. Technol.*, **2014**, 48 (3), pp 1843–1850

3. Booklet for Exemplary Results of HOC Mass Transfer Model for the Effectiveness of Activated Carbon Amendment

Booklet for Exemplary Results of HOC Mass Transfer Model for the Effectiveness of Activated Carbon Amendment

This booklet is aimed to assist those who consider the application of in-situ activated carbon (AC) amendment as a remediation technique for sediment sites impacted by hydrophobic organic contaminants (HOCs). An HOC mass transfer model, which has been validated for reliable prediction of the effectiveness of AC amendment by laboratory and pilot-scale studies, was used to generate simulation results for each field site shown as pore-water HOC concentrations. The modeling results are presented for ten field sites with different site characteristics and HOCs of concern.

The readers are suggested to first briefly review the general information given for each field site in the booklet to select a site that is most similar to the site of their own interest. After reviewing the site-specific model input parameters for the corresponding site, the readers can check the example modeling results shown for two or three representative HOCs for the site. The example modeling results will guide readers to decide whether or not in-situ AC amendment will be effective for the sediment site of their concern.

Site#1: Hunters Point Shipyard, CA, USA

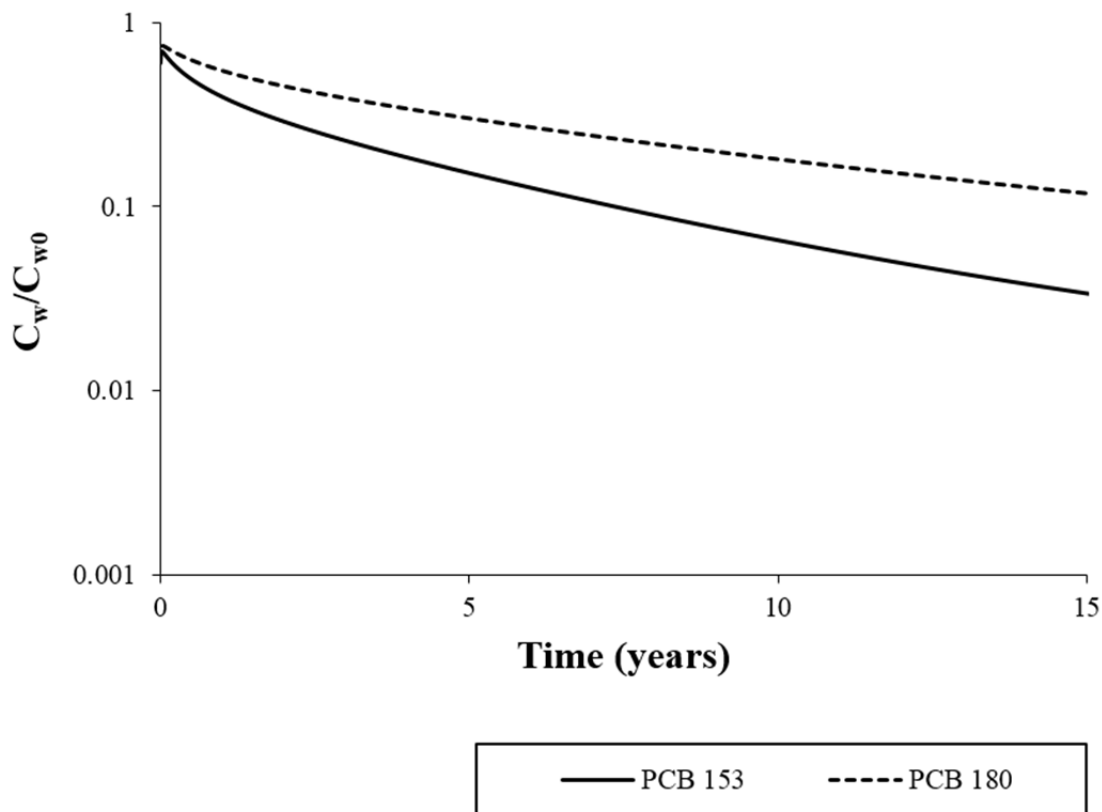
A. General information

Site information	tidal mudflat, former naval shipyard, site closure in 1991
Contaminants of concern	PCBs; 1.09 mg/kg as total (for the pilot study plot)
Sediment & contaminant information	moderate PCB release rate; PCB abundance order hepta- > hexa- > octa-chlorobiphenyls; very small amount of fine coal-like fragments
Total organic carbon (%)	1.7
Black carbon (%)	0.29

B. Model input parameters

Parameters	Unit	Symbol	Model compounds	
			PCB 153	PCB 180
Initial pore-water concentration	ng cm ⁻³	C _{w0}	9.4×10 ⁻⁴	7.3×10 ⁻⁴
Sediment-water distribution coefficient	cm ³ g ⁻¹	K _d	9.2×10 ⁴	1.7×10 ⁵
Fast-HOC-releasing rate	s ⁻¹	k _{fast}	6.8×10 ⁻⁸	6.8×10 ⁻⁸
Slow-HOC-releasing rate	s ⁻¹	k _{slow}	1.5×10 ⁻⁹	1.1×10 ⁻⁹
Fraction of slow-releasing HOC	-	f _{slow}	0.75	0.76
AC-water partitioning coefficient	cm ³ g ⁻¹	K _{AC}	8.8×10 ⁸	1.5×10 ⁹
Apparent AC intra-particle diffusion coefficient	cm ² s ⁻¹	D _{AC,app}	2.9×10 ⁻¹⁵	2.8×10 ⁻¹⁵

C. Model results



C_{w0} = model compound pore-water concentration before AC deployment

C_w = model compound pore-water concentration as a function of time after AC deployment

D. Related references

- Zimmerman, J. R.; Ghosh, U.; Millward, R. N.; Bridges, T. S.; Luthy, R. G. (2004) Addition of carbon sorbents to reduce PCB and PAH bioavailability in marine sediments: Physicochemical tests. *Environ. Sci. Technol.* 38, 5458-5464.
- Werner, D.; Hale, S. E.; Ghosh, U.; Luthy, R. G. (2010) Polychlorinated biphenyl sorption and availability in field-contaminated sediments. *Environ. Sci. Technol.* 44, 2809-2815.
- Choi, Y.; Cho, Y. -M.; Werner, D.; Luthy, R. -G. (2014) In situ sequestration of hydrophobic organic contaminants in sediments. 2. Mass transfer modeling. *Environ. Sci. Technol.* 48, 1843-1850.

Site#2: Lake Hartwell, SC, USA

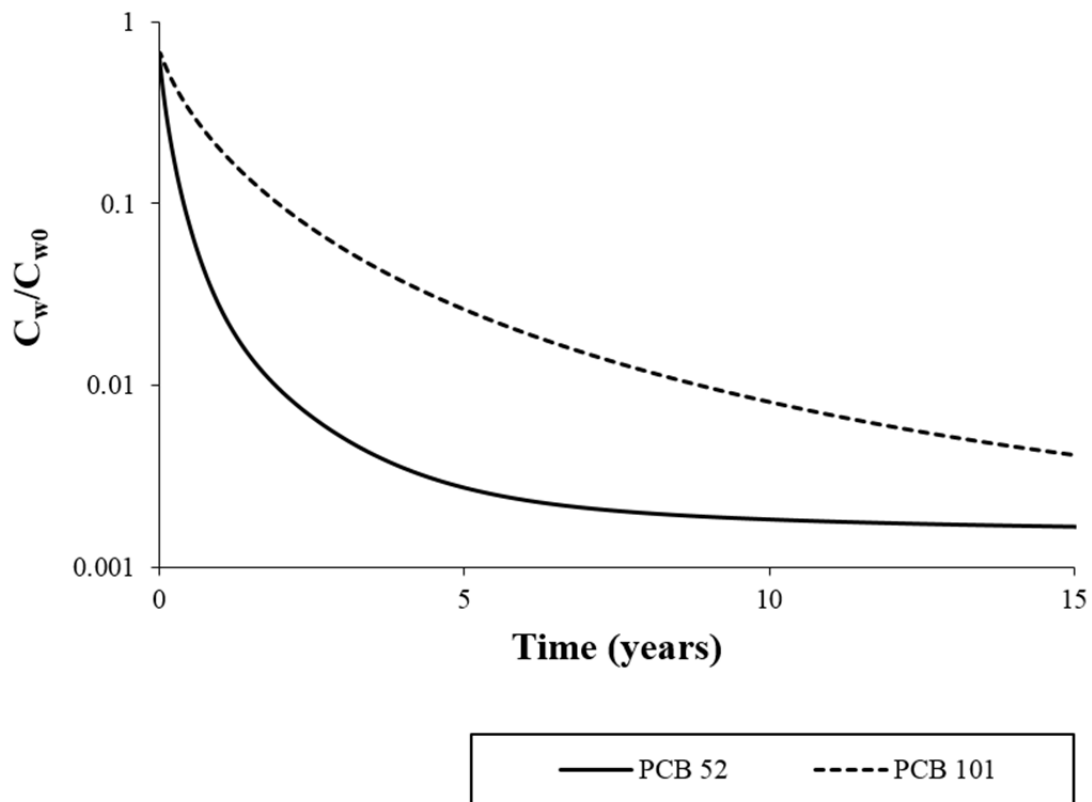
A. General information

Site information	freshwater sediment; site operation from 1955 to 1987
Contaminants of concern	PCBs; 1.25 mg/kg as total
Sediment & contaminant information	tetra- and penta-chlorobiphenyls dominant; fast PCB release rate (57% desorbs in 2 days); little coal-like fragments (<1% by volume)
Total organic carbon (%)	2.8
Black carbon (%)	Not available

B. Model input parameters

Parameters	Unit	Symbol	Model compounds	
			PCB 52	PCB 101
Initial pore-water concentration	ng cm ⁻³	C _{w0}	4.9×10 ⁻³	9.5×10 ⁻⁴
Sediment-water distribution coefficient	cm ³ g ⁻¹	K _d	1.1×10 ⁴	4.8×10 ⁴
Fast-HOC-releasing rate	s ⁻¹	k _{fast}	2.8×10 ⁻⁷	1.9×10 ⁻⁷
Slow-HOC-releasing rate	s ⁻¹	k _{slow}	2.3×10 ⁻¹³	6.6×10 ⁻¹³
Fraction of slow-releasing HOC	-	f _{slow}	0.21	0.22
AC-water partitioning coefficient	cm ³ g ⁻¹	K _{AC}	2.3×10 ⁸	1.5×10 ⁹
Apparent AC intra-particle diffusion coefficient	cm ² s ⁻¹	D _{AC,app}	1.4×10 ⁻¹⁴	2.1×10 ⁻¹⁵

C. Model results



C_{w0} = model compound pore-water concentration before AC deployment

C_w = model compound pore-water concentration as a function of time after AC deployment

D. Related references

Werner, D. ; Higgins, C. P.; Luthy, R. G. (2005) The sequestration of PCBs in Lake Hartwell sediment with activated carbon. *Water Res.* 39, 2105-2113.

Werner, D.; Ghosh, U.; Luthy, R. G. (2006) Modeling polychlorinated biphenyl mass transfer after amendment of contaminated sediment with activated carbon. *Environ. Sci. Technol.* 40, 4211-4218.

Werner, D.; Hale, S. E.; Ghosh, U.; Luthy, R. G. (2010) Polychlorinated biphenyl sorption and availability in field-contaminated sediments. *Environ. Sci. Technol.* 44, 2809-2815.

Site#3: Crab Orchard Lake, IL, USA

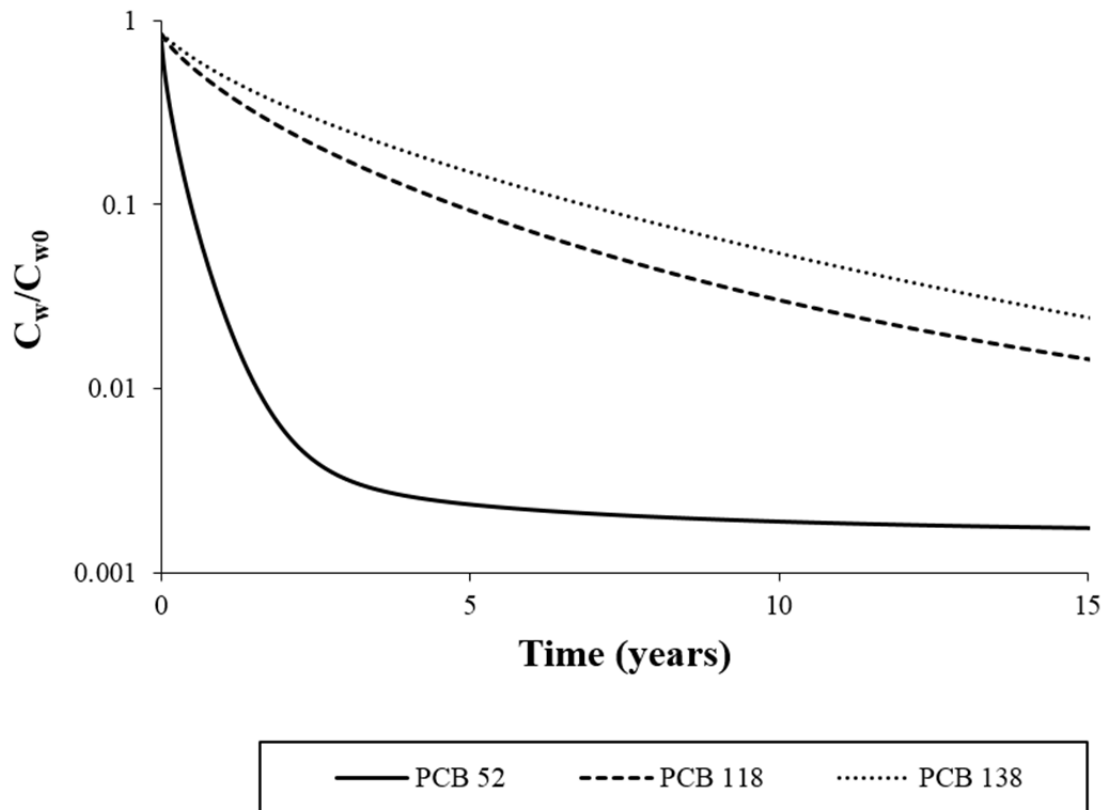
A. General information

Site information	freshwater sediment; legacy contamination (contaminated before 1970)
Contaminants of concern	PCBs; 29.15 mg/kg as aroclor 1254 PCBs
Sediment & contaminant information	high clay/silt fraction (86%); PCB abundance order penta- > hexa- > tetra-chlorobiphenyls
Total organic carbon (%)	0.59
Black carbon (%)	Not available

B. Model input parameters

Parameters	Unit	Symbol	Model compounds		
			PCB 52	PCB 118	PCB 138
Initial pore-water concentration	ng cm ⁻³	C _{w0}	3.0×10 ⁻³	6.0×10 ⁻⁴	3.9×10 ⁻⁴
Sediment-water distribution coefficient	cm ³ g ⁻¹	K _d	2.1×10 ³	1.9×10 ⁴	3.1×10 ⁴
Fast-HOC-releasing rate	s ⁻¹	k _{fast}	6.8×10 ⁻⁷	8.8×10 ⁻⁷	8.8×10 ⁻⁷
Slow-HOC-releasing rate	s ⁻¹	k _{slow}	6.8×10 ⁻⁸	1.9×10 ⁻⁸	3.2×10 ⁻⁸
Fraction of slow-releasing HOC	-	f _{slow}	0.52	0.62	0.56
AC-water partitioning coefficient	cm ³ g ⁻¹	K _{AC}	2.3×10 ⁸	2.8×10 ⁹	3.6×10 ⁹
Apparent AC intra-particle diffusion coefficient	cm ² s ⁻¹	D _{AC,app}	1.5×10 ⁻¹⁴	1.2×10 ⁻¹⁵	8.8×10 ⁻¹⁶

C. Model results



C_{w0} = model compound pore-water concentration before AC deployment
 C_w = model compound pore-water concentration as a function of time after AC deployment

D. Related references

- You, J.; Landrum, P. E.; Trimble, T. A.; Lydy, M. J. (2007) Availability of polychlorinated biphenyls in field-contaminated sediment. *Environ. Toxicol. Chem.* 26, 1940-1948.
- Werner, D.; Hale, S. E.; Ghosh, U.; Luthy, R. G. (2010) Polychlorinated biphenyl sorption and availability in field-contaminated sediments. *Environ. Sci. Technol.* 44, 2809-2815.

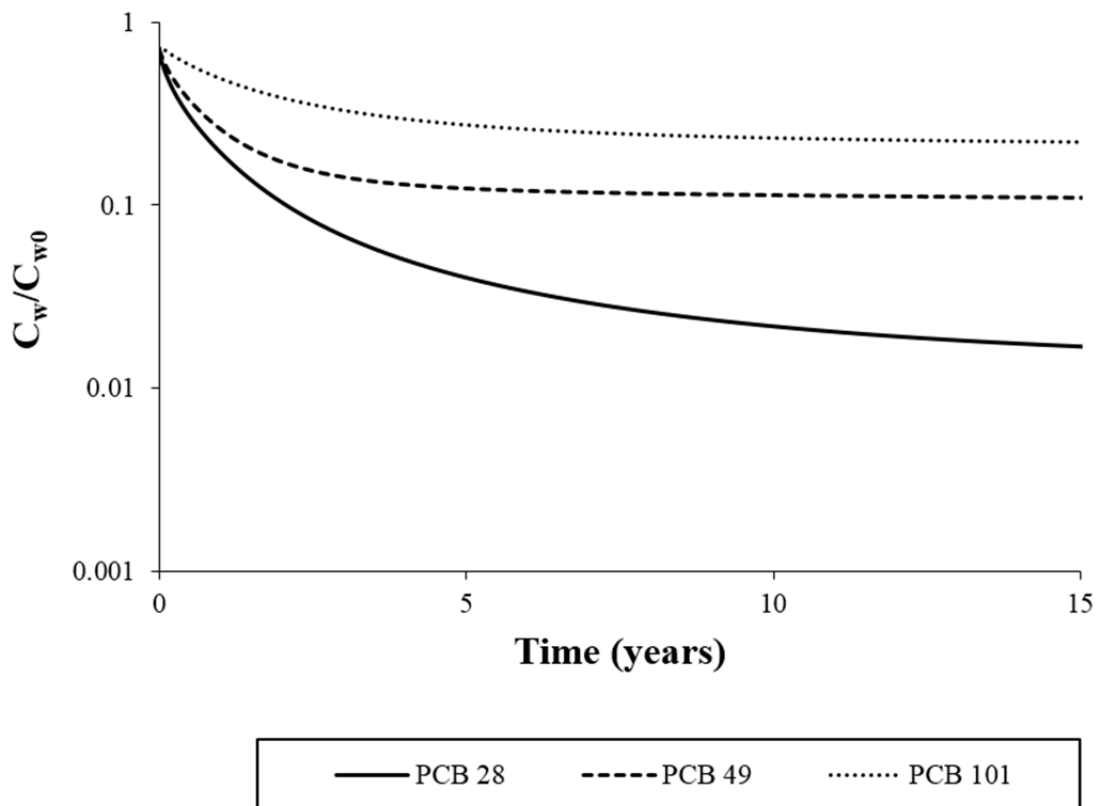
Site#4: Eastbrook Park, Milwaukee River, WI, USA, location 1**A. General information**

Site information	freshwater sediment from the Great Lakes
Contaminants of concern	PCBs; 45.2 mg/kg
Sediment & contaminant information	PCB abundance order tetra- > tri- > penta-chlorobiphenyls; presence of some coal-derived particles
Total organic carbon (%)	3.22
Black carbon (%)	0.64

B. Model input parameters

Parameters	Unit	Symbol	Model compounds		
			PCB 28	PCB 49	PCB 101
Initial pore-water concentration	ng cm ⁻³	C _{w0}	6.0×10 ⁻²	3.3×10 ⁻²	6.9×10 ⁻³
Sediment-water distribution coefficient	cm ³ g ⁻¹	K _d	3.9×10 ⁴	4.8×10 ⁴	1.6×10 ⁵
Fast-HOC-releasing rate	s ⁻¹	k _{fast}	5.3×10 ⁻⁷	4.1×10 ⁻⁷	8.8×10 ⁻⁸
Slow-HOC-releasing rate	s ⁻¹	k _{slow}	1.1×10 ⁻⁸	1.9×10 ⁻⁸	3.2×10 ⁻¹⁴
Fraction of slow-releasing HOC	-	f _{slow}	0.40	0.39	0.09
AC-water partitioning coefficient	cm ³ g ⁻¹	K _{AC}	1.2×10 ⁸	1.2×10 ⁷	1.7×10 ⁷
Apparent AC intra-particle diffusion coefficient	cm ² s ⁻¹	D _{AC,app}	3.0×10 ⁻¹⁴	2.8×10 ⁻¹³	1.9×10 ⁻¹³

C. Model results



C_{w0} = model compound pore-water concentration before AC deployment

C_w = model compound pore-water concentration as a function of time after AC deployment

D. Related references

Sun, X.; Ghosh, U. (2008) The effect of activated carbon on partitioning, desorption, and biouptake of native polychlorinated biphenyls in four freshwater sediments. *Environ. Toxicol. Chem.* 27, 2287-2295.

Werner, D.; Hale, S. E.; Ghosh, U.; Luthy, R. G. (2010) Polychlorinated biphenyl sorption and availability in field-contaminated sediments. *Environ. Sci. Technol.* 44, 2809-2815.

Hale, S. E.; Kwon, S.; Ghosh, U.; Werner, D. (2010) Polychlorinated biphenyl sorption to activated carbon and the attenuation caused by sediment. *Global NEST J.* 12, 318-326.

Site#5: Eastbrook Park, Milwaukee River, WI, USA, location 2

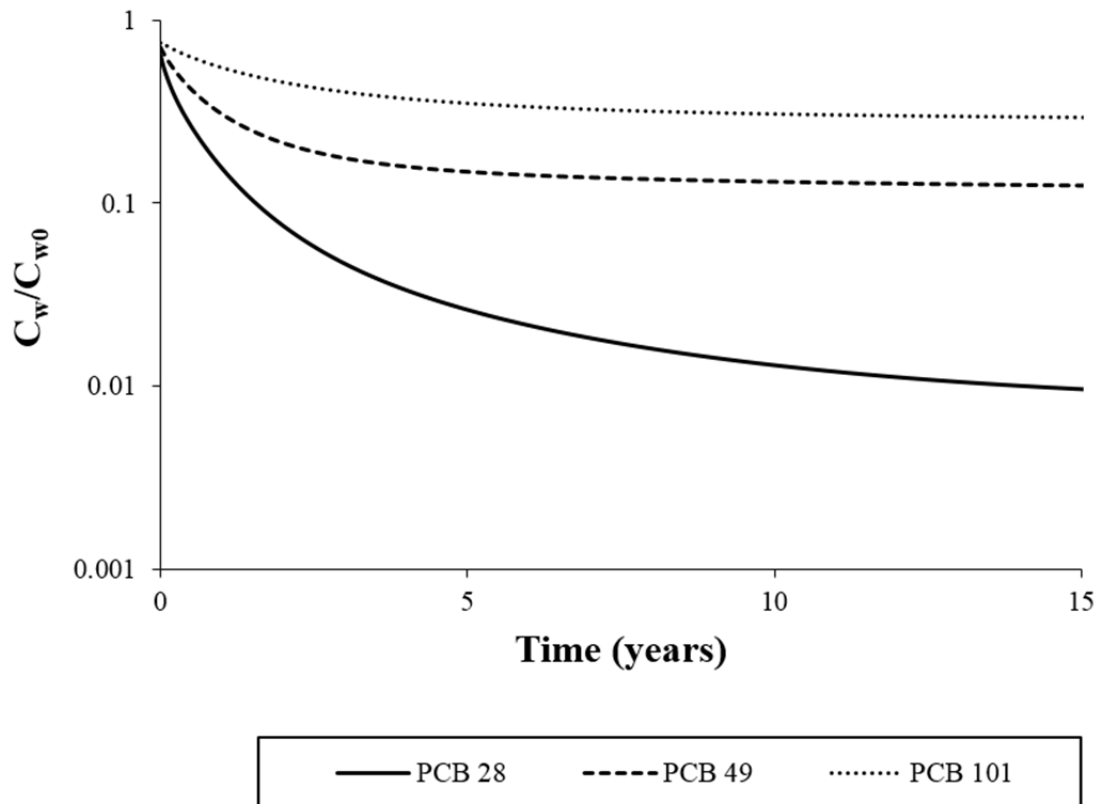
A. General information

Site information	freshwater sediment from the Great Lakes
Contaminants of concern	PCBs; 87.4 mg/kg
Sediment & contaminant information	PCB abundance order tetra- > tri- > penta-chlorobiphenyls; presence of some coal-derived particles
Total organic carbon (%)	3.70
Black carbon (%)	0.62

B. Model input parameters

Parameters	Unit	Symbol	Model compounds		
			PCB 28	PCB 49	PCB 101
Initial pore-water concentration	ng cm ⁻³	C _{w0}	1.7×10 ⁻¹	5.1×10 ⁻²	7.5×10 ⁻³
Sediment-water distribution coefficient	cm ³ g ⁻¹	K _d	4.0×10 ⁴	5.7×10 ⁴	2.0×10 ⁵
Fast-HOC-releasing rate	s ⁻¹	k _{fast}	8.8×10 ⁻⁷	6.8×10 ⁻⁷	1.0×10 ⁻⁷
Slow-HOC-releasing rate	s ⁻¹	k _{slow}	1.5×10 ⁻⁸	8.8×10 ⁻⁸	1.0×10 ⁻⁹
Fraction of slow-releasing HOC	-	f _{slow}	0.34	0.73	0.11
AC-water partitioning coefficient	cm ³ g ⁻¹	K _{AC}	1.7×10 ⁸	1.3×10 ⁷	1.5×10 ⁷
Apparent AC intra-particle diffusion coefficient	cm ² s ⁻¹	D _{AC,app}	2.1×10 ⁻¹⁴	2.6×10 ⁻¹³	2.2×10 ⁻¹³

C. Model results



C_{w0} = model compound pore-water concentration before AC deployment

C_w = model compound pore-water concentration as a function of time after AC deployment

D. Related references

- Sun, X.; Ghosh, U. (2008) The effect of activated carbon on partitioning, desorption, and biouptake of native polychlorinated biphenyls in four freshwater sediments. *Environ. Toxicol. Chem.* 27, 2287-2295.
- Werner, D.; Hale, S. E.; Ghosh, U.; Luthy, R. G. (2010) Polychlorinated biphenyl sorption and availability in field-contaminated sediments. *Environ. Sci. Technol.* 44, 2809-2815.
- Hale, S. E.; Kwon, S.; Ghosh, U.; Werner, D. (2010) Polychlorinated biphenyl sorption to activated carbon and the attenuation caused by sediment. *Global NEST J.* 12, 318-326.

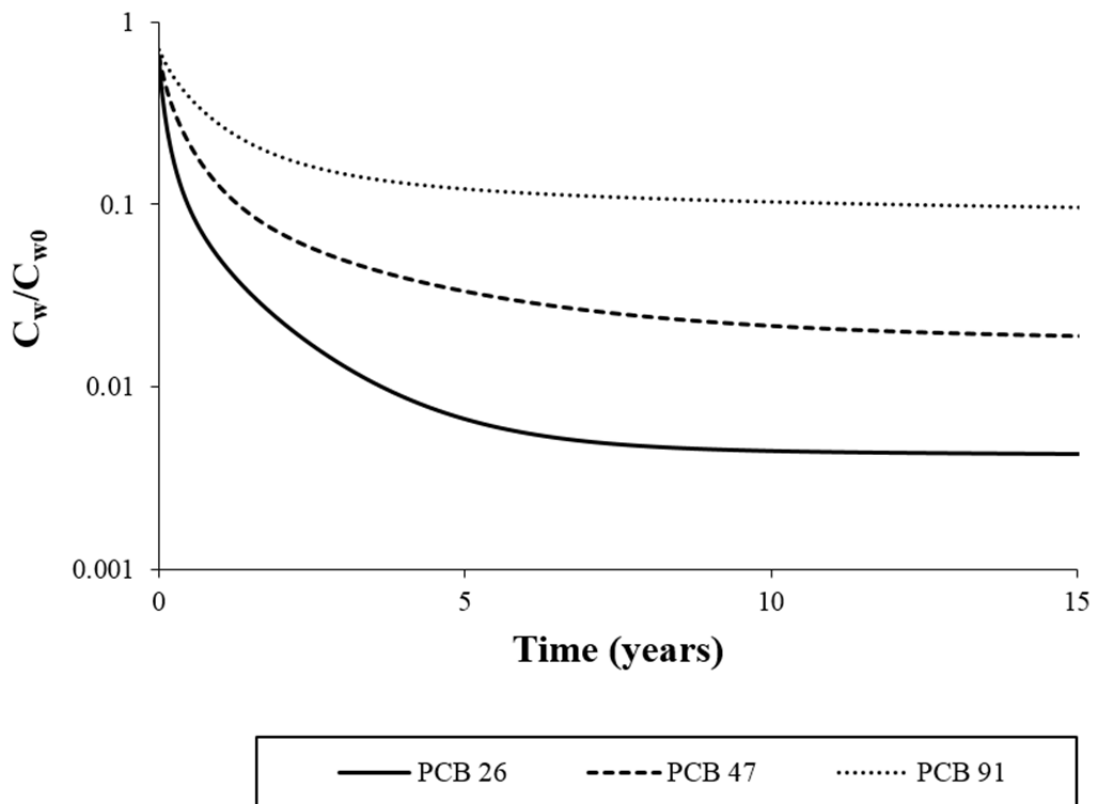
Site#6: Grasse River, NY, USA**A. General information**

Site information	freshwater sediment from the Great Lakes
Contaminants of concern	PCBs; 6.8 mg/kg as total
Sediment & contaminant information	tri- and tetra-chlorobiphenyls dominant; organic matter is mostly vegetative debris
Total organic carbon (%)	5.17
Black carbon (%)	0.365

B. Model input parameters

Parameters	Unit	Symbol	Model compounds		
			PCB 26	PCB 47	PCB 91
Initial pore-water concentration	ng cm ⁻³	C _{w0}	2.4×10 ⁻²	1.2×10 ⁻²	1.9×10 ⁻³
Sediment-water distribution coefficient	cm ³ g ⁻¹	K _d	9.8×10 ³	2.2×10 ⁴	4.7×10 ⁴
Fast-HOC-releasing rate	s ⁻¹	k _{fast}	1.0×10 ⁻⁶	6.0×10 ⁻⁷	4.0×10 ⁻⁷
Slow-HOC-releasing rate	s ⁻¹	k _{slow}	9.0×10 ⁻⁹	2.0×10 ⁻⁸	2.0×10 ⁻⁸
Fraction of slow-releasing HOC	-	f _{slow}	0.18	0.24	0.20
AC-water partitioning coefficient	cm ³ g ⁻¹	K _{AC}	7.9×10 ⁷	4.0×10 ⁷	1.6×10 ⁷
Apparent AC intra-particle diffusion coefficient	cm ² s ⁻¹	D _{AC,app}	4.4×10 ⁻¹⁴	8.4×10 ⁻¹⁴	2.1×10 ⁻¹³

C. Model results



C_{w0} = model compound pore-water concentration before AC deployment

C_w = model compound pore-water concentration as a function of time after AC deployment

D. Related references

Sun, X.; Ghosh, U. (2008) The effect of activated carbon on partitioning, desorption, and biouptake of native polychlorinated biphenyls in four freshwater sediments. *Environ. Toxicol. Chem.* 27, 2287-2295.

Werner, D.; Hale, S. E.; Ghosh, U.; Luthy, R. G. (2010) Polychlorinated biphenyl sorption and availability in field-contaminated sediments. *Environ. Sci. Technol.* 44, 2809-2815.

Hale, S. E.; Kwon, S.; Ghosh, U.; Werner, D. (2010) Polychlorinated biphenyl sorption to activated carbon and the attenuation caused by sediment. *Global NEST J.* 12, 318-326.

Site#7: River Tyne, Newcastle upon Tyne, U.K.

A. General information

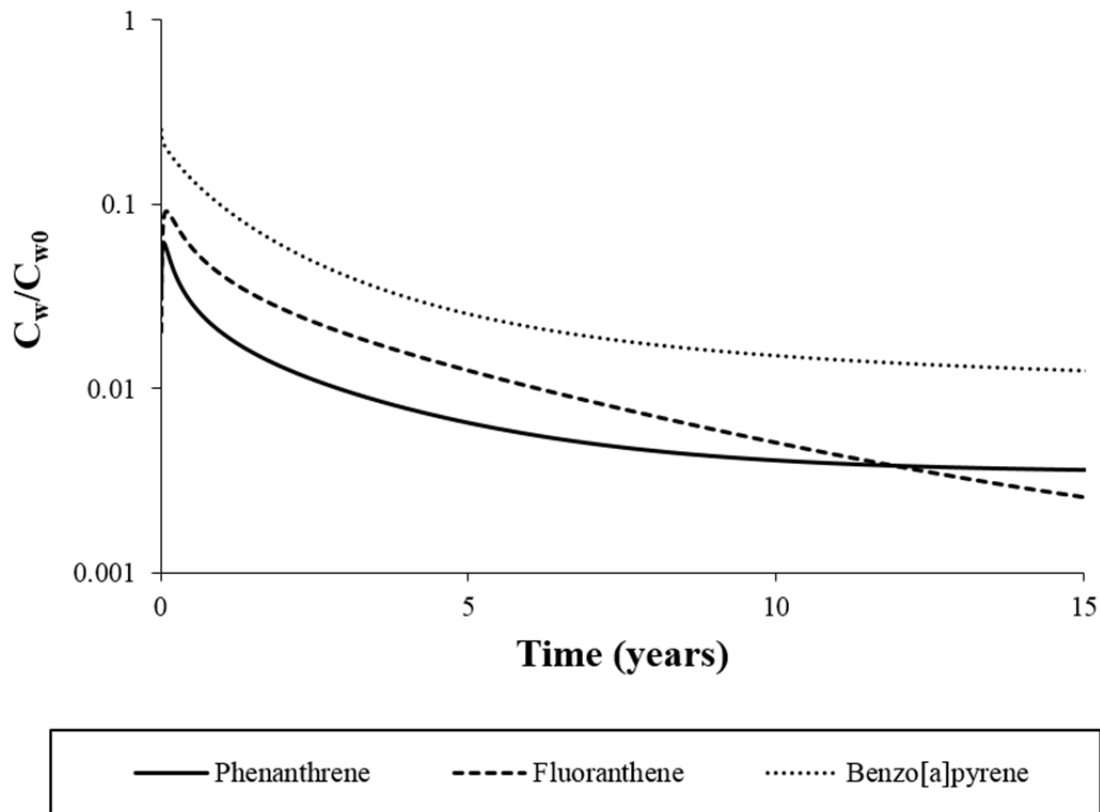
Site information	freshwater sediment
Contaminants of concern	PAHs; 25 mg/kg as total parent PAHs
Sediment & contaminant information	very slow PAH release rate (9% of total PAHs desorbs in 112 days); dominance of fine particles; majority of organic matter is coal-like particles
Total organic carbon (%)	5.06
Black carbon (%)	N/A

B. Model input parameters

Parameters	Unit	Symbol	Model compounds		
			PHEN	FLUA	BaP
Initial pore-water concentration	ng cm ⁻³	C _{w0}	3.0×10 ⁻¹	1.7×10 ⁻¹	1.4×10 ⁻³
Sediment-water distribution coefficient	cm ³ g ⁻¹	K _d	1.0×10 ⁴	3.2×10 ⁴	1.3×10 ⁶
Fast-HOC-releasing rate	s ⁻¹	k _{fast}	1.3×10 ⁻⁹	7.9×10 ⁻¹⁰	3.2×10 ⁻¹⁴
Slow-HOC-releasing rate	s ⁻¹	k _{slow}	3.2×10 ⁻¹²	3.2×10 ⁻¹⁴	3.2×10 ⁻¹⁴
Fraction of slow-releasing HOC	-	f _{slow}	0.47	0.56	0.46
AC-water partitioning coefficient	cm ³ g ⁻¹	K _{AC}	6.3×10 ⁷	5.0×10 ⁸	4.0×10 ⁸
Apparent AC intra-particle diffusion coefficient	cm ² s ⁻¹	D _{AC,app}	7.9×10 ⁻¹⁴	7.9×10 ⁻¹⁵	7.9×10 ⁻¹⁵

* Abbreviations: PHEN, phenanthrene; FLUA, fluoranthene; BaP, benzo(a)pyrene

C. Model results



C_{w0} = model compound pore-water concentration before AC deployment

C_w = model compound pore-water concentration as a function of time after AC deployment

D. Related reference

Hale, S. E.; Werner, D. (2010) Modeling the mass transfer of hydrophobic organic pollutants in briefly and continuously mixed sediment after amendment with activated carbon. Environ. Sci. Technol. 44, 3381-3387.

Site#8: Undisclosed, petroleum-impacted site, USA

A. General information

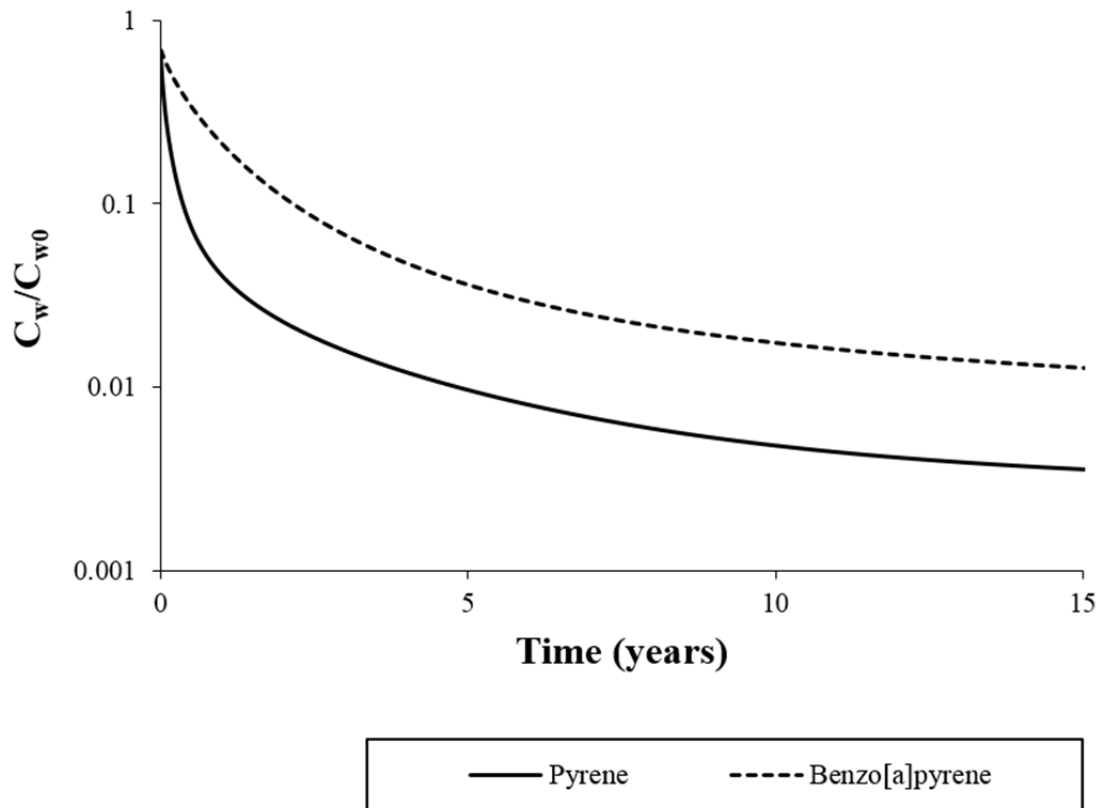
Site information	estuarine channel sediment, impacted by petroleum
Contaminants of concern	PAHs; 125 mg/kg as total (parent + alkylated) and 11.6 mg/kg as total parent PAHs
Sediment & contaminant information	very fast PAH release rate; high alkylated-PAH abundance; 4-ring dominant for parent PAHs and C4-naphthalenes/C3-fluorenes dominant for alkylated PAHs; 1.1% oil & grease content
Total organic carbon (%)	4.0
Black carbon (%)	0.73

B. Model input parameters

Parameters	Unit	Symbol	Model compounds	
			PYR	BaP
Initial pore-water concentration	ng cm ⁻³	C _{w0}	1.5×10 ⁻¹	7.3×10 ⁻³
Sediment-water distribution coefficient	cm ³ g ⁻¹	K _d	6.3×10 ³	4.8×10 ⁴
Fast-HOC-releasing rate	s ⁻¹	k _{fast}	4.1×10 ⁻⁶	5.3×10 ⁻⁷
Slow-HOC-releasing rate	s ⁻¹	k _{slow}	5.3×10 ⁻⁸	2.5×10 ⁻⁸
Fraction of slow-releasing HOC	-	f _{slow}	0.18	0.25
AC-water partitioning coefficient	cm ³ g ⁻¹	K _{AC}	1.0×10 ⁸	2.0×10 ⁸
Apparent AC intra-particle diffusion coefficient	cm ² s ⁻¹	D _{AC,app}	5.1×10 ⁻¹⁵	5.0×10 ⁻¹⁵

* Abbreviations: PYR, pyrene; BaP, benzo(a)pyrene

C. Model results



C_{w0} = model compound pore-water concentration before AC deployment

C_w = model compound pore-water concentration as a function of time after AC deployment

D. Related references

- Choi, Y.; Cho, Y. -M.; Gala, W. -R.; Luthy, R. G. (2013) Measurement and modeling of activated carbon performance for the sequestration of parent- and alkylated-polycyclic aromatic hydrocarbons in petroleum-impacted sediments. *Environ. Sci. Technol.* 47, 1024-1032.
- Choi, Y.; Cho, Y. -M.; Werner, D.; Luthy, R. -G. (2014) In situ sequestration of hydrophobic organic contaminants in sediments. 2. Mass transfer modeling. *Environ. Sci. Technol.* 48, 1843-1850.

Site#9: Lauritzen Channel, Richmond, CA, USA

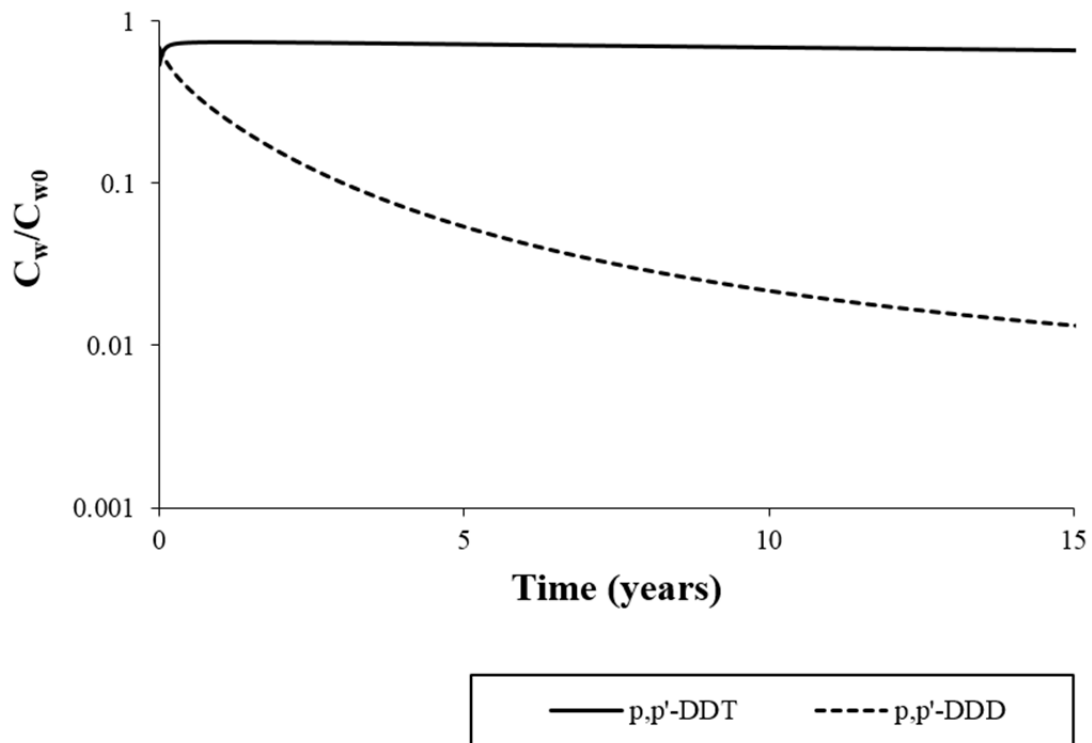
A. General information

Site information	estuarine channel; site operation from 1947 to 1966
Contaminants of concern	DDTs; 7.5-252 mg/kg as total (including metabolites)
Sediment & contaminant information	high clay/silt fraction (82%); very little black carbon particles (0.6% by volume); DDT desorbs 20% or less in 55 days but DDD, DDE, and DDMU desorbs >57% in 55 days
Total organic carbon (%)	2.8
Black carbon (%)	Not available

B. Model input parameters

Parameters	Unit	Symbol	Model compounds	
			p,p'-DDT	p,p'-DDD
Initial pore-water concentration	ng cm ⁻³	C _{w0}	1.3×10 ⁻²	1.5×10 ⁻¹
Sediment-water distribution coefficient	cm ³ g ⁻¹	K _d	5.6×10 ⁶	6.1×10 ⁴
Fast-HOC-releasing rate	s ⁻¹	k _{fast}	8.8×10 ⁻¹⁰	1.5×10 ⁻⁶
Slow-HOC-releasing rate	s ⁻¹	k _{slow}	2.5×10 ⁻¹⁰	3.2×10 ⁻¹⁰
Fraction of slow-releasing HOC	-	f _{slow}	0.36	0.25
AC-water partitioning coefficient	cm ³ g ⁻¹	K _{AC}	9.1×10 ⁸	3.0×10 ⁸
Apparent AC intra-particle diffusion coefficient	cm ² s ⁻¹	D _{AC,app}	2.9×10 ⁻¹⁵	9.5×10 ⁻¹⁵

C. Model results



C_{w0} = model compound pore-water concentration before AC deployment

C_w = model compound pore-water concentration as a function of time after AC deployment

D. Related references

Tomaszewski, J. E.; Werner, D.; Luthy, R. G. (2007) Activated carbon amendment as a treatment for residual DDT in sediment from a Superfund site in San Francisco Bay, Richmond, California, USA. *Environ. Toxicol. Chem.* 26, 2143-2150.

Hale, S. E.; Tomaszewski, J. E.; Luthy, R. G.; Werner, D. (2009) Sorption of dichlorodiphenyltrichloroethylene (DDT) and its metabolites by activated carbon in clean water and sediment slurries. *Water Res.* 43, 4336-4346.

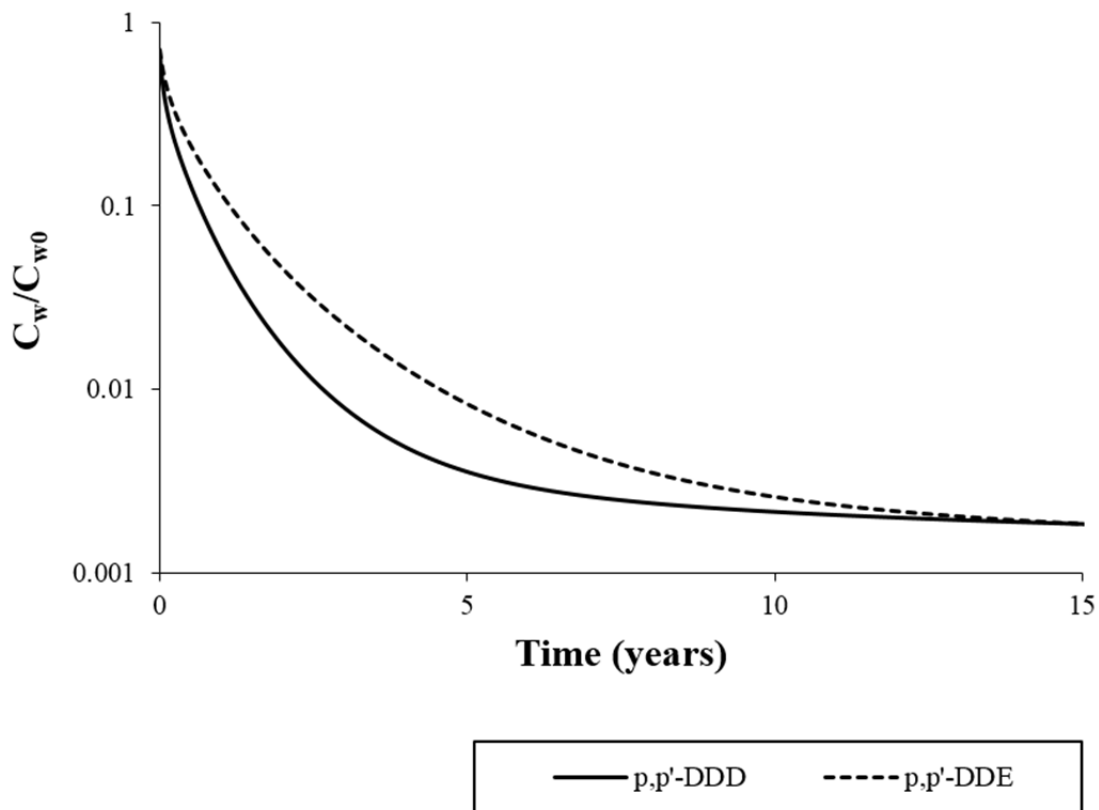
Site#10: Undisclosed, freshwater lake, Italy**A. General information**

Site information	Freshwater sediment
Contaminants of concern	DDTs; 1.8 mg/kg as total (including metabolites)
Sediment & contaminant information	very fine clayey silt
Total organic carbon (%)	1.9
Black carbon (%)	Not available

B. Model input parameters

Parameters	Unit	Symbol	Model compounds	
			p,p'-DDD	p,p'-DDE
Initial pore-water concentration	ng cm ⁻³	C _{w0}	1.5×10 ⁻¹	2.1×10 ⁻²
Sediment-water distribution coefficient	cm ³ g ⁻¹	K _d	6.8×10 ³	1.3×10 ⁴
Fast-HOC-releasing rate	s ⁻¹	k _{fast}	1.9×10 ⁻⁶	1.1×10 ⁻⁶
Slow-HOC-releasing rate	s ⁻¹	k _{slow}	1.5×10 ⁻⁸	1.1×10 ⁻⁸
Fraction of slow-releasing HOC	-	f _{slow}	0.63	0.53
AC-water partitioning coefficient	cm ³ g ⁻¹	K _{AC}	3.0×10 ⁸	8.1×10 ⁸
Apparent AC intra-particle diffusion coefficient	cm ² s ⁻¹	D _{AC,app}	5.2×10 ⁻¹⁵	1.9×10 ⁻¹⁵

C. Model results



C_{w0} = model compound pore-water concentration before AC deployment

C_w = model compound pore-water concentration as a function of time after AC deployment

D. Related references

- Hale, S. E.; Tomaszewski, J. E.; Luthy, R. G.; Werner, D. (2009) Sorption of dichlorodiphenyltrichloroethylene (DDT) and its metabolites by activated carbon in clean water and sediment slurries. *Water Res.* 43, 4336-4346.
- Hale, S. E.; Werner, D. (2010) Modeling the mass transfer of hydrophobic organic pollutants in briefly and continuously mixed sediment after amendment with activated carbon. *Environ. Sci. Technol.* 44, 3381-3387.
- Lin, D.; Cho, Y. -M.; Werner, D.; Luthy, R. G. (2014) Bioturbation delays attenuation of DDT by clean sediment cap but promotes sequestration by thin-layered activated carbon. *Environ. Sci. Technol.* 48, 1175-1183.

Appendix C. Numerical Data for Figures

As supporting information, numerical data used to construct Figures 4, 5, and 7-14 are provided in this section.

Table C1. Numerical data for Figure 4: 1-d and 28-d Tenax uptake relative to the total amount of PCBs in sediment slurry immediately after PCB sequestration ($n=3$, average \pm standard deviation).

Compound	Treatment	1-d Tenax uptake	28-d Tenax uptake
PCB101	Untreated	0.2813 \pm 0.0238	0.3662 \pm 0.0254
	PCB sequestered	0.0094 \pm 0.0028	0.0615 \pm 0.0134
PCB153	Untreated	0.2380 \pm 0.0231	0.3192 \pm 0.0212
	PCB sequestered	0.0093 \pm 0.0034	0.0430 \pm 0.0066
PCB 180	Untreated	0.1656 \pm 0.0223	0.2365 \pm 0.0238
	PCB sequestered	0.0075 \pm 0.0039	0.0351 \pm 0.0108

Table C2. Numerical data for Figure 5: 1-d and Tenax uptake relative to the total amount of PCBs applying different mixing times of mixing after PCB sequestration ($n=3$, average \pm standard deviation).

Compound	Mixing time	Treatment	1-d Tenax uptake
PCB101	0 month	Untreated	0.2813 \pm 0.0238
		PCB sequestered	0.0094 \pm 0.0028
	1 month	Untreated	0.2804 \pm 0.0387
		PCB sequestered	0.0370 \pm 0.0206
	3 months	Untreated	0.3434 \pm 0.0905
		PCB sequestered	0.0167 \pm 0.0010
	6 months	Untreated	0.2874 \pm 0.0235
		PCB sequestered	0.0159 \pm 0.0001
	12 months	Untreated	0.2933 \pm 0.0903
		PCB sequestered	0.0362 \pm 0.0046
	0 month	Untreated	0.2380 \pm 0.0231
		PCB sequestered	0.0093 \pm 0.0034
PCB153	1 month	Untreated	0.2642 \pm 0.0263
		PCB sequestered	0.0367 \pm 0.0224
	3 months	Untreated	0.2646 \pm 0.1359
		PCB sequestered	0.0180 \pm 0.0004
	6 months	Untreated	0.2571 \pm 0.0137
		PCB sequestered	0.0165 \pm 0.0027

PCB 180	12 months	Untreated	0.3189±0.0763
		PCB sequestered	0.0283±0.0030
	0 month	Untreated	0.1656±0.0223
		PCB sequestered	0.0075±0.0039
	1 month	Untreated	0.2123±0.0148
		PCB sequestered	0.0339±0.0184
	3 months	Untreated	0.2313±0.1312
		PCB sequestered	0.0172±0.0013
	6 months	Untreated	0.1938±0.0099
		PCB sequestered	0.0177±0.0037
	12 months	Untreated	0.3000±0.0547
		PCB sequestered	0.0228±0.0070

Table C3. Numerical data for Figure 7: Uptake and release kinetics of five PCB congeners for PE in water. The experimental values are shown as mass fraction remaining in PE relative to the amount at equilibrium for uptake kinetics and relative to the initially spiked amount for release kinetics ($n=3$, average±standard deviation).

Compound	Uptake kinetics		Release kinetics	
	Time (hr)	Mass fraction	Time (hr)	Mass fraction
PCB 29	0	0.000±0.000	0	1.000±0.000
	5	0.483±0.147	5	0.741±0.010
	24	0.932±0.085	24	0.365±0.014
	120	0.991±0.042	120	0.155±0.035
PCB 69	0	0.000±0.000	0	1.000±0.000
	5	0.321±0.098	5	0.866±0.008
	24	0.745±0.033	24	0.601±0.004
	120	0.996±0.044	120	0.272±0.006
PCB 103	0	0.000±0.000	0	1.000±0.000
	5	0.193±0.071	5	0.924±0.011
	24	0.507±0.012	24	0.766±0.010
	120	0.866±0.041	120	0.444±0.035
PCB 155	600	0.963±0.023	696	0.170±0.032
	0	0.000±0.000	0	1.000±0.000
	5	0.113±0.046	5	0.951±0.010
	24	0.316±0.066	24	0.889±0.008
PCB 192	120	0.731±0.074	120	0.667±0.063
	600	0.968±0.030	696	0.197±0.009
	1200	0.967±0.037	1200	0.132±0.008
	0	0.000±0.000	0	1.000±0.000

5	0.000±0.000	5	0.994±0.002
24	0.038±0.006	24	0.970±0.011
120	0.165±0.028	120	0.870±0.033
600	0.504±0.100	696	0.460±0.036
1200	0.711±0.051	1200	0.369±0.032
1920	0.842±0.095	1920	0.309±0.030
3000	0.900±0.020	3000	0.045±0.039

Table C4. Numerical data for Figure 8: PE concentrations for PCB PRCs, congeners 29, 69, 103, 155, and 192, in different types of PEs relative to the PE concentrations in 51 µm Brentwood PE after equilibrating in a single batch of 80:20 (v:v) methanol:water solution ($n=3$, average±standard deviation).

Compound	51 µm Brentwood	17 µm Husky	51 µm Husky	102 µm Husky
PCB 29	1.000±0.020	0.843±0.008	1.104±0.036	1.085±0.041
PCB 69	1.000±0.022	0.927±0.012	1.168±0.026	1.115±0.043
PCB 103	1.000±0.031	0.907±0.013	1.186±0.022	1.126±0.043
PCB 155	1.000±0.103	0.852±0.015	1.122±0.096	1.156±0.034
PCB 192	1.000±0.030	0.858±0.010	1.172±0.054	1.276±0.024

Table C5. Numerical data for Figure 9: PE concentrations for PCB congeners 43, 101, 153, and 180 in different types of PEs relative to the PE concentrations in 51 µm Brentwood PE after equilibrating in a single batch Hunters Point sediment slurry ($n=3$, average±standard deviation).

Compound	51 µm Brentwood	17 µm Husky	51 µm Husky	102 µm Husky
PCB 43	1.000±0.033	1.018±0.263	1.218±0.050	1.228±0.066
PCB 101	1.000±0.173	0.860±0.135	1.191±0.224	1.219±0.252
PCB 153	1.000±0.093	0.909±0.065	1.186±0.124	1.198±0.160
PCB 180	1.000±0.057	0.959±0.026	1.181±0.074	1.127±0.128

Table C6. Numerical data for Figures 10, 11, 12, and 13: PCB uptake kinetics in quiescent sediment for PCB congeners 43, 101, 153, and 180 shown as the PE concentration at each contact time relative to the equilibrium PE concentration ($C_{PE}(t)/C_{PE,eq}$) ($n=3$, average±standard deviation).

Compound	Contact time (d)	17 µm Husky	51 µm Husky	102 µm Husky
PCB 43	1	0.070±0.015	0.021±0.001	0.011±0.001

PCB 101	4	0.121±0.005	0.040±0.002	0.023±0.002
	16	0.233±0.012	0.074±0.001	0.043±0.001
	64	0.361±0.011	0.167±0.041	0.091±0.004
	132	0.386±0.034	0.201±0.003	0.153±0.017
	264	0.528±0.038	0.284±0.041	0.194±0.036
	1	0.028±0.006	0.007±0.000	0.004±0.000
PCB 153	4	0.049±0.002	0.015±0.001	0.007±0.001
	16	0.115±0.006	0.027±0.000	0.015±0.000
	64	0.183±0.008	0.054±0.006	0.028±0.001
	132	0.210±0.012	0.073±0.004	0.048±0.006
	264	0.295±0.017	0.095±0.008	0.060±0.008
	1	0.012±0.002	0.003±0.000	0.002±0.000
PCB 180	4	0.023±0.001	0.007±0.000	0.003±0.000
	16	0.044±0.015	0.012±0.000	0.007±0.000
	64	0.090±0.004	0.025±0.002	0.013±0.001
	132	0.107±0.006	0.033±0.001	0.022±0.003
	264	0.165±0.010	0.046±0.003	0.027±0.004
	1	0.005±0.001	0.001±0.000	0.001±0.000
PCB 180	4	0.012±0.001	0.004±0.000	0.002±0.000
	16	0.029±0.002	0.007±0.000	0.004±0.000
	64	0.046±0.001	0.013±0.001	0.007±0.000
	132	0.060±0.003	0.018±0.001	0.013±0.002
	264	0.094±0.009	0.026±0.001	0.015±0.001

Table C7. Numerical data for Figure 14: PCB release kinetics in quiescent sediment for congeners 29, 69, 103, 155, and 192 shown as the PE concentration at each contact time relative to the initial PE concentration ($C_{PE}(t)/C_{PE0}$) ($n=3$, average±standard deviation).

Compound	Contact time (d)	17 μ m Husky	51 μ m Husky	102 μ m Husky
PCB 29	0	1.000±0.010	1.000±0.033	1.000±0.038
	1	0.917±0.021	0.998±0.015	0.975±0.018
	4	0.765±0.031	0.913±0.040	0.982±0.048
	16	0.566±0.039	0.870±0.049	0.951±0.021

PCB 69	64	0.330±0.004	0.668±0.030	0.854±0.006
	132	0.237±0.008	0.612±0.025	0.788±0.008
	264	0.147±0.018	0.485±0.007	0.719±0.021
	0	1.000±0.013	1.000±0.022	1.000±0.039
	1	0.924±0.014	0.971±0.026	1.016±0.019
	4	0.891±0.030	0.944±0.027	1.040±0.042
	16	0.747±0.021	0.930±0.041	1.018±0.013
PCB 103	64	0.525±0.007	0.801±0.014	0.956±0.008
	132	0.418±0.011	0.802±0.035	0.936±0.023
	264	0.309±0.028	0.683±0.002	0.903±0.006
	0	1.000±0.014	1.000±0.019	1.000±0.038
	1	0.995±0.018	0.996±0.028	1.026±0.021
	4	0.973±0.034	0.975±0.025	1.057±0.045
	16	0.890±0.018	0.980±0.038	1.046±0.013
PCB 155	64	0.711±0.006	0.887±0.015	1.003±0.010
	132	0.435±0.014	0.674±0.032	0.748±0.024
	264	0.393±0.022	0.612±0.005	0.750±0.016
	0	1.000±0.018	1.000±0.085	1.000±0.029
	1	1.055±0.013	0.940±0.032	0.902±0.016
	4	0.975±0.025	0.905±0.015	0.917±0.031
	16	0.944±0.016	0.904±0.028	0.904±0.007
PCB 192	64	0.829±0.008	0.837±0.014	0.869±0.011
	132	0.783±0.041	1.011±0.032	1.078±0.037
	264	0.723±0.010	0.848±0.000	0.930±0.024
	0	1.000±0.011	1.000±0.046	1.000±0.019
	1	1.054±0.005	0.987±0.041	0.907±0.007
	4	1.021±0.025	0.947±0.007	0.924±0.021
	16	0.982±0.028	0.954±0.025	0.913±0.003
	64	0.899±0.008	0.891±0.010	0.879±0.009
	132	0.905±0.012	1.050±0.023	1.083±0.041
	264	0.798±0.004	0.881±0.008	0.887±0.031

Appendix D. Electronic Files

The standalone HOC mass transfer model and the standalone HOC sediment desorption model developed in this study are submitted as separate files (zip files) along with this report.